

PROGRESS IN PHOTOVOLTAIC CELLS BASED ON ORGANIC THIN FILMS&ORGANIC/INORGANIC HYBRID STRUCTURES

S. ANTOHE,

*University of Bucharest, Faculty of Physics,
Research and Development Centre for Materials and Electronic and
Optoelectronic Devices,*

P.O. Box MG-11, Magurele, Ilfov, 077125, ROMANIA,

E-mail: santohe@solid.fizica.unibuc.ro

Telefon: +40214574535/4574419, fax: +40214574418/4574521



Outline

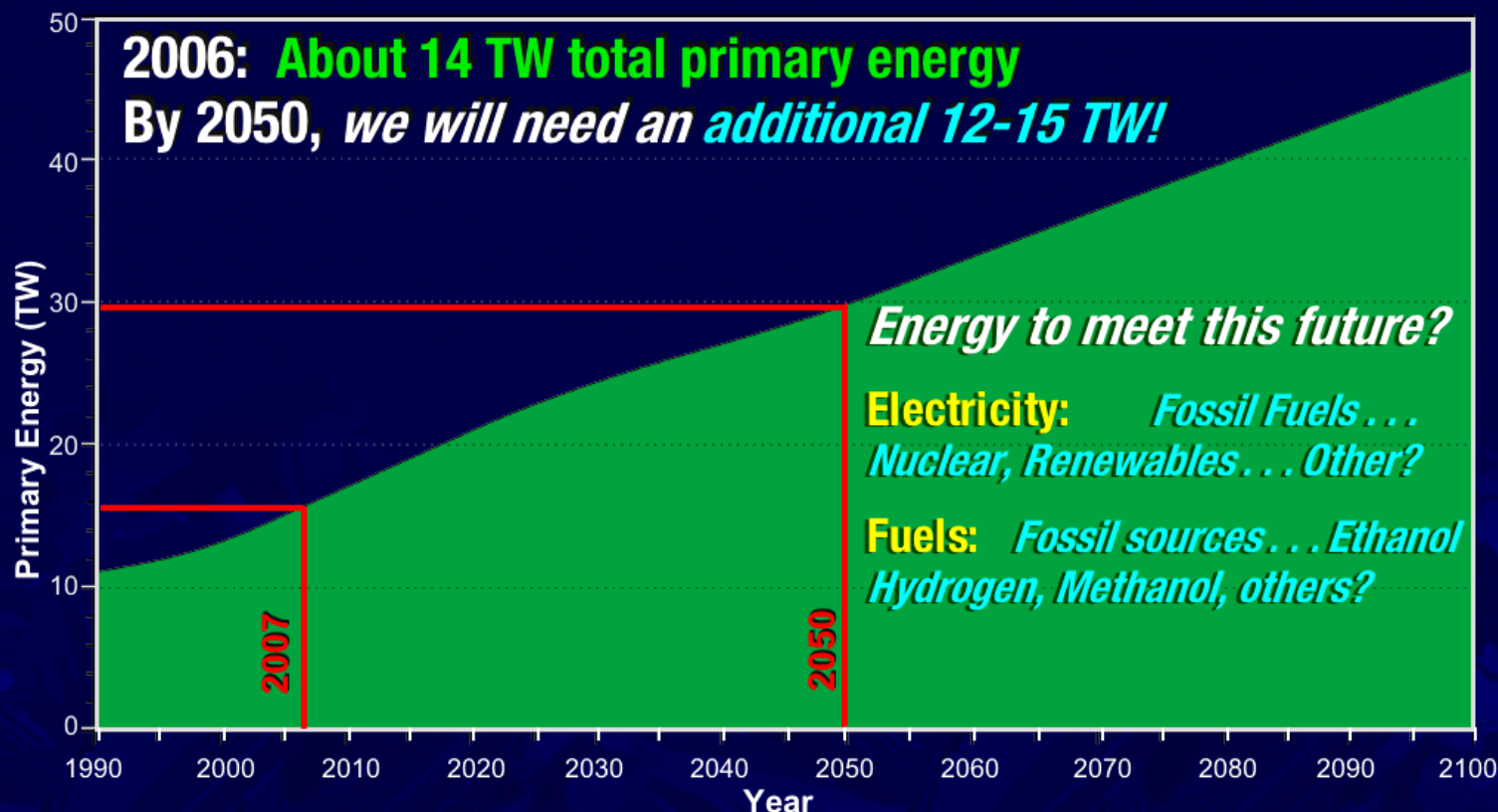
- Motivation
- Organic semiconductors good light absorbers, produced from non-toxic precursors, by very cheap thin film technologies
- Hybrid inorganic/organic structures – a route towards efficient and low-cost photovoltaic cells
 - Problem: excitonic absorption mechanisms
→ charge extraction?
 - Layered structures;
 - Structures engineered at sub-micron or nanoscale
- Conclusions



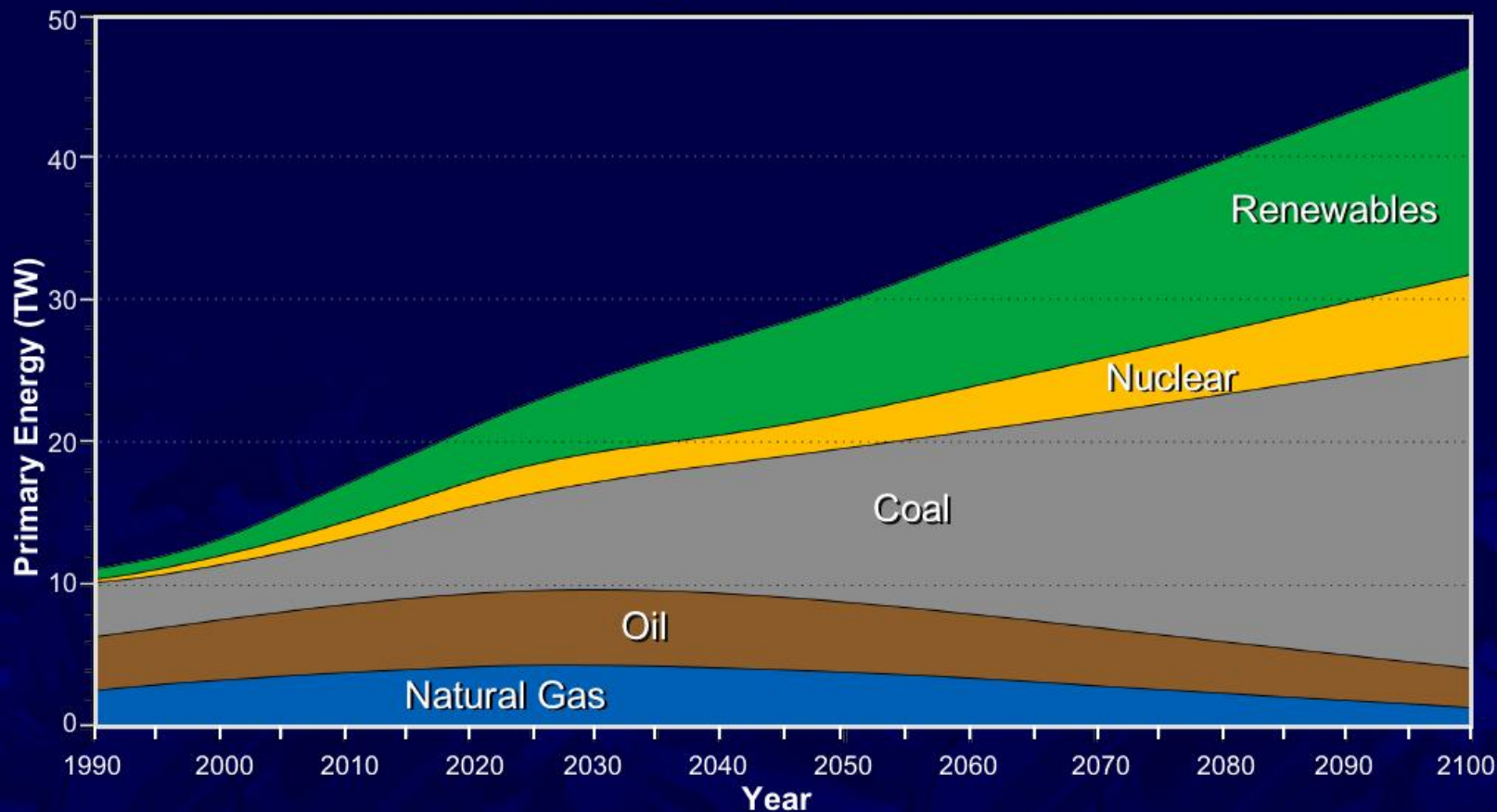
Motivation

The Challenges (*The Terawatt Dilemma . . .*) Worldwide Energy Consumption (now to the future):

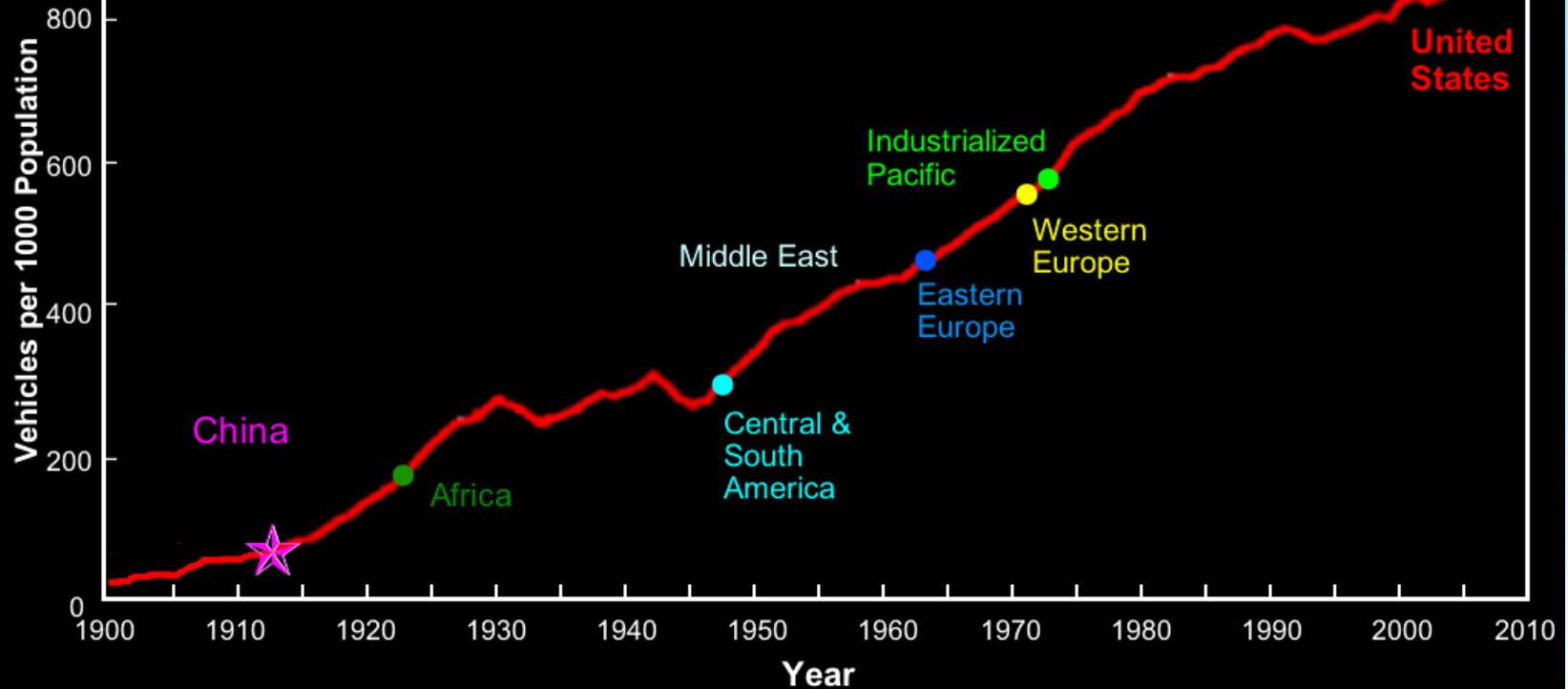
Primary Energy Projections in Terawatts



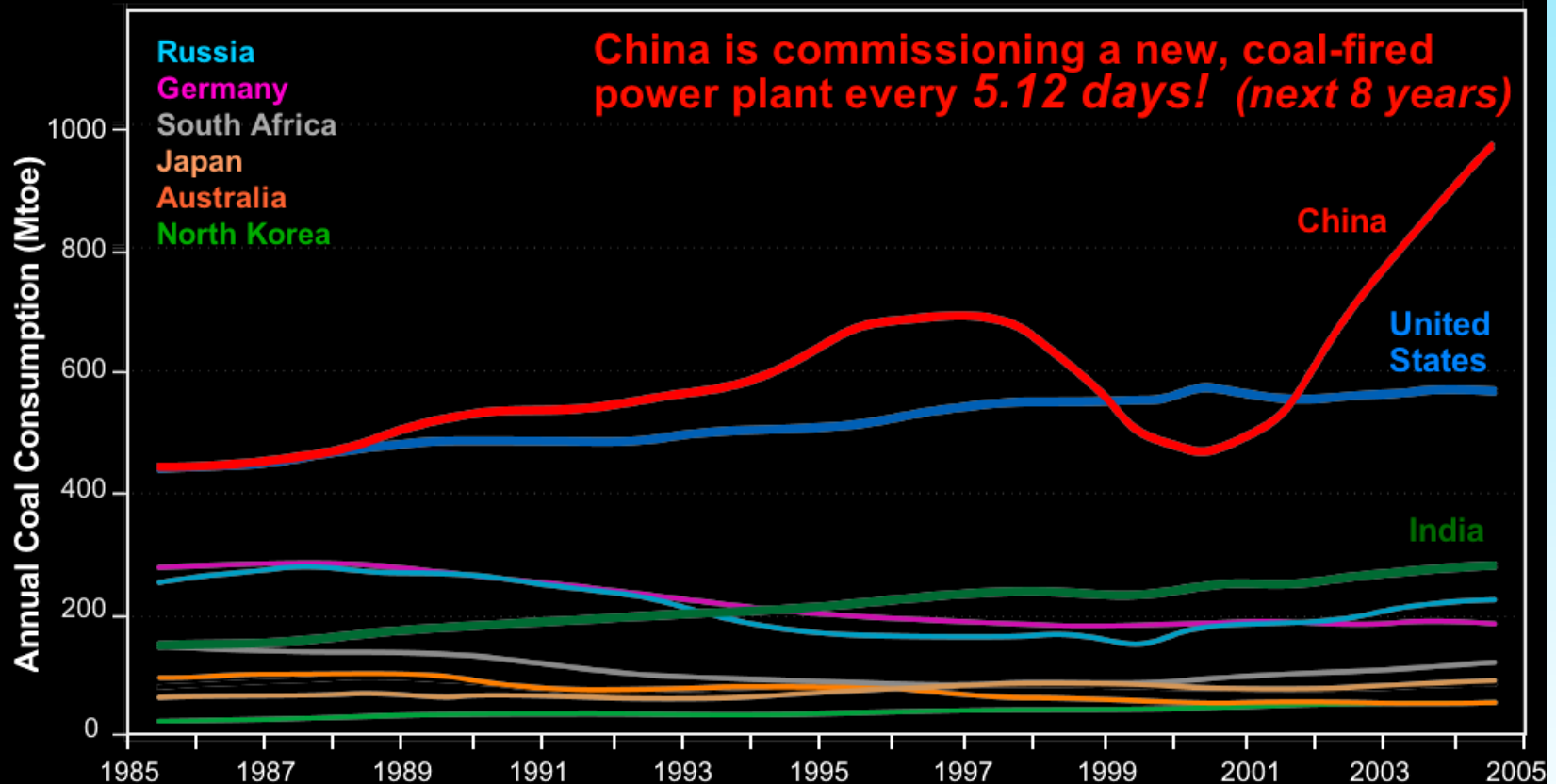
Primary Energy Projections in Terawatts



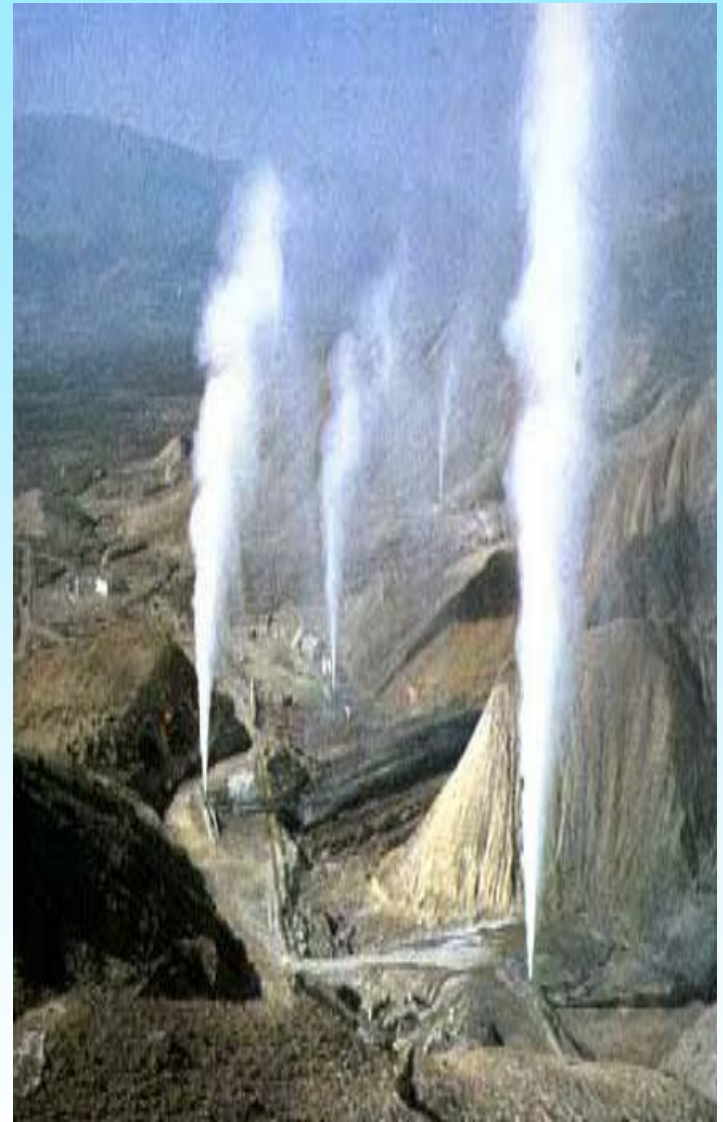
"The History of the Car" Vehicles per Capita History



Annual Coal Consumption by Country



RENEWABLES



How much *solar* will be part of the solution?

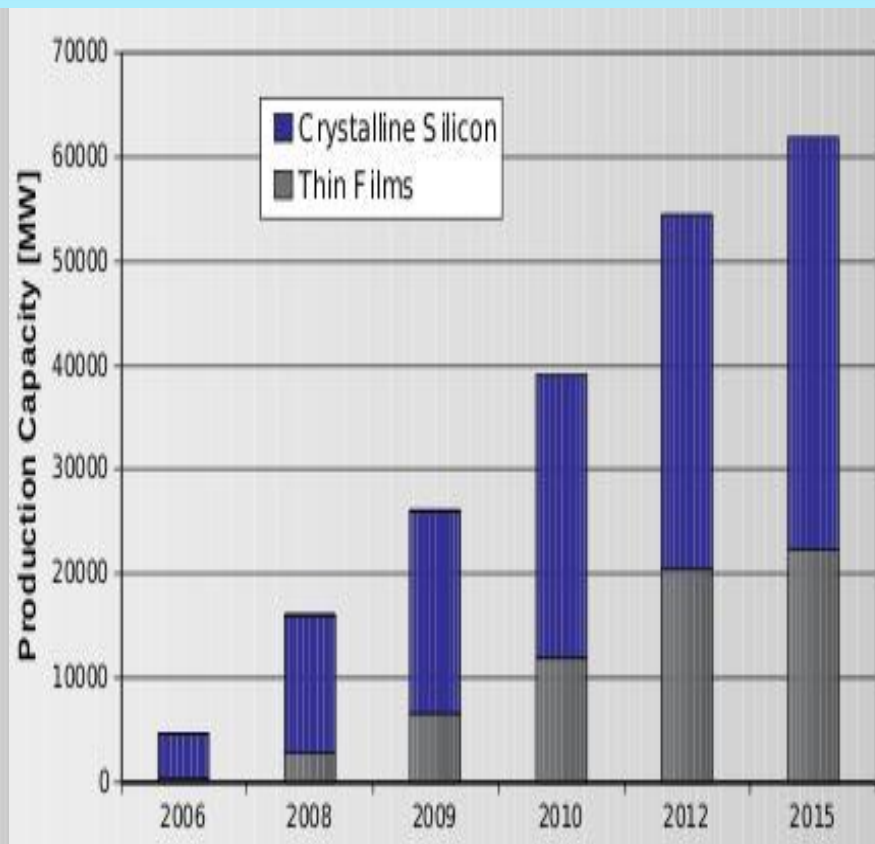
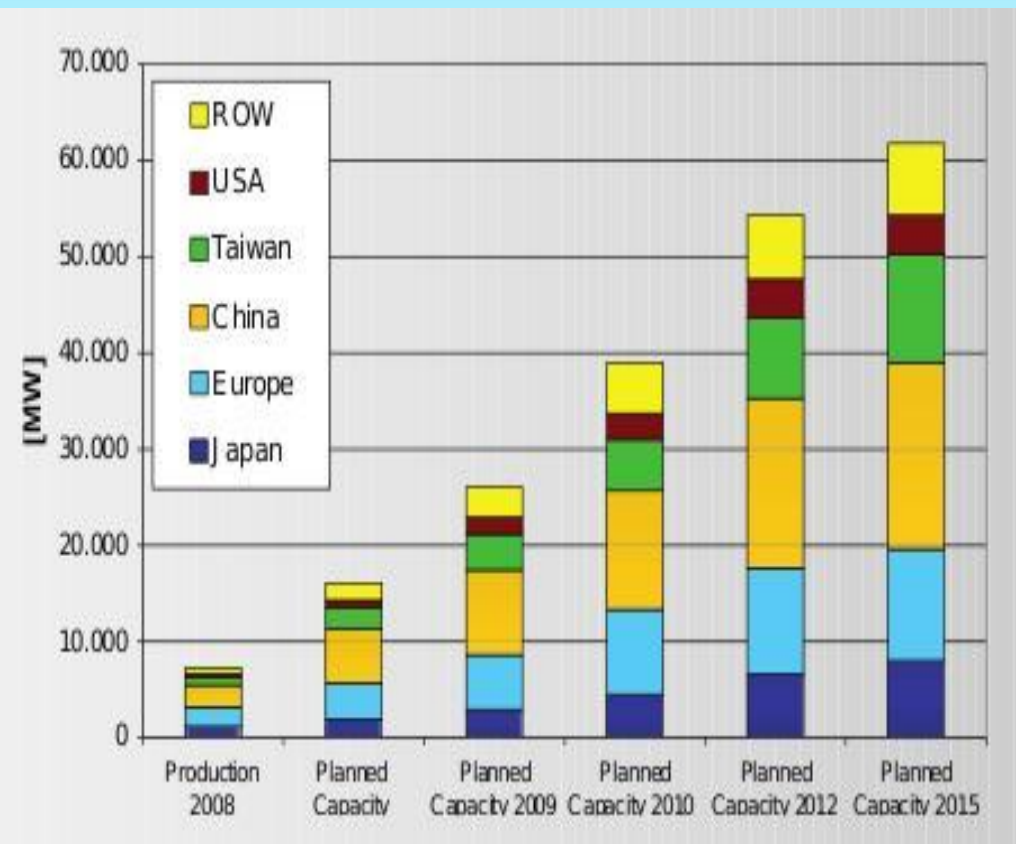


SOLAR is real....

now and for our future



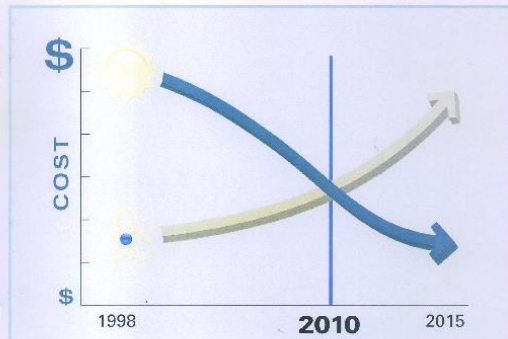
Joint Research Centre - European Commission Renewable Energy Unit PV STATUS REPORT 2009, www.jrc.ec.europa.eu



Study: Solar power is cheaper than nuclear

Solar and Nuclear Costs — The Historic Crossover

Solar Energy is Now the Better Buy



John O. Blackburn
Sam Cunningham
July 2010

Prepared for **NC WARN**

NC WARN

CONTENTS

Summary	3
The Backdrop for Change	5
The Sun is Changing the Game	5
Who Pays for New Nuclear?	7
Wiring the Crossover — in North Carolina	9
Jobs and Manufacturing — in North Carolina	10
Is the Public Ahead of the Utilities?	10
Financing Solar Equipment	11
What About Subsidies?	11
Conclusion	13
Notes	14
Appendix A: Methodology	17
Appendix B: Nuclear plant cost estimates and upward revisions per reactor	19

John O. Blackburn, Ph.D., Professor Emeritus of Economics and former Chancellor, Duke University. Dr. Blackburn has conducted research into energy efficiency and renewable energy over a period of more than thirty years. He has authored six booklets and numerous articles on the future of energy and has served on the Advisory Boards of the Florida Solar Energy Center and the Biomass Research Program at the University of Florida. He has testified before the NC Utilities Commission in several utility dockets on electricity supply and demand, energy efficiency, and renewable energy.

Sam Cunningham, Master of International Management, Duke University. Mr. Cunningham's professional and academic interests are focused on policy applications of natural resource economics. He is an Economics and Environmental Studies graduate of Emory University.

NC WARN: Water Awareness & Reduction Network is a member-based nonprofit building the accelerating, critical path to climate change — along with the various risks of nuclear power — by watchdogging utility practices and working for a safer North Carolina transition to energy efficiency and clean power generation. In partnership with other citizen groups, NC WARN uses sound scientific research to inform and involve the public in key decisions regarding their water buy.

NC WARN: Water Awareness & Reduction Network
PO Box 6161, Durham, NC 27715, 919.414.5077
www.ncwarn.org

NC WARN

SUMMARY

Solar photovoltaic system costs have fallen steadily for decades. They are projected to fall even farther over the next 10 years. Meanwhile, projected costs for construction of new nuclear plants have risen steadily over the last decade, and they continue to rise.

In the past year, the lines have crossed in North Carolina. Electricity from new solar installations is now cheaper than electricity from proposed new nuclear plants.

This new development has profound implications for North Carolina's energy and economic future. Each and every stakeholder in North Carolina's energy sector — citizens, elected officials, solar power installers and manufacturers, and electric utilities — should recognize this watershed moment.

Solar-Nuclear Kilowatt-Hour Cost Comparison

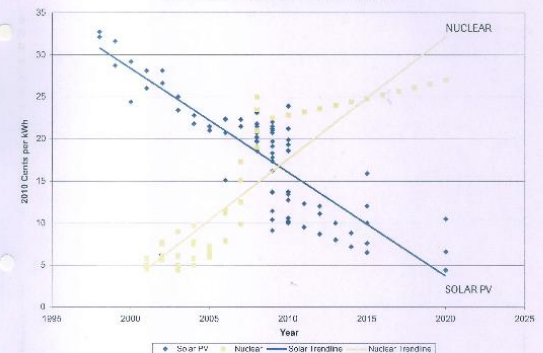


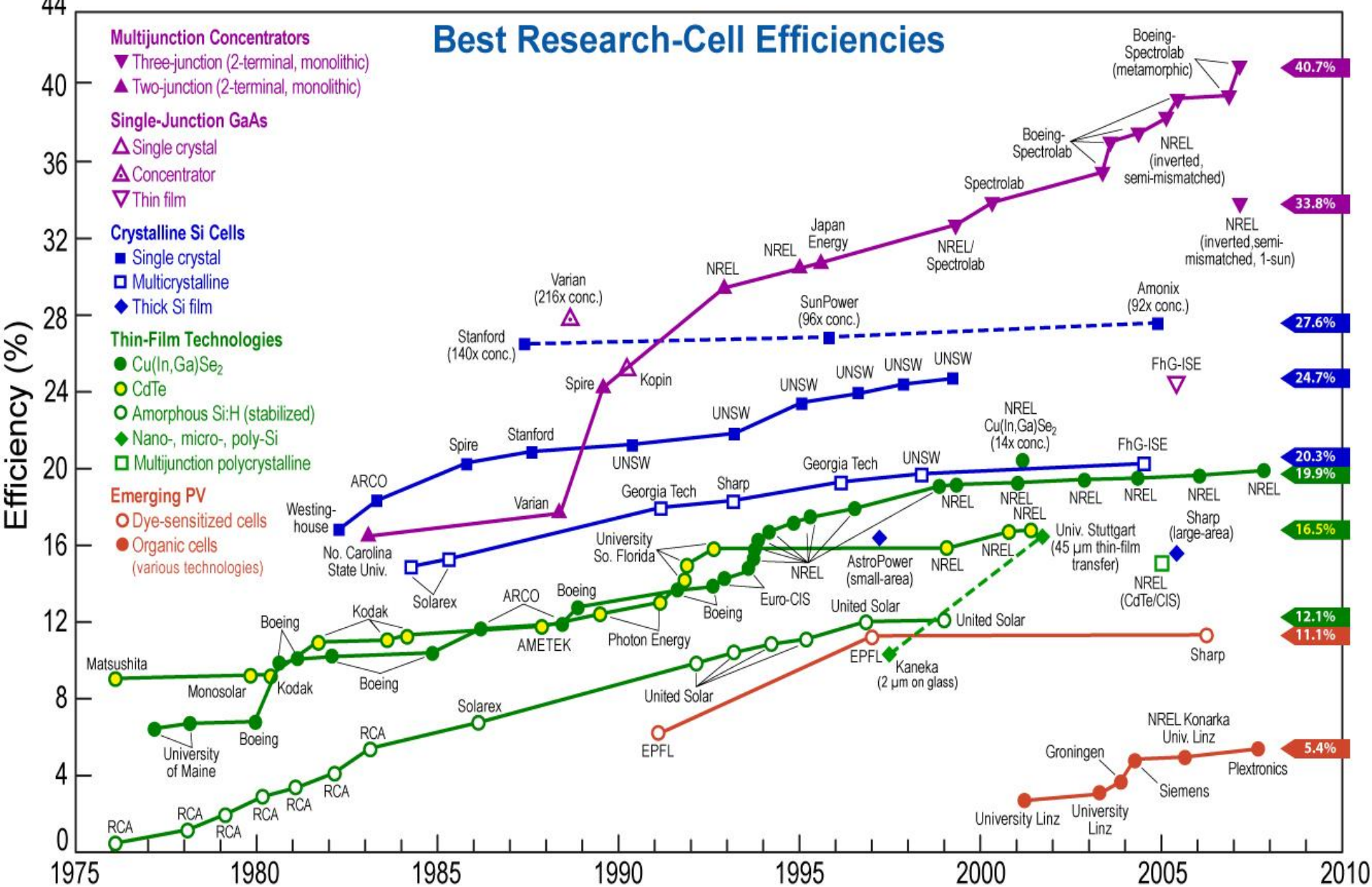
Figure 1: The Historic Crossover — Solar photovoltaic costs are falling as new nuclear costs are rising.¹

The Solar PV least squares trendline is fit to 1) data points representing the actual cost of producing a kilowatt-hour in the year shown through 2010 in the U.S.; 2) 2010 costs from North Carolina installers; and 3) national cost projections from 2010 to 2020. The nuclear trendline is fit to national cost projections made in the year shown on the x-axis of eventual kilowatt-hour cost if projects reach completion. See complete methodology in Appendix A.

THE HISTORIC CROSSOVER

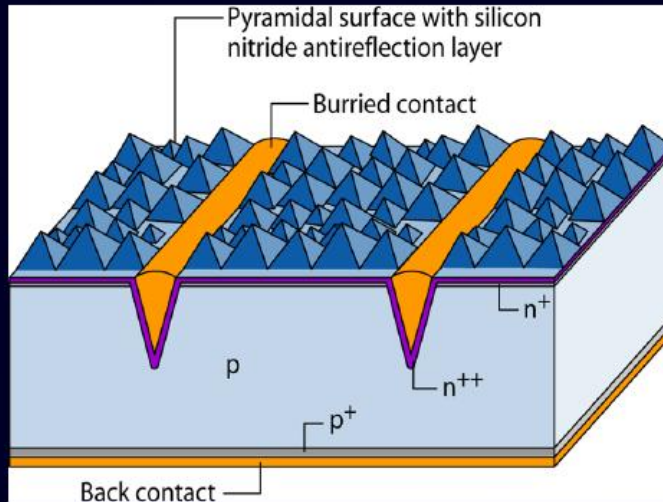
3



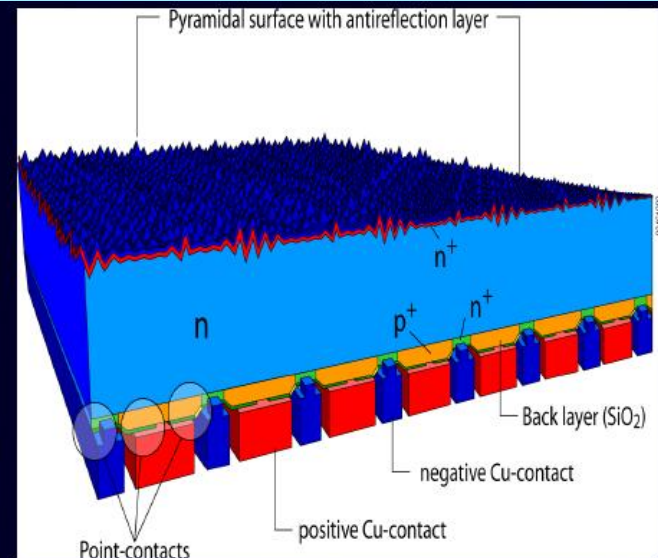


1st Generation PV

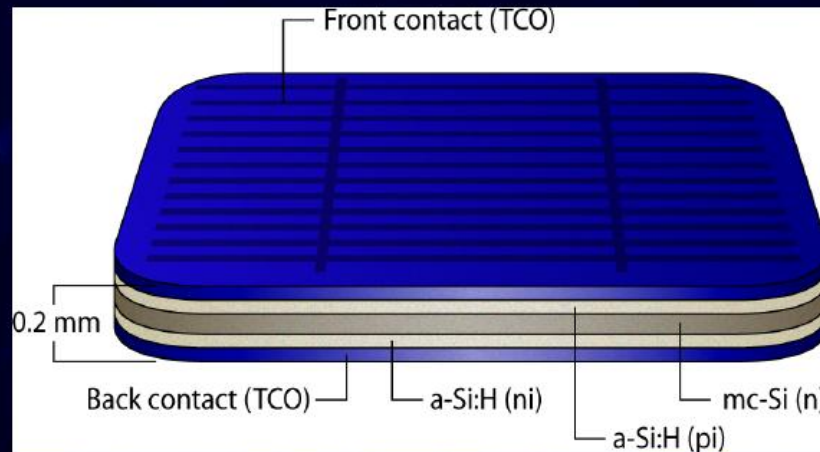
PV Si 20% Club



BP Saturn



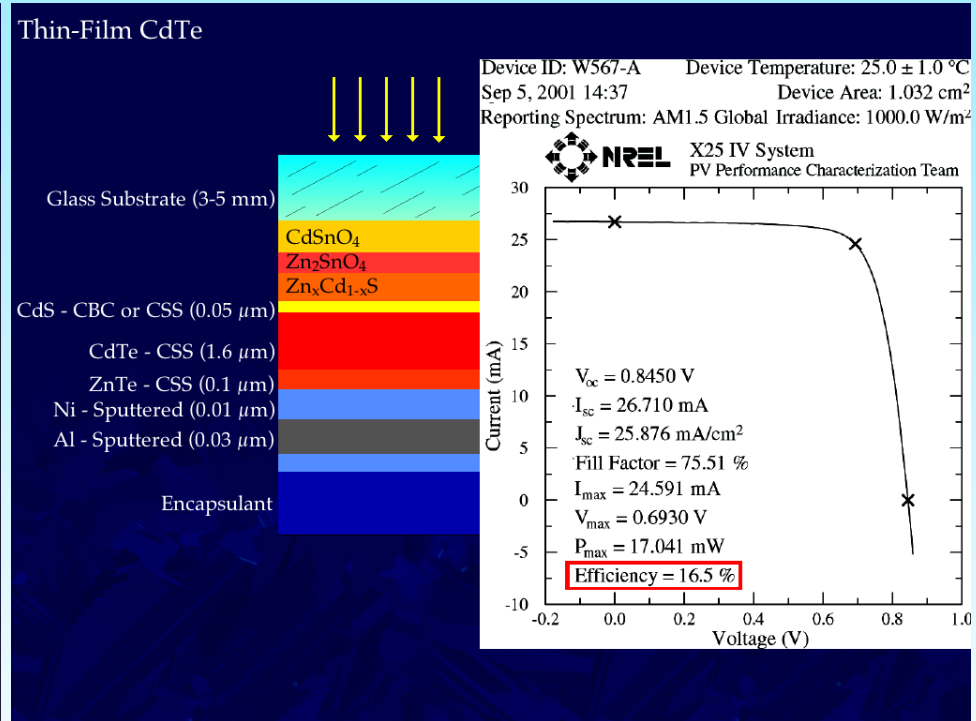
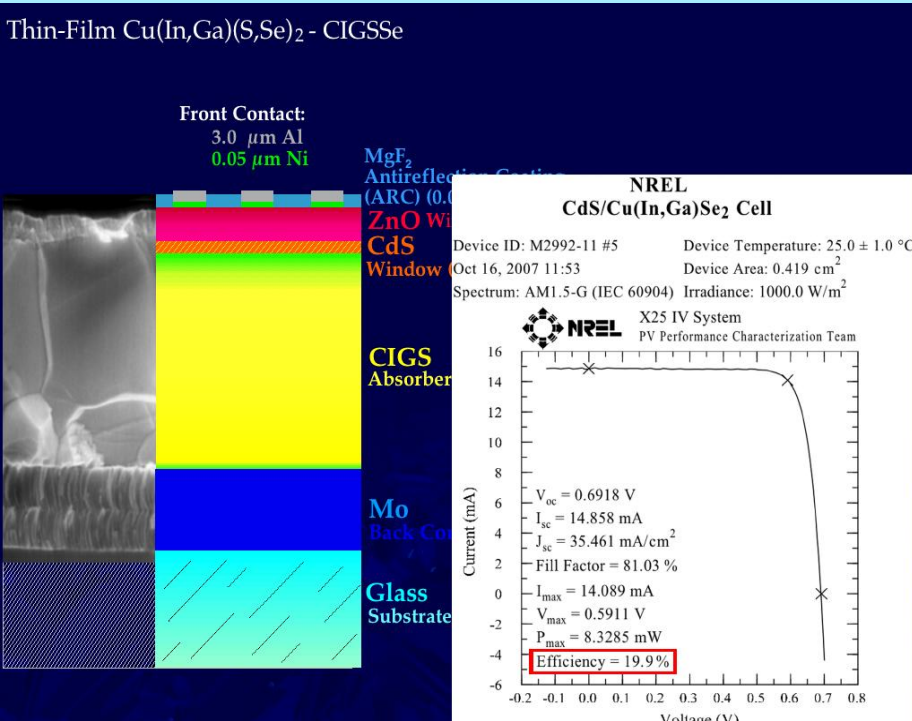
SunPower Cell



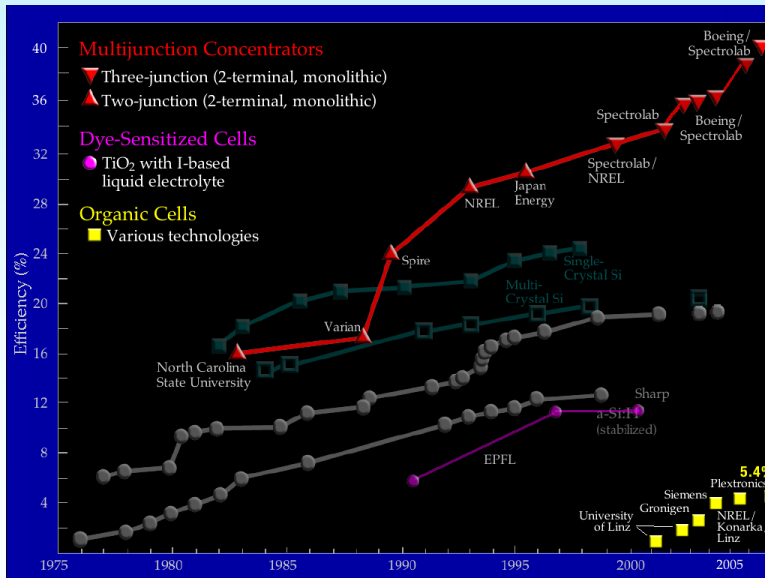
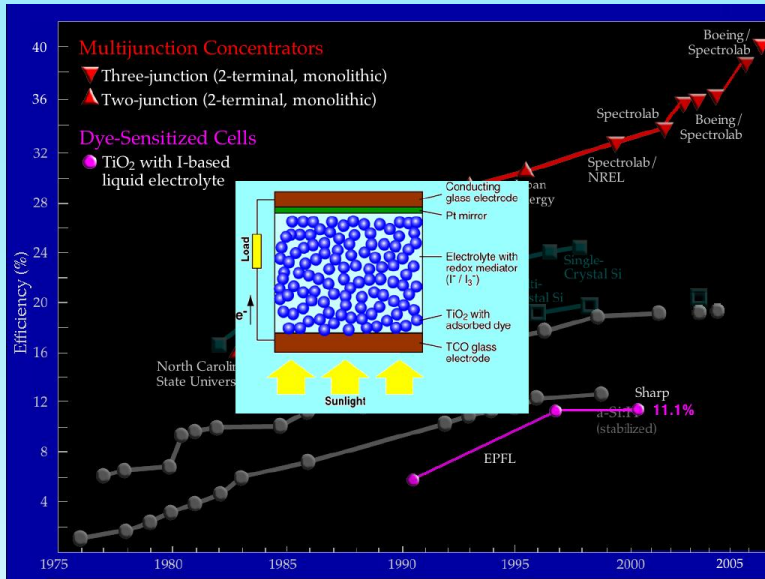
Sanyo HIT Cell



2nd Generation PV



3rd Generation PV —Emerging PV: DSSC, Organic Cells, Plastic Cells



Konarka Power Plastic®

A new generation of solar technology.

Flexible film panels can be applied to virtually any surface — to create true energy independence. The window of opportunity is wide open.

Let's put the light to work.




4th Generation PV—Hybrid Organic/Inorganic Structures

Multijunction Concentrators, Nanostructured thin films

3rd, 4th, ... Future Generations
Revolutionary Technologies for Our Next Generations of Consumers

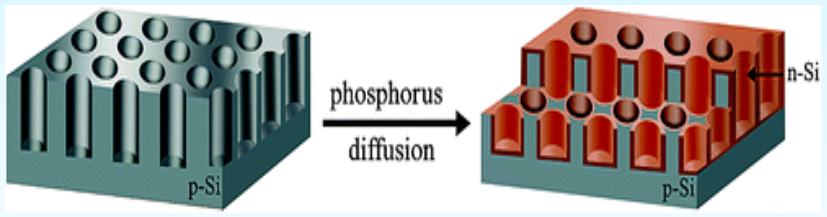
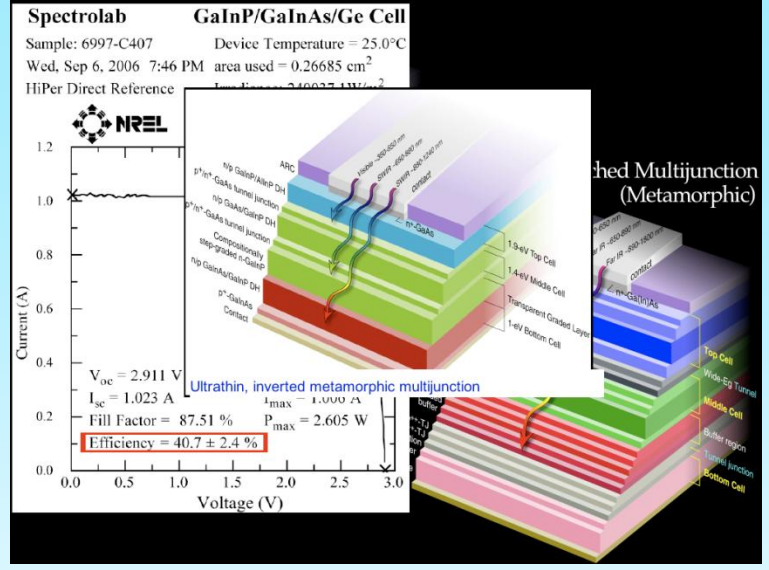
- ... quantum dot, pod, rod and other novel structures; nanotechnologies; multiple-junctions...
- ... with efficiencies 2-3 times those for conventional PV
- ... high-risk research
- ... the fringes of technology exploration



Efficiencies for Ideal Future Generation Solar Cells

Ideal converter; $T_s = 6000K, T_a = 300K$ isotropic illumination	Efficiency
Carnot	0.950
Landsberg	0.933
Multijunction	0.868
Impact ionisation, best Q	0.868
Solar thermal	0.854
Hot electrons	0.854
Thermophotovoltaic	0.854
Thermophotonic	0.854
Intermediate band, (MQD or alloy)	0.632
2nd photon pumped MQW	0.632
Shockley & Queisser limit	0.403

Multiband
Triple Iron-Hole Pairs



Si nanohole arrays Silicon nanohole solar cells aim to make photovoltaics cost-competitive.

Under 1 sun AM1.5G illumination, a Si nanohole solar cell with p-n junctions via P diffusion exhibited an $U_{oc} = 566.6 mV$, a $J_{sc} = 32.2 mA/cm^2$, and a remarkable $\eta = 9.51\%$. *The nanohole array geometry solar cells possesses :* i) a robust structure compared with fragile free-standing nanowire geometry ,ii) a better ability for capturing sunlight than nanowire arrays, iii) the radial p-n junctions allowing for enhanced carrier collection.

Since 2002, photovoltaic production worldwide has been **doubling every two years**, making it the world's fastest-growing energy technology. However, the overall energy conversion efficiency of photovoltaics is still too low to be cost-competitive with fossil fuels, that is why new efforts must be done to increase the performances of solar cells and decrease their cost. For example the recent paper of **Kui-Qing Peng, Shuit-Tong Lee**, City University of Hong Kong, **Journal of the American Chemical Society**, **7 May, 2010** shows that

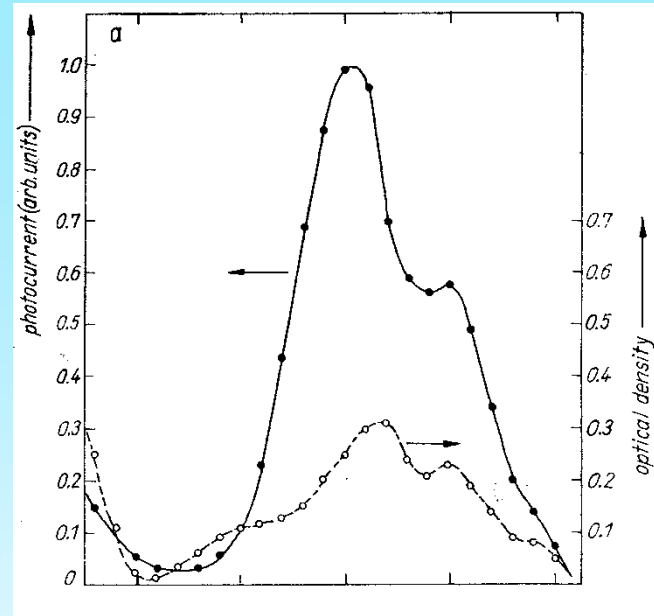
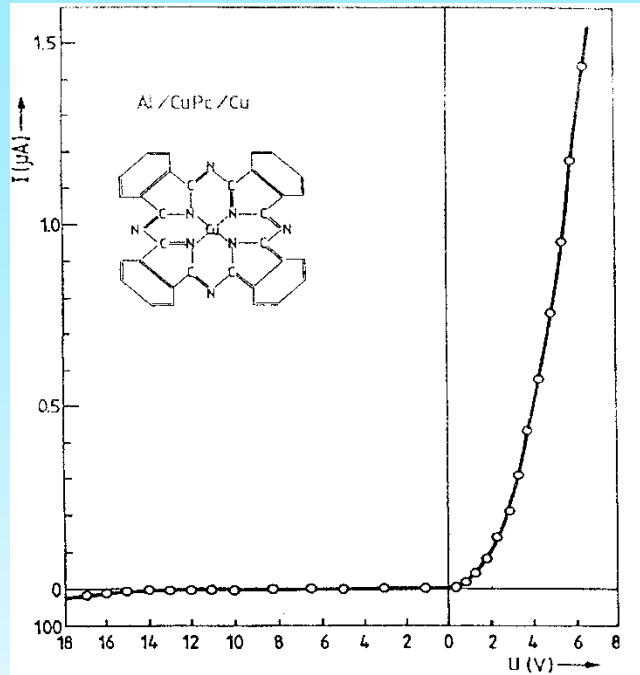


I - Photovoltaic Cells Based on Organic Monomeric and Polymeric Thin Films



Mono-layer cells based on CuPc and TPyP

ITO/CuPc/Al



Action spectrum of short - circuit photocurrent and absorption spectrum of the organic layers for the Schottky cells ITO/CuPc/Al

Dark current-voltage characteristics of a ITO/CuPc/Al cell, at room temperature The chemical structural formula of CuPc is shown in inset

■ Transport parameters:

- hole equilibrium concentration $\rho_0 = 2.3 \times 10^{13} \text{ cm}^{-3}$,
- mobility $\mu_p = 1.1 \times 10^{-2} \text{ cm}^2/\text{Vs}$,
- dark electrical conductivity $\sigma_p = 4 \times 10^{-8} \Omega^{-1} \text{ cm}^{-1}$ and
- equilibrium Fermi level located at 0.455 eV above the valence band

■ Typical cell parameters at illumination through ITO electrode with monochromatic light ($\lambda = 620 \text{ nm}$ and $\sim 10^5 \text{ photons/cm}^2\text{s}$) are:

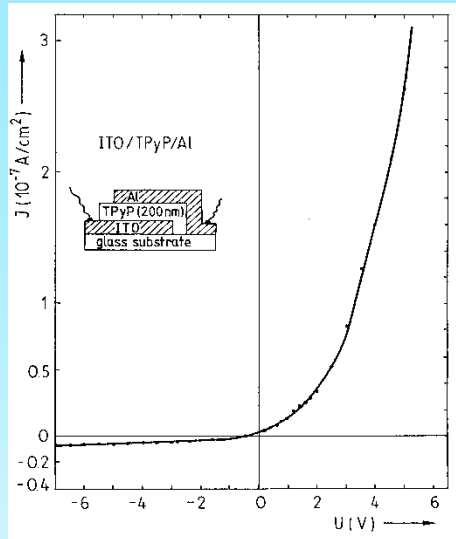
- open-circuit photovoltage $U_{oc} = 0.675 \text{ V}$,
- short-circuit photocurrent $I_{sc} = 8 \text{ nA}$, and
- fill factor $ff = 0.35$.
- $\eta_e = 0.6 \times 10^{-2} \%$.

S. Antohe, Journal of Optoelectronics and Advanced Materials, 2, 498 (2000)



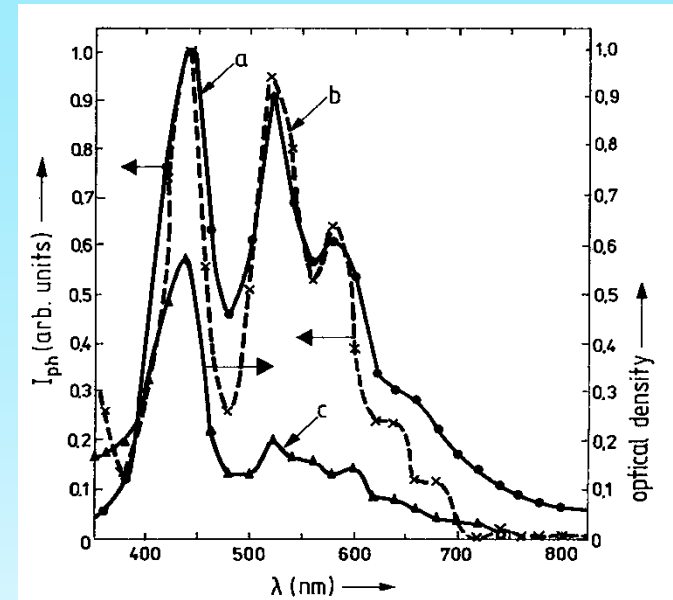
Mono-layer cells based on CuPc and TPyP

ITO/TPyP/Al



Dark current - voltage characteristic of ITO/TPyP/Al cell

- Transport parameters:
- Ohmic region:
 - $n_0 = 3 \times 10^9 \text{ cm}^{-3}$
 - $E_{F0} = 0.66 \text{ eV below (CB)}$
 - $\mu = 6 \times 10^{-4} \text{ cm}^2/\text{Vs}$
 - $\sigma_0 = 3 \times 10^{-13} \Omega^{-1} \text{ cm}^{-1}$
- SCLC region:
 - $N_t = 1.7 \times 10^{14} \text{ cm}^{-3}$
 - $E_c - E_t = 0.75 \text{ eV}$

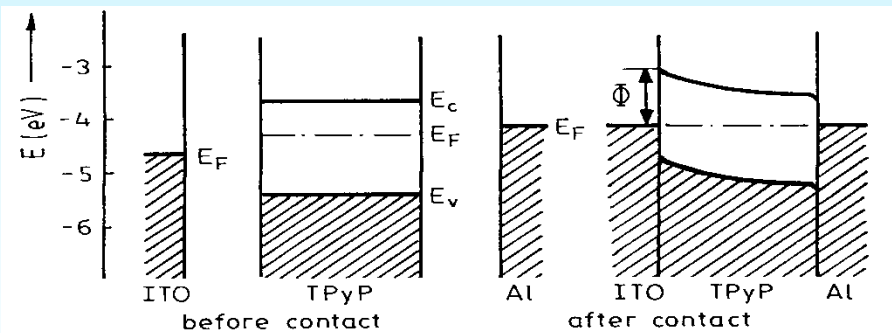


Action spectra and absorption spectrum of the ITO/TPyP/Al cell

- Typical cell parameters at illumination through ITO electrode with monochromatic light of $32 \mu\text{W}/\text{cm}^2$ at $\lambda = 440 \text{ nm}$:

- $U_{oc} = 0.175 \text{ V}$
- $J_{sc} = 42 \text{ nA}/\text{cm}^2$
- $ff = 0.13$
- $\eta = 0.27 \times 10^{-2} \%$

S. Antohe, Phys. Stat. Sol. (a), 136 (1993) 401

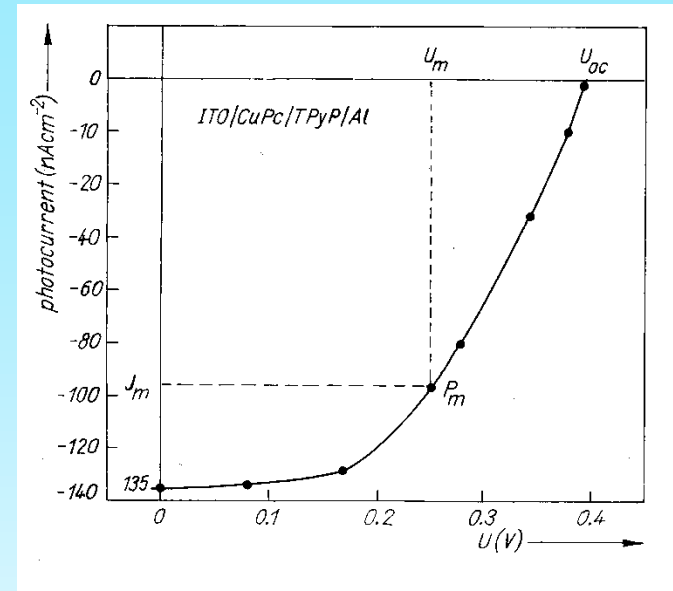
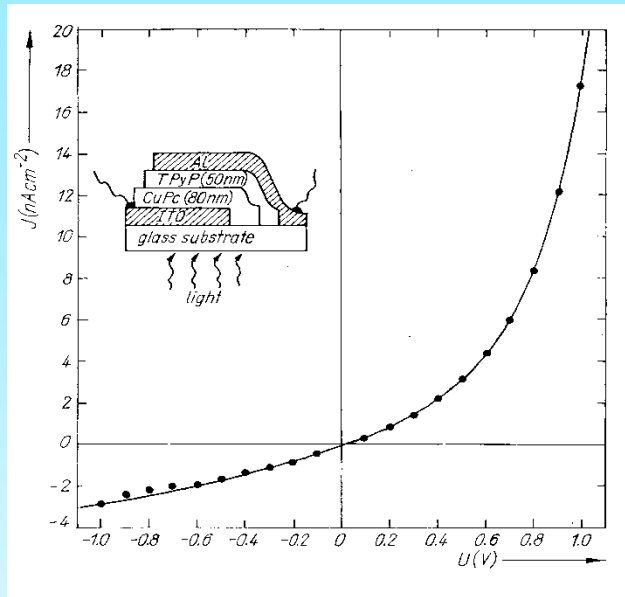


Schematic representation of energy bands at the ITO/TPyP(50 nm)/Al junction. $\Phi = 0.68 \text{ eV}$ the barrier height at ITO/TPyP interface; wide of barrier $w \in [193, 50] \text{ nm}$, when the temperature increases from 295 to 360 K



Two-Layer Organic Photovoltaic Cells

ITO/CuPc/TPyP/Al



Cell configuration (inset) and dark current-voltage characteristics of ITO/CuPc/TPyP/Al

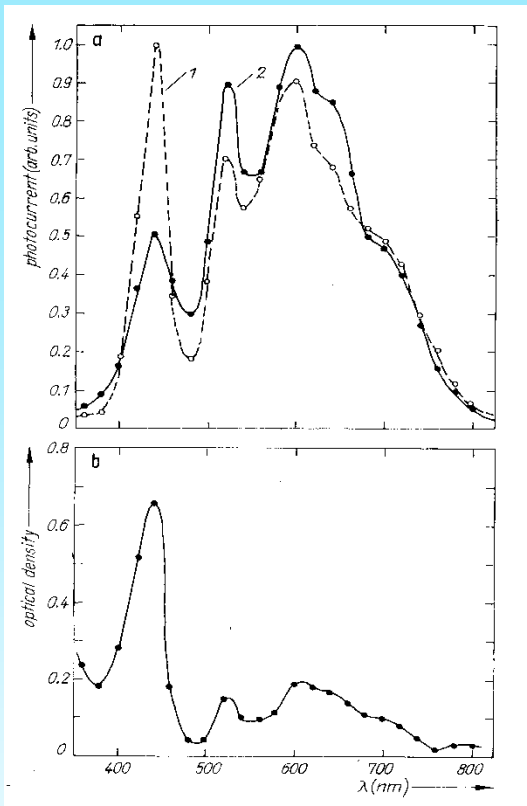
Current - voltage characteristics for a ITO/CuPc/TPyP/Al photovoltaic cell in the fourth quadrant, under illumination with monochromatic light of $20 \mu \text{ W/cm}^2$ at 440 nm

■ Typical cell parameters at illumination through ITO with $20 \mu \text{ W/cm}^2$ at 440 nm:

- ➔ $U_{oc} = 400 \text{ mV}$
- ➔ $J_{sc} = 135 \text{ nA/cm}^2$
- ➔ $ff = 0.44$ and
- ➔ $\eta_e = 0.12\%$.

S. Antohe and L. Tugulea, phys. stat. sol. (a) 128, 253 (1991)



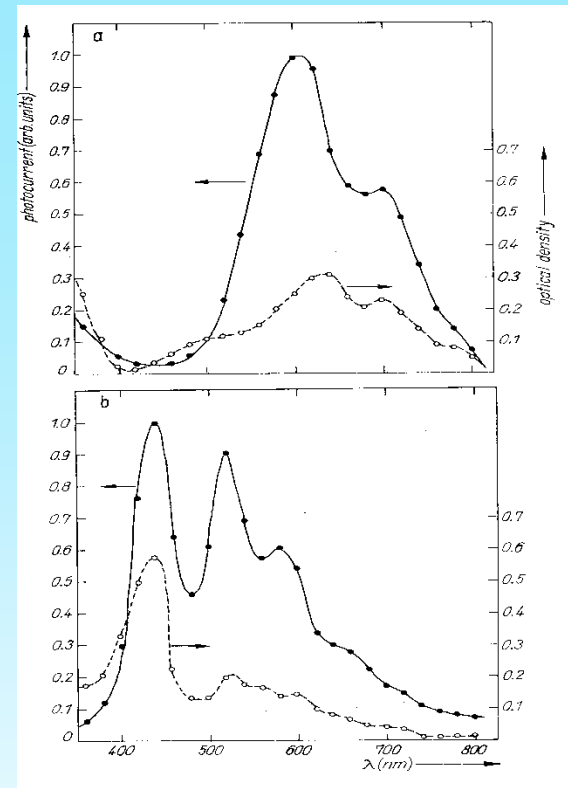


(a) Action spectra of short - circuit photo-current for the p-n junction cell of ITO/CuPc/TPyP/Al. Curves (1) and (2) are obtained at illumination of the Al and ITO electrodes, respectively

$$(1) J_{\text{ph } 400 \text{ nm}} = 0.845 \text{ nA/cm}^2$$

$$(2) J_{\text{ph } 600 \text{ nm}} = 223 \text{ nA/cm}^2.$$

(b) Optical absorption spectrum of the CuPc/TPyP two layer film.



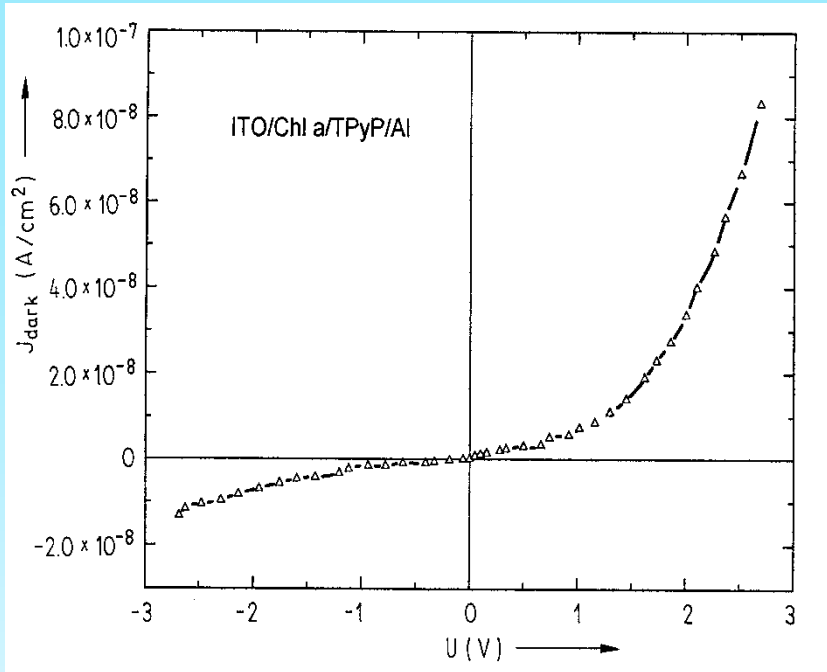
Action spectrum of short - circuit photocurrent for the Schottky cells of: (a) ITO/CuPc/Al; (b) ITO/TPyP/Al, at illumination through the ITO electrode, and the absorption spectrum of the: a) CuPc; b) TPyP layer

$$a) J_{\text{ph } 600 \text{ nm}} = 37.2 \text{ nA/cm}^2,$$

$$b) J_{\text{ph } 440 \text{ nm}} = 28.8 \text{ nA/cm}^2.$$

S. Antohe and L. Tugulea, phys. stat. sol. (a) 128, 253 (1991)



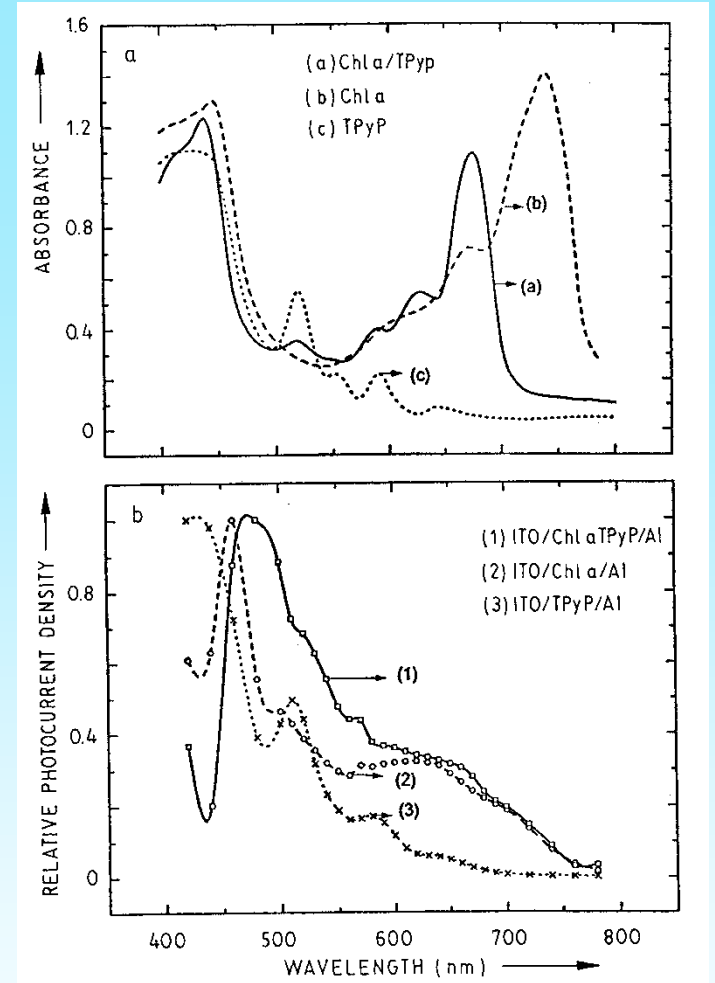


Dark Current - voltage characteristic of ITO/Chl a(200 nm)/TPyP (100nm)/Al cell at room temperature

■ Typical photovoltaic cell parameters under monochromatic light of $20 \mu\text{W}/\text{cm}^2$ at 470 nm:

- $U_{oc} = 490 \text{ mV}$, $J_{sc} = 13 \text{ nA}/\text{cm}^2$, $ff = 0.34$ and $\eta = 1.1 \times 10^{-2}\%$
- $ff = 0.34$ is better than the values of 0.09 and 0.13 for ITO/Chla/Al and ITO/TPyP/Al Schottky cells, respectively.
- η is about 2-3 times higher than for ITO/Chla/Al cell.

S. Antohe, L. Tugulea, V. Gheorghe, V. Ruxandra, I. Caplanusi and L. Ion, phys. stat. sol. (a) 153, 581 (1996)



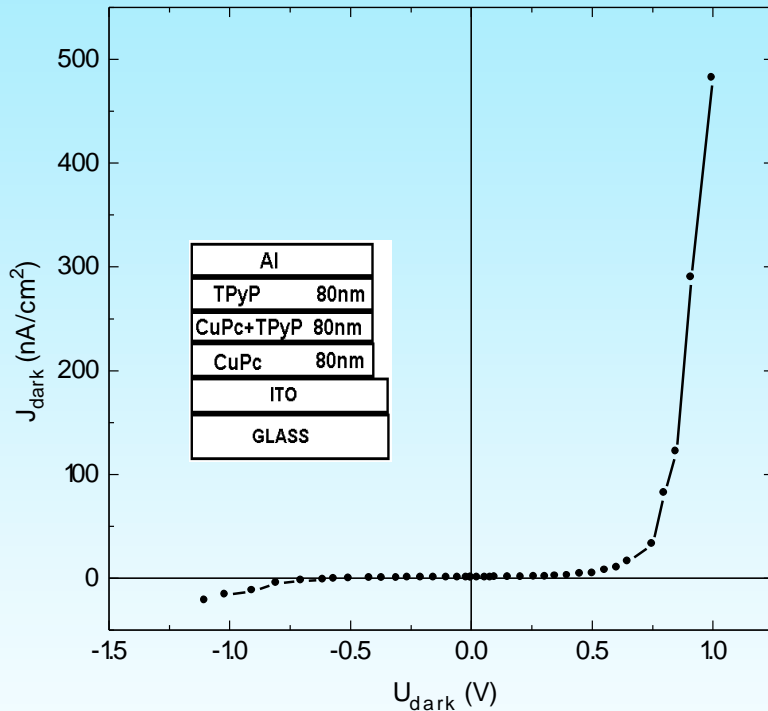
- (a) Absorption spectrum of Chl a/TPyP films, Chl a layer, and TPyP layer
- (b) Action spectra of cells illuminated through ITO: ITO/Chl a/TPyP/Al (1), ITO/Chl a/Al (2), and ITO/TPyP/Al (3)



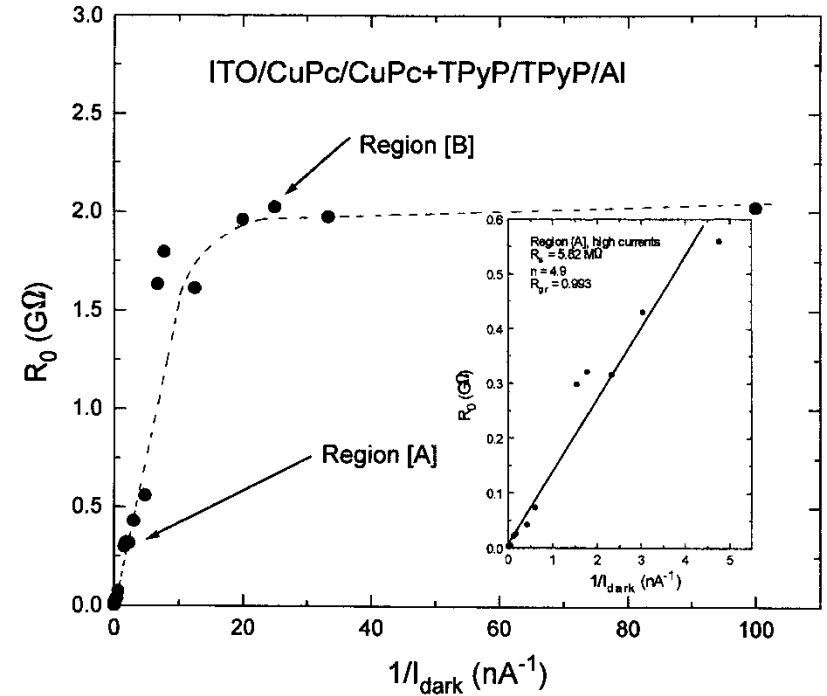
Three - Layered Photovoltaic Cell

ITO/CuPc/(CuPc+TPyP)/TPyP/Al

a) Dark current-voltage characteristics



Cell configuration (inset) and the dark current-voltage characteristics of the ITO/CuPc/(CuPc+TPyP)/TPyP/Al cell at room temperature



Variation of junction resistance R_0 as a function of reciprocal forward current $1/I$. The insert zooms on region A of high currents

S. Antohe, V. Ruxandra, L. Tugulea, V. Gheorghe and D. Ionascu, *J. Phys. III France 6, 1133 (1996)*



Forward characteristic of the cell up to 1V can be fitted well by the modified Shockley equation:

$$I = I_0 \left\{ \exp \left[\frac{q(U - IR_s)}{nkT} \right] - 1 \right\} + \frac{U - IR_s}{R_{sh}} \quad (1)$$

► The junction resistance R_0 is

$$R_0 = dU/dI = R_s + 1/\{\beta I_0 \exp[\beta(U - IR_s)] + 1/R_{sh}\} \quad (2)$$

when $\beta = q/nkT$

► For higher forward bias, where R_s affects the curves, eq (1) can be approximated as $I = I_0 \exp[(U - IR_s)]$, and since $1/R_{sh} \ll I$, eq (2) can be written as:

$$R_0 \cong R_s + 1/\beta I \quad (3)$$

► For low voltages, where R_{sh} acts, the approximation $\beta I_0 \exp[(U - IR_s)] \ll 1/R_{sh}$ is valid, and eq. (2) becomes: $R_0 \approx R_s + R_{sh}$ (4)

► From the extrapolated linear region [A], the determined value of R_s is 5.82 MΩ, the value of R_{sh} , obtained from region [B] being ~ 2 GΩ.

► To improve the linearity of $\ln(I)$ -U plot, for determination of n and I_0 , we firstly removed the effect of R_s . This was achieved by making the following change in variable: $Y = U - IR_s$ (5)

► With this change, eq. (1) becomes: $I = I_0 [\exp(Y) - 1] + Y/R_{sh}$ (6)

► For high forward biases, eq. (6) can be written as: $I \approx I_0 \exp(\beta Y)$ (7)

► Plotting $\ln(I - Y/R_{sh})$ vs. Y we remove the effect of the R_{sh} .

► from 0.3V to 0.1V and at higher The removal of R_{sh} and R_s has lead to the increase in the linearity of the curve at lower biases biases from 0.7 to 0.8 V, respectively.

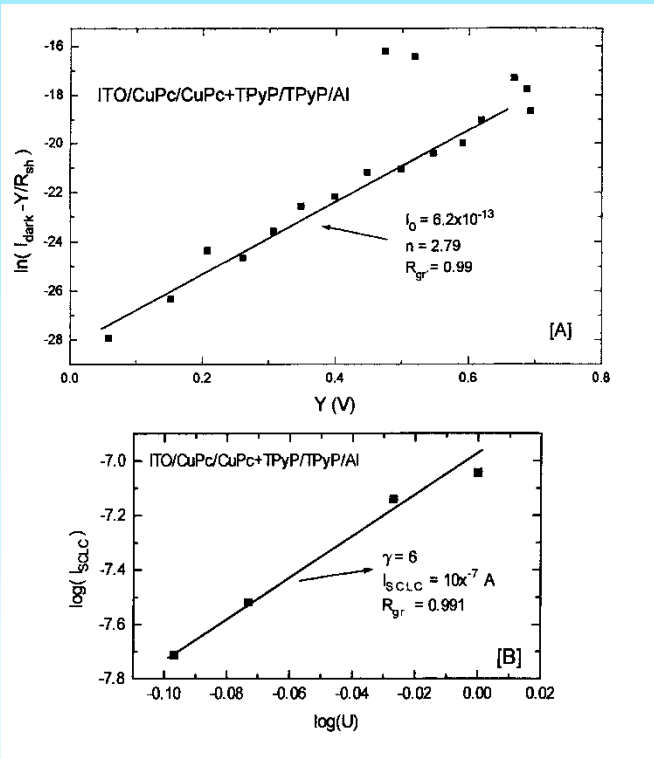
► The whole linear region of $\ln(I)$ -U plot is extended in the range 0.1-0.8V.

► n and I_0 obtained from the slope and the intercept are 2.79 and $6.2 \times 10^{-13} A$, respectively and are more reliable than those obtained after the removal of R_s only.

► For biases > 0.8 V, the current follows the relation $I \sim U^m$, where $m = 7$. this suggests that the dark current is a (SCLC) in the presence of exponentially distributed traps.

$$J_{SCLC} = N_{eff} \mu q^{1-\gamma} [\epsilon \gamma / N_t (\gamma + 1)]^\gamma [(2\gamma + 1) / \gamma + 1]^{\gamma+1} (U^{\gamma+1} / d^{2\gamma+1}) \quad (8)$$

where $= T_c/JT$, and T_c is a "characteristic temperature"

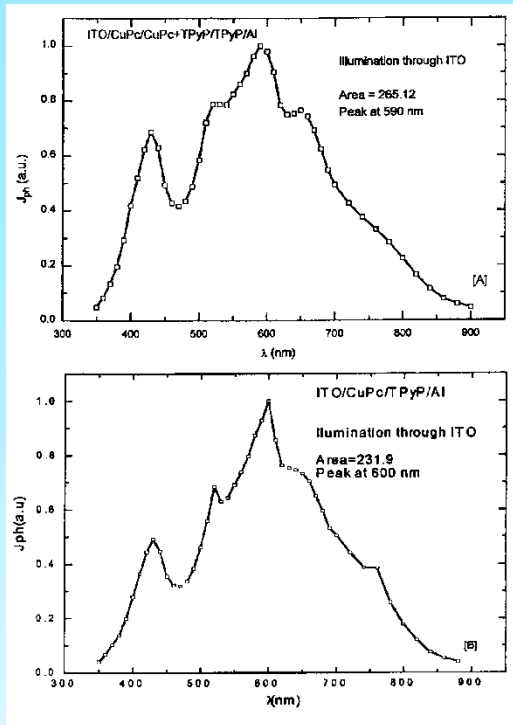


[A] Semi logarithmic plots of the forward-biased dark current: $I - Y/R_{sh}$ vs Y . [B] Logarithmic plot of SCLC current vs voltage for high forward biases

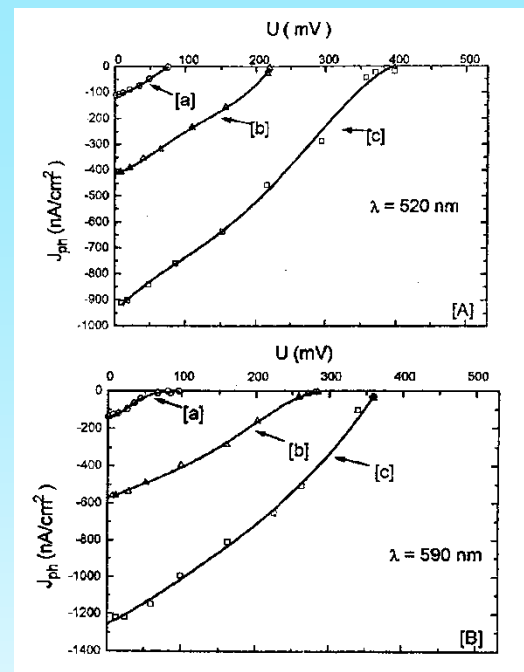
S. Antohe, V. Ruxandra, L. Tugulea, V. Gheorghe and D. Ionascu, *J. Phys. III France 6, 1133 (1996)*



b) Photovoltaic Properties



Action spectra of the cells: [A] ITO/CuPc/(CuPc+TPyP)/TPyP/Al; [B] ITO/CuPc/TPyP/Al, illuminated through ITO electrode



Photocurrent- photovoltage characteristics of the ITO/CuPc/(CuPc+TPyP)/TPyP/Al cell illuminated through ITO electrode with: [A] 520 nm wavelength of varying intensity as ($3 \mu\text{W}/\text{cm}^2$ [a], $12 \mu\text{W}/\text{cm}^2$ [b] and $30 \mu\text{W}/\text{cm}^2$ [c]); [B] 590 nm wavelength of varying intensity as ($6 \mu\text{W}/\text{cm}^2$ [a], $30 \mu\text{W}/\text{cm}^2$ [b] and $72 \mu\text{W}/\text{cm}^2$ [c])

Fill factors of this particular cell have different values ranging from 0.11 to 0.32.

S. Antohe, Chapter 11 „Electronic and Optoelectronic Devices Based on Organic Thin Films “ in *HANDBOOK OF ORGANIC ELECTRONICS AND PHOTONICS*, Electronic Materials and Devices, Edited by Hari Singh Nalwa, Volume 1 : Pages: 433, 440, AMERICAN SCIENTIFIC PUBLISHERS, Los Angeles, California, USA, 2007, ISBN : 1-58883-096-9



Table 3. The typical parameters of ITO/CuPc/(CuPc+TPyP)/TPyP/Al cells. **S. Antohe, V. Ruxandra, L. Tugulea, V. Gheorghe and D. Ionascu, *J. Phys. III France* 6, 1133 (1996), Copyright EDP Sciences (1996)**

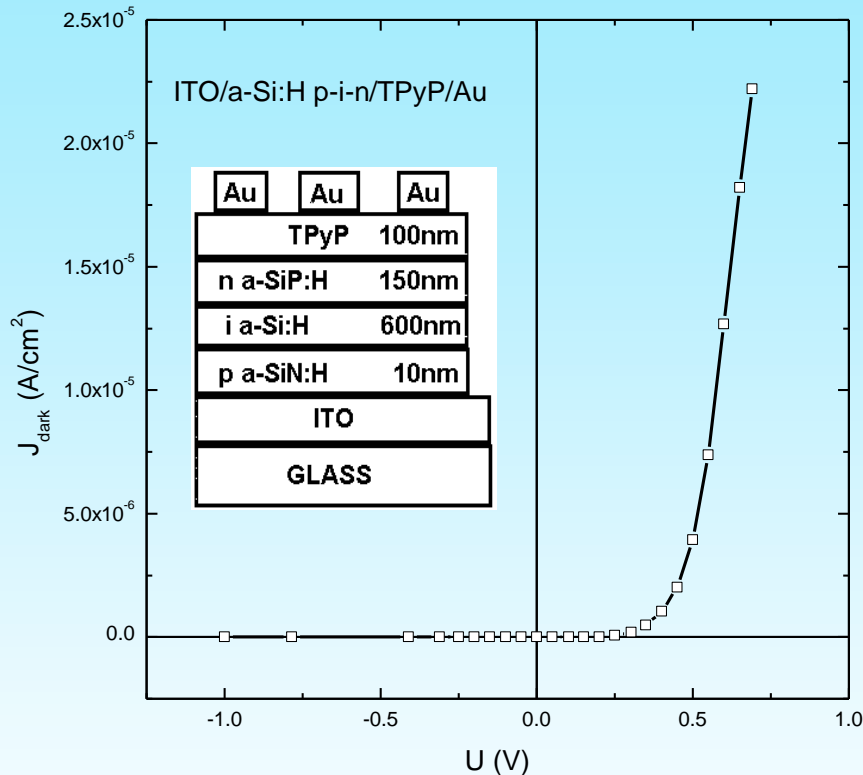
λ (nm)	Curve See Fig.	I'_{inc} ($\mu\text{W}/\text{cm}^2$)	J_{sc} (nA/cm^2)	U_{oc} (mV)	ff	η (%)
520	[a]	3	107	75	0.32	0.09
520	[b]	12	410	220	0.29	0.22
520	[c]	30	916	405	0.28	0.35
590	[a]	6	136	87	0.23	0.05
590	[b]	30	528	277	0.31	0.15
590	[c]	72	1250	350	0.11	0.07



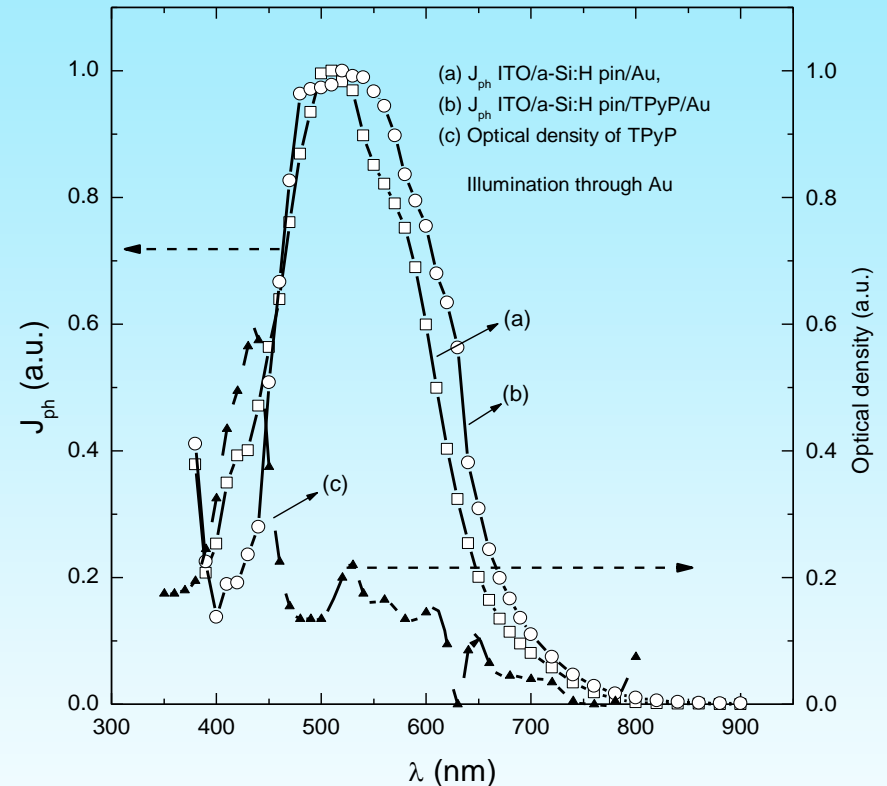
- As a conclusion, this new type of three-layered organic photovoltaic cells having a co deposited layer of (CuPc +TPyP), between the CuPc and TPyP films, clearly suggest an improvement, although modest, over two-layered cells.
- The co deposited interlayer, has been found to act as an efficient carrier photogeneration layer because: on the one hand, the built-in potential drops across it and, on the other hand, here there is the region of maximum photogeneration rate, as a result of exciton dissociation via the exciplex of (CuPc-TPyP+)^{*} dyes.
- The **fill factors of 0.11-0.32** represent an improvement over single and double-layered cells.
- Moreover, the **power conversion efficiencies of three-layered cells, ranging from 0.07 to 0.35%, are 2-3 times greater as compared to those for double-layered cells.**
- The thickness of about 400 nm of our three-layered cells is mainly responsible for the high internal resistance, which limits again the performances of the cells.
- By obtaining of an optimized structure as regarding the thickness of the layers and the architecture of the cells, substantial improvement of the organic photovoltaic cells would be possible.



Electrical and photovoltaic properties of photosensitized ITO/a-Si:H p-i-n/TPyP/Au cells



Cell configuration (inset) and current-voltage characteristics of ITO/a-Si:H p-i-n/TPyP/Au cell



Action spectra of short-circuit photocurrent of: (a) ITO/a-Si:H p-i-n/Au and (b) ITO/a-Si:H p-i-n/TPyP/Au cells. (c) Optical absorption spectrum of TPyP layer

S. Antohe, L. Ion, N. Tomozeiu, T. Stoica, E. Barna, *Solar Energy Materials & Solar Cells* 62, 207 (2000)



Photovoltaic Structures Based on Polymeric Materials: poly(3-hexylthiophene); 1-(3-methoxycarbonyl)-propyl-1-phenyl-(6,6) C_{61} and Their Blend P3HT:PCBM

- Enlarging the photoactive region in the case of three-layered structures an increased efficiency was obtained, due to the increased number of sites for exciton dissociation [4].
- Following the photovoltaic mechanism, an excitonic one, which takes place in this kind of cells, the structures based on polymeric blends, seem to be more promising for photovoltaic cells with relatively high efficiency about 4-5 %, but more cheap than the organic monomeric thin films [5].
- Polymer-fullerene bulk heterojunction solar cells have shown promising perspectives because of the high quality of these materials in terms of mobility and thermal stability [6-10].
- Here we present structural, morphological, electrical and photoelectrical properties of organic photovoltaic cell based on poly(3-hexylthiophene) [P3HT], 1-(3-methoxycarbonyl)-propyl-1-phenyl-(6,6) C_{61} [PCBM]
- We stress the differences observed for the devices based on single components and those fabricated from blend of the above polymers.



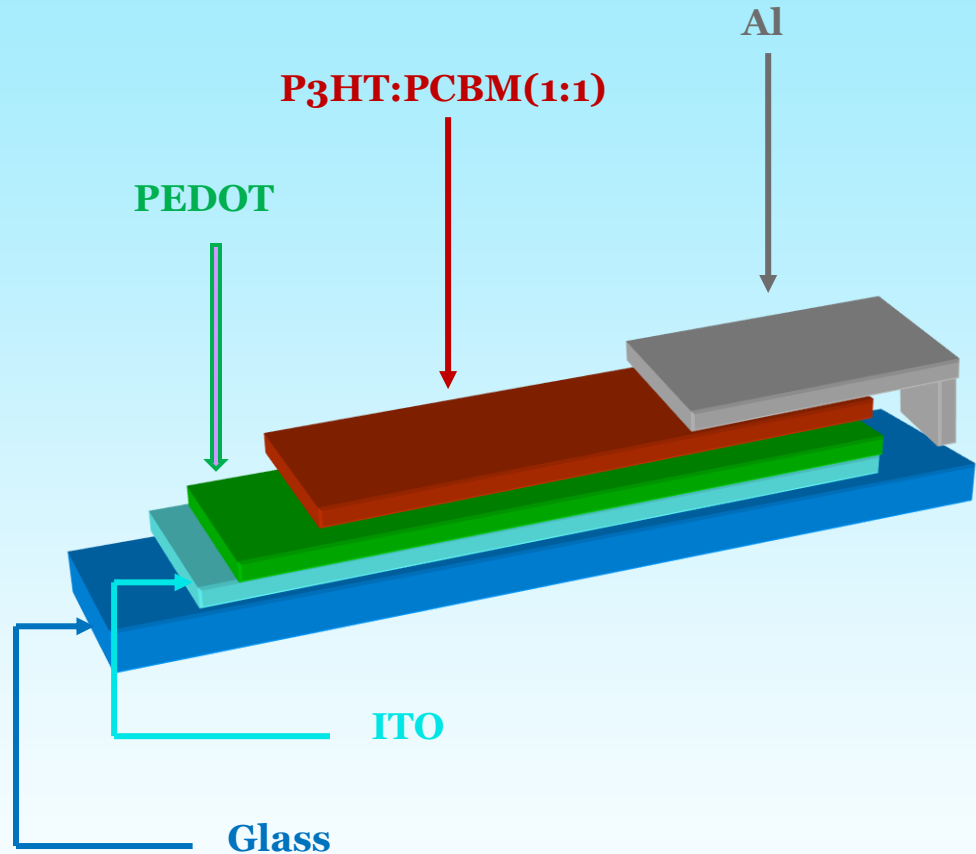
Sample preparation

- Photovoltaic cells based on polymer blends in the sequence

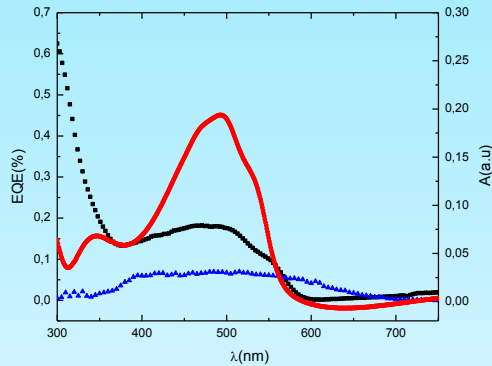
ITO/PEDOT/P3HT:PCBM(1:1)/Al

were prepared, using optical glass substrates covered with ITO , 300 nm thickness and $25 \Omega/\square$

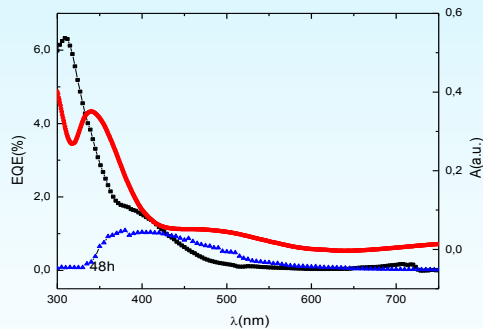
- PEDOT, P3HT and PCBM layers were deposited by spin-coating technique, while Al back electrode was deposited by thermal vacuum evaporation.



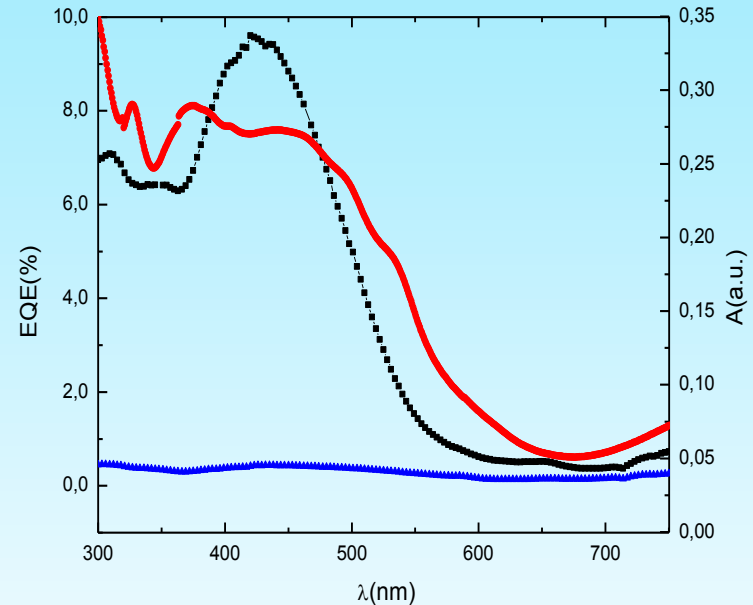
Action Spectra of: ITO/PEDOT/P3HT/Al , ITO/PEDOT/PCBM/Al, ITO/PEDOT/P3HT:PCBM (1:1)/Al structures and the Absorption Spectra of the organic absorbers



Photocurrent normalized to the power of the light source for ITO/PEDOT/P3HT/Al structure



Photocurrent normalized to the power of the light source for ITO/PEDOT/PCBM/Al structure



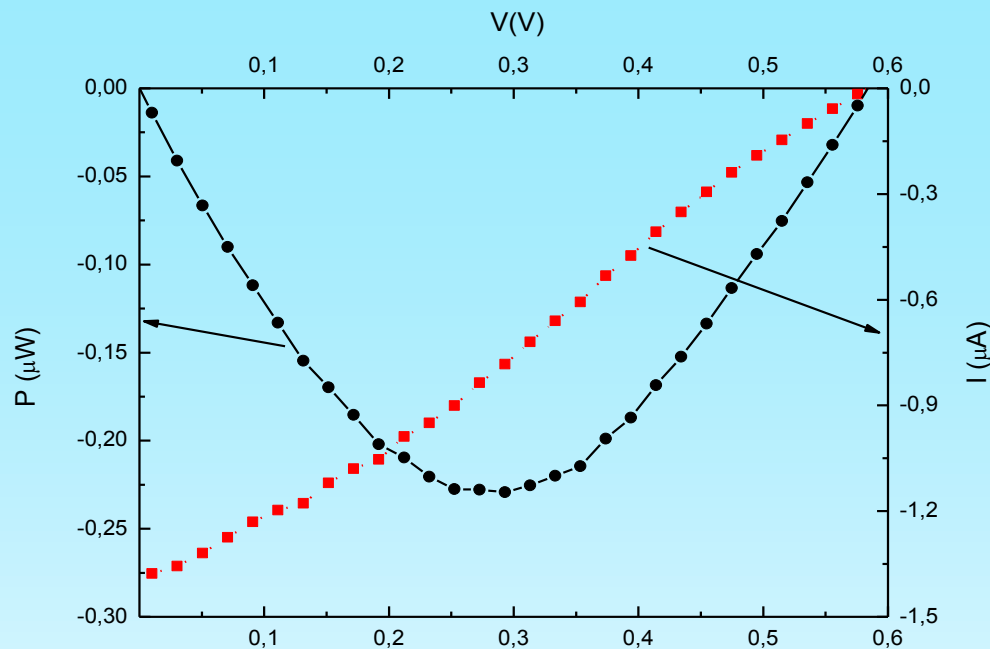
Photocurrent normalized to the power of the light source for ITO/PEDOT/P3HT:PCBM(1:1)/Al structure

Larisa Magherusan, Polona Skraba, Cristina Besleaga, Sorina Iftimie, Nicoleta Dina, Mirela Bulgariu, Carmen-Gabriela Bostan, C. Tazlaoanu, A. Radu, L. Ion, M. Radu, A. Tanase, G. Bratina, S. Antohe, **Journal of Optoelectronics and Advanced Materials, Vol. 12 , No. 2, February 18, 2010, p. 212-218**



- The absorption spectrum of the blend was enlarged from 300 nm until 700 nm, showing that the so called „*co - sensitization effect*” still exist in the case of blend structures like in the case of D/A bilayer cell, [13, 14].
- The action spectra are enlarged too, in the range (300-600 nm) with increased photocurrent,.
- The number of Donor/Acceptor (D/A) interfaces was significantly increased by blending the two donor and acceptor materials, giving rise to the so called „*bulk heterojunctions*”, in which the dimension of photon-capturing domain becomes on the same order of the average exciton diffusion lengths, (5 to 80 nm for most organic semiconductors).
- The larger D/A interface *reduces the exciton loss*, then the blend film *harvest more photons* than in the case of single P3HT or PCBM layer cells.
- *A stronger photo generation* take place in a blend, but *the carrier loss seem to be a major problem*, due to the fact that the charge carriers can be easily *trapped in the isolated phase donor or acceptor domains* which still coexist with the blend. More that, if the *donor and acceptor are in direct contact with both collector electrodes*, the *recombination of the non-equilibrium charge carriers* at the blend/electrode interfaces could be strong enough.
- The action spectra of blend structure, has an „*anti-batic*” behavior. Even though the energy offsets between Donor-LUMO and Acceptor –LUMO represent the key driving force for the exciton dissociation, then for the enhanced photocurrent in a blend structure, [15], the presence of the internal *electric field across the blend/electrode interfaces*, has an important contribution to the photovoltaic response, too, [16]. The observed anti-batic spectra, could be explained in terms of „*filtering effect*”.





The fourth quadrant I - V characteristic of the ITO/P3HT:PCBM (1:1)/Al device under illumination with 400 nm monochromatic light and

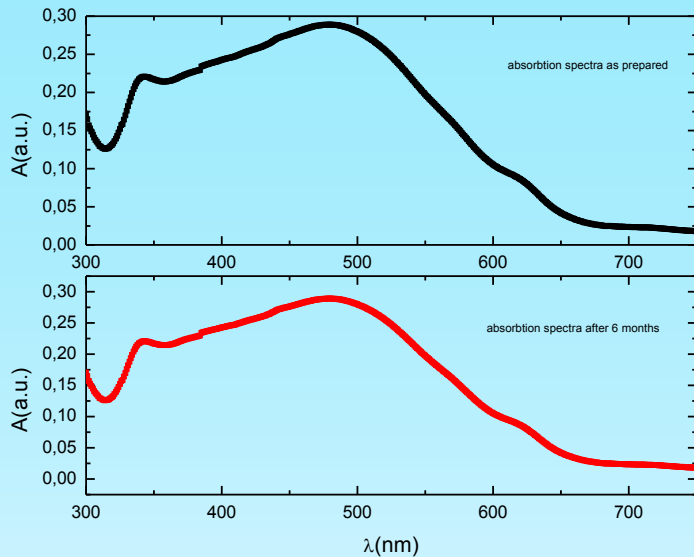
$$P_{in} = 5,19 \times 10^{-5} \text{ W}$$

	ITO/PEDOT/P3HT/Al	ITO/PEDOT/PCBM/Al	ITO/PEDOT/P3HT:PCBM(1:1)/Al
V_{oc} (V)	0.84	0.1	0.58
I_{ph} (A)	1.85×10^{-8}	4.1×10^{-8}	1.35×10^{-6}
P_m (W)	1.7×10^{-9}	5.88×10^{-10}	2.25×10^{-5}
P_{in} (W)	2.15×10^{-5}	3.3×10^{-5}	5.19×10^{-5}
FF (%)	10	14	28
η (%)	0.01%	0.0017%	0.44%

Larisa Magherusan, Polona Skraba, Cristina Besleaga, Sorina Iftimie, Nicoleta Dina, Mirela Bulgariu, Carmen-Gabriela Bostan, C. Tazlaoanu, A. Radu, L. Ion, M. Radu, A. Tanase, G. Bratina, **S. Antohe**,

Journal of Optoelectronics and Advanced Materials, Vol. 12, No. 2, February 18, 2010, p. 212-218



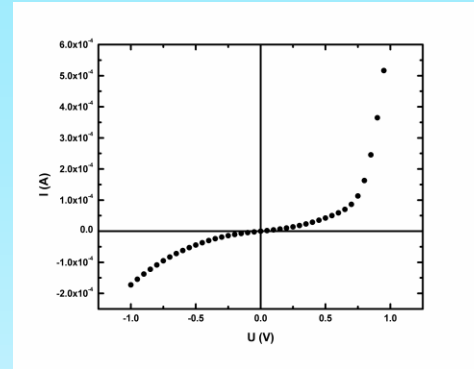
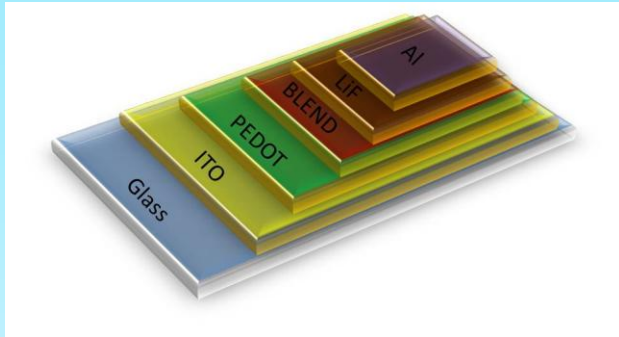


Absorption spectra of the blend P3HT:PCBM (1:1) layer as prepared (black line) and after 6 months (red line)

- **Very poor stability**
- **The action spectra measured after 2 hours and 48 hours from the Al contact deposition, respectively, showed a permanently decreasing of the photocurrent**
- **Trying to explain this behavior, the absorption spectra for all the polymeric layers (P3HT, PCBM, and P3HT: PCBM (1:1), respectively), were measured at different intervals of time.**
- **It do not appear changes in the above absorption spectra of the blend P3HT: PCBM (1:1) layer as prepared (black line) and after 6 months (red line), resulting that *no changes takes place in the optical processes giving rise to the excitons creation in these materials. But dramatically changes seem to be present in physical processes involved in the photo generation of the charge carriers, their separation and collection to the electrodes.***
- **Now, systematically studies are carried out, devoted to explain these processes in view to the increasing the stability of the promising photovoltaic structures.**

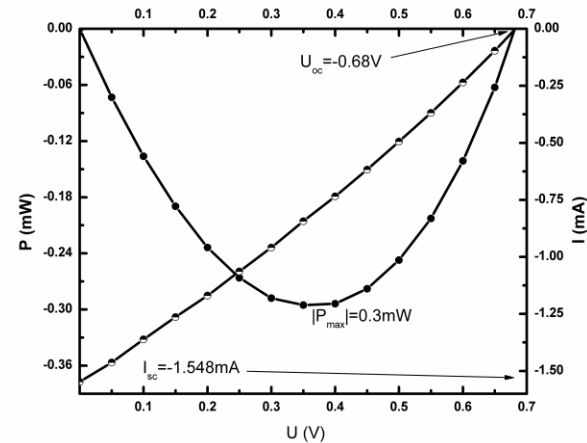
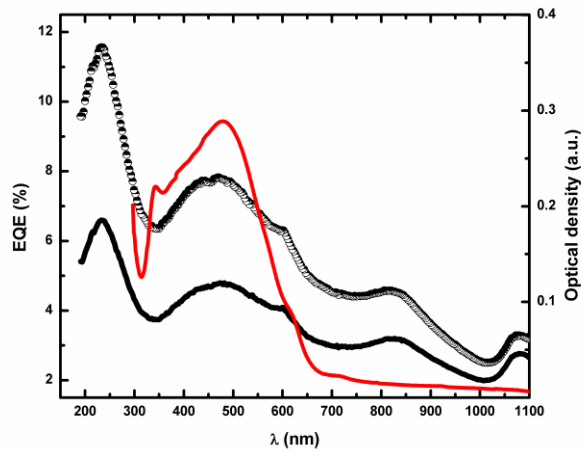


ITO/PEDOT/P3HT:PCBM(1:1)/LiF/Al



Structure of ITO/PEDOT/P3HT:PCBM(1:1)/LiF/Al

I-V dark characteristic



Absorption spectrum of ITO/PEDOT/P3HT:PCBM/LiF (red curve) and action spectra for as prepared sample (black/white curve) and after 24 hours (black curve)

The fourth quadrant I-V characteristic in A.M.1.5,

Sorina Iftimie, A. Majkic, Cristina Besleaga, V. A. Antohe, A. Radu, M. Radu, Iulia Arghir, Camelia Florica, L. Ion, G. Bratina, S. Antohe,

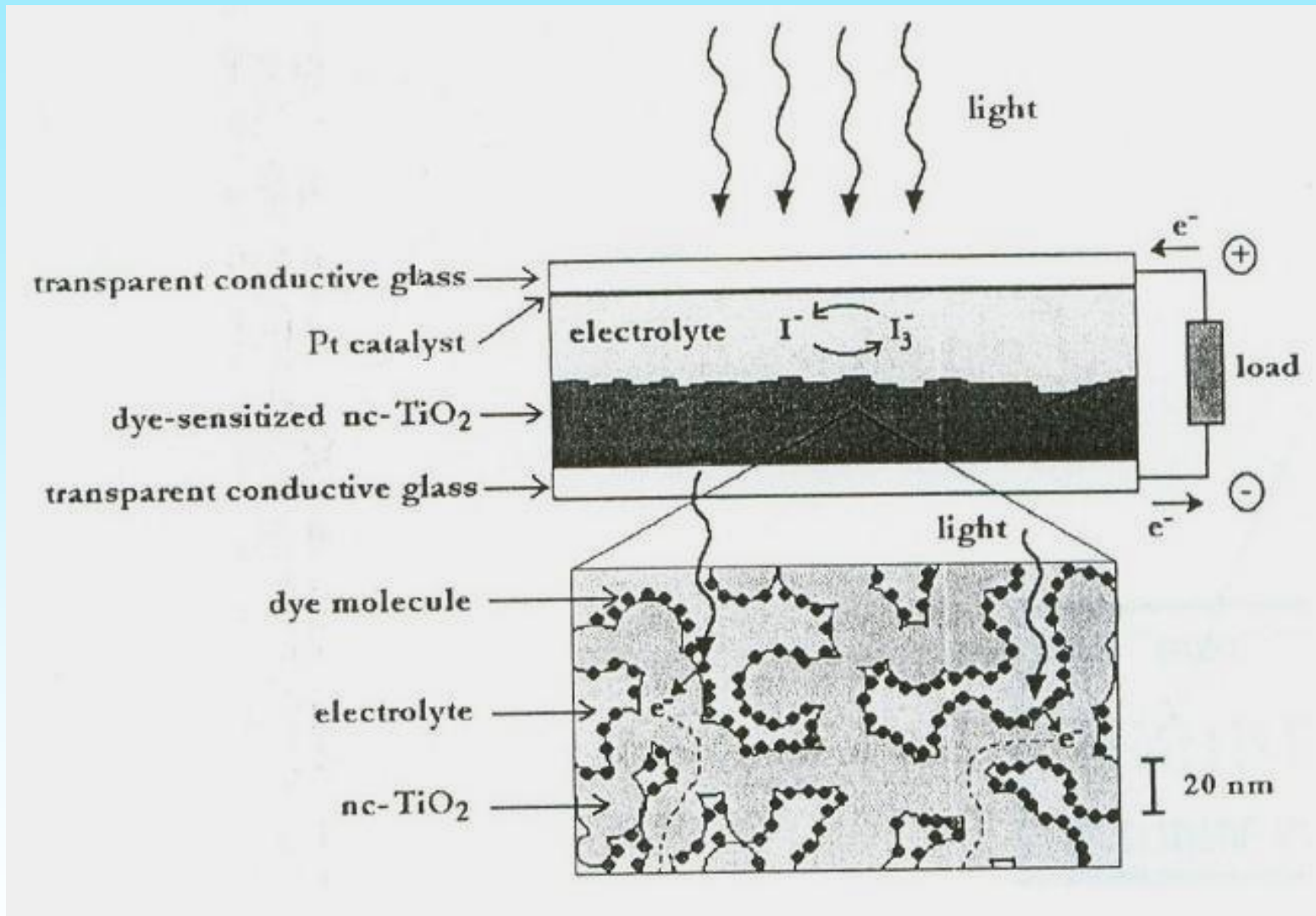
E-MRS 2010 Symposium L, in press at Thin Solid Films 2010



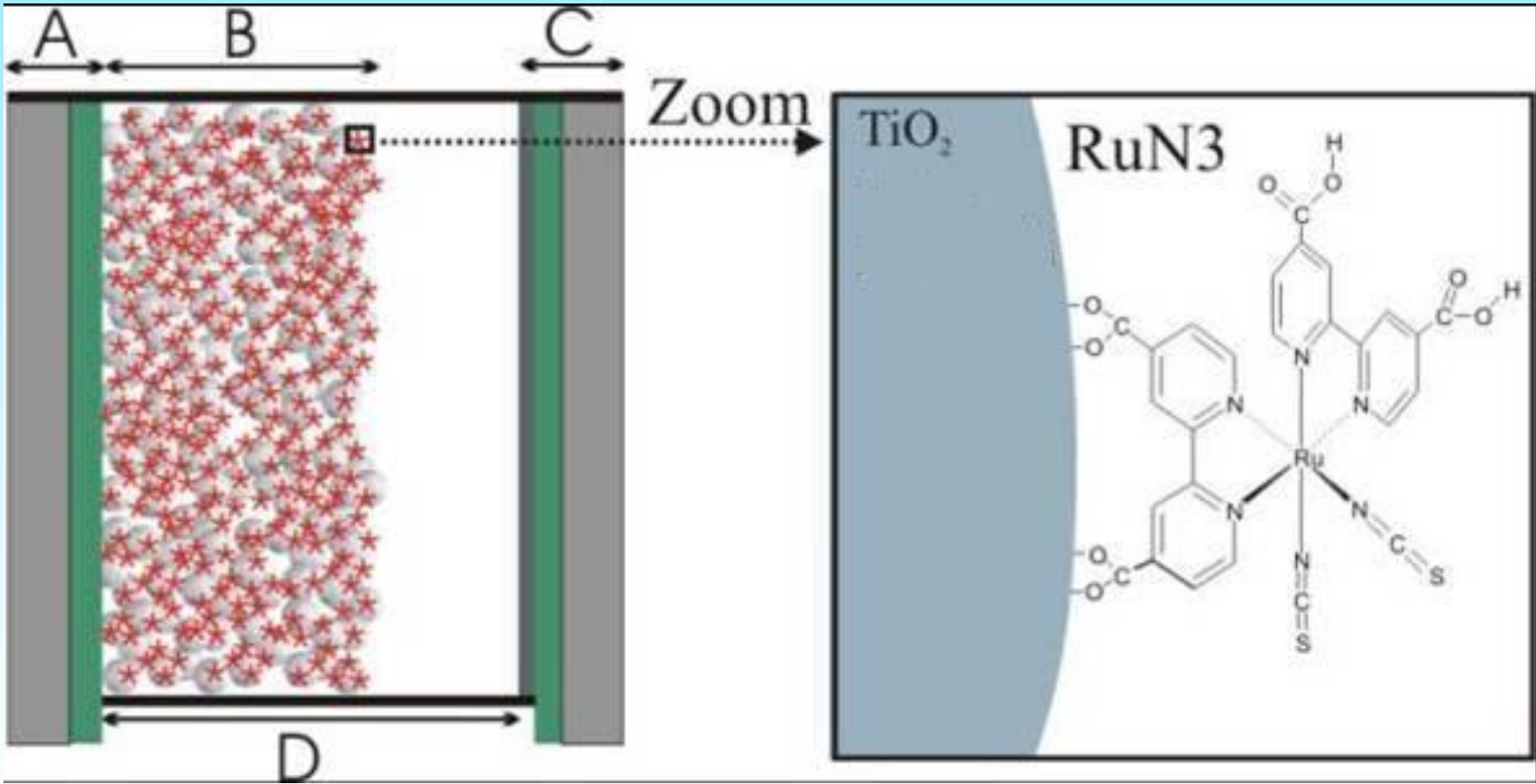
Hybrid Inorganic/Organic Structures for Photovoltaic Applications



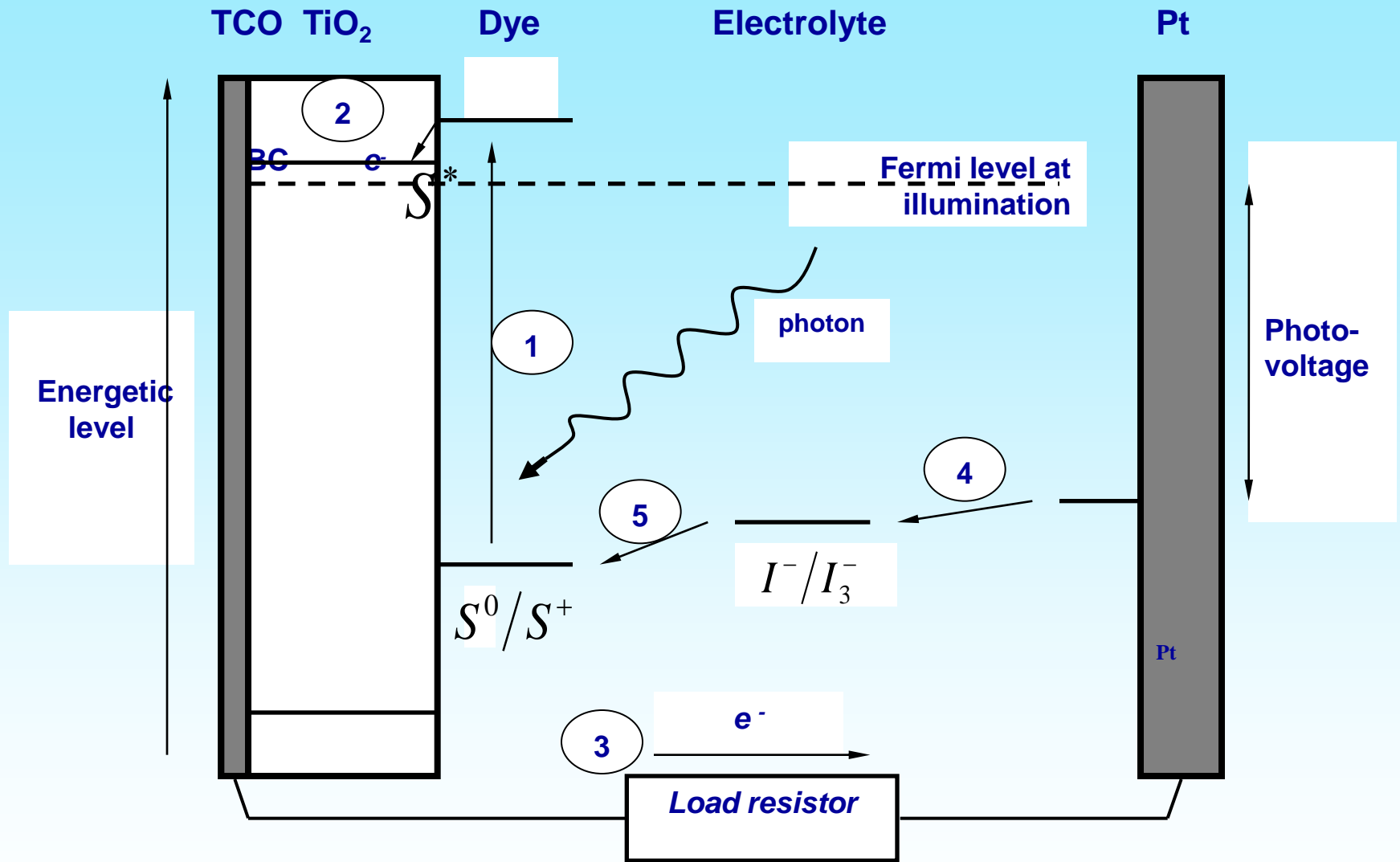
Dye Sensitized Solar Cells



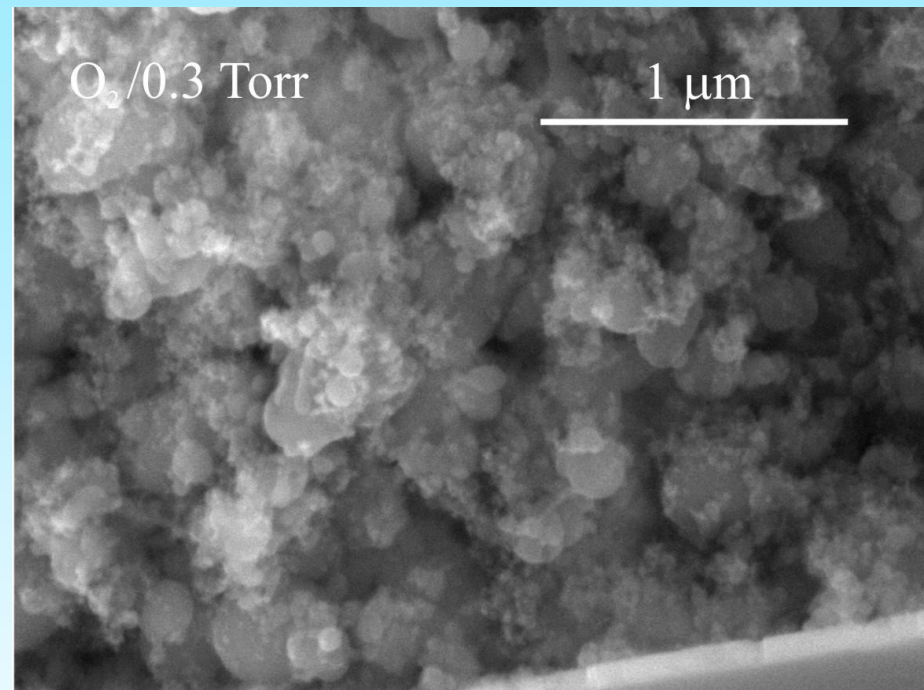
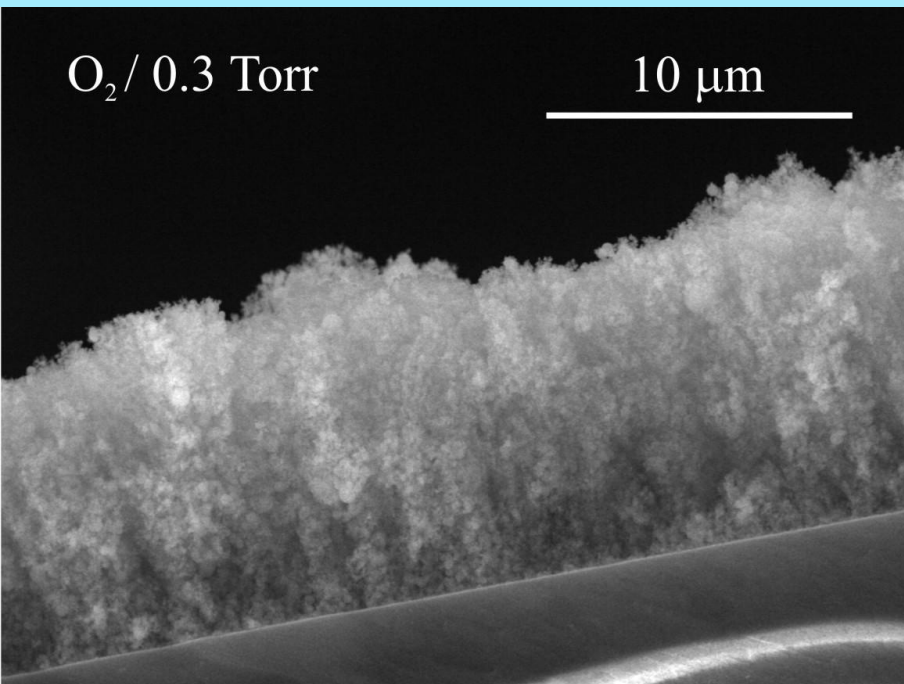
Dye Sensitized Solar Cells based on Nanostructured TiO_2 Thin Films



Dye Sensitized Solar Cells based on Nanostructured TiO_2 Thin Films



Dye Sensitized Solar Cells based on Nanostructured TiO₂ Thin Films



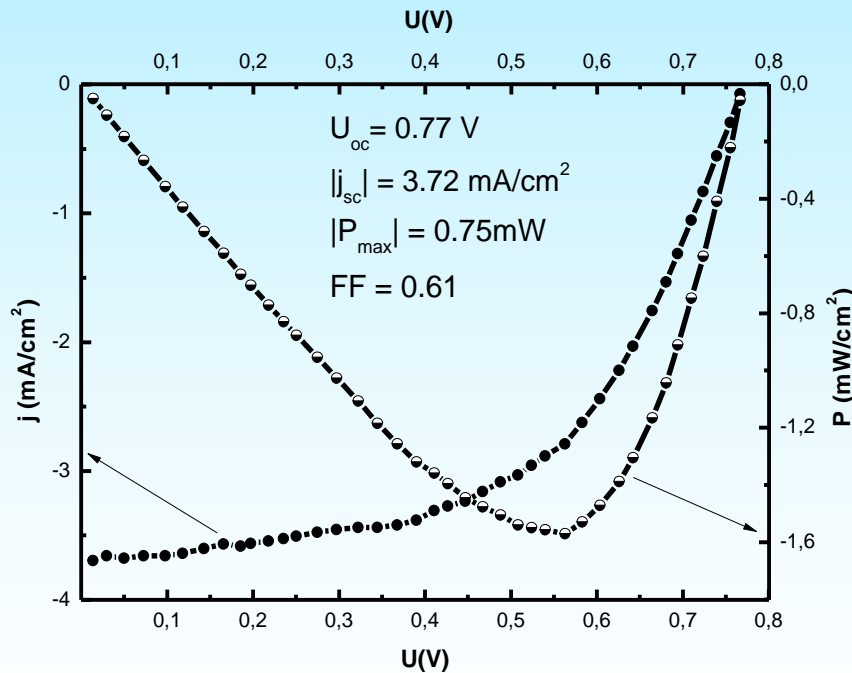
TiO₂ thin films were prepared by PLD technique using a Nd:YVO₄ laser (puls duration 8ps, $\lambda=532\text{nm}$, average power 1W, rate 50kHz, flux of 0.17J/cm²)

Cornelia Sima, C. Grigoriu, S. Antohe, **Thin Solid Films (2010), doi:10.1016/j.tsf.2010.07.002**



Cell	Oxygen pressure (Torr)	TiO ₂ film thickness (μm)	t (°C)	U _{oc} (mV)	j _{sc} (mA/cm ²)	P _{max} (mW)	η(%)
1	1	11.4	450	532	0.32	0.09	0.10
2	0.5	13.4	450	730	1.66	0.29	0.69
3	0.3	8.3	450	723	4.16	0.72	1.74
4	0.3	13.0	450	767	3.72	0.75	1.81
5	0.3	8.0	RT	488	0.83	0.07	0.16
6	0.04	5.7	450	348	0.41	0.03	0.07

The typical cell parameters in regim of photoelement of the cells based on TiO₂ nanostructured thin films deposited at different pressures and with diferent thickness



Current- Voltage (I-V) characteristics in fourth quadrant of a DSSC, based on TiO₂ electrode (thickness of 13 μm, oxygen pressure in the reaction chamber - 0.3Torr, thermal treatment at 450°C), under AM1.5. illumination conditions

Cornelia Sima, Constantin Grigoriu, Stefan Antohe **Thin Solid Films (2010)**, doi:10.1016/j.tsf.2010.07.002



Hybrid inorganic/organic structures – a route towards efficient and low-cost photovoltaic cells

- In the last decade hybrid structures, based on nanostructured inorganic materials and organic thin films have attracted a great deal of interest for producing low-cost solar cells.
- Among the organic semiconductors envisaged to be used in such structures, metal-doped phthalocyanines (MePc, with Me=Cu, Mg, Zn, etc.) are the most studied, due to their peculiar properties:
- Their optical absorption in the visible range of the solar spectrum is strong, but based on an excitonic mechanism. Most of the photogenerated excitons annihilate by direct recombination before the occurring of the charge separation in the internal field of the structure.
- This charge extraction problem can be avoided by creating a large area heterostructure at the interface with an inorganic semiconductor, where the photogenerated excitons will dissociate by electronic transfer.
- A typical value for the diffusion length of the exciton in organic semiconductors is of 30-80 nm, while in order to achieve the required efficiency in light absorption, the absorber layer has to be at least 100 nm thick.
- One way to improve the extraction of the charge carriers will consist in significantly increasing of the area of the interface between the two components of the heterostructure, then reducing the dimensions of D/A heterojunctions to the dimension of exciton diffusion length in the organic absorber.
- In this way the driving forces, due to potential difference between Donor LUMO and Acceptor LUMO, will acts efficiently for exciton dissociation and photo charge carrier generation, what is expected for the efficient fourth generation solar cells.



Problem: excitonic absorption mechanisms and charge extraction?

- Two kind of hybrid structures were prepared and characterized:
 - hybrid structures based on nanostructured ZnO electrode, photosensitized by CuPC, as organic absorber
 - hybrid structures based on CdTe wires arrays/ZnPc or TPyP
- Three type of hybrid structures based on ZnO electrodes:
 - *Nanostructured ZnO thin films/CuPc*
 - *ZnO wires aray/CuPc*
 - *ZnO hexagonal column array/CuPc*
- For **second type**, a template method has been used to produce quasi-one-dimensional (q-1D) nanostructured systems based on CdTe. *The hybrid cells, based on the heterostructure at the interface between wire array of CdTe, and the organic film ZnPc and TPyP, were produced and characterized.*



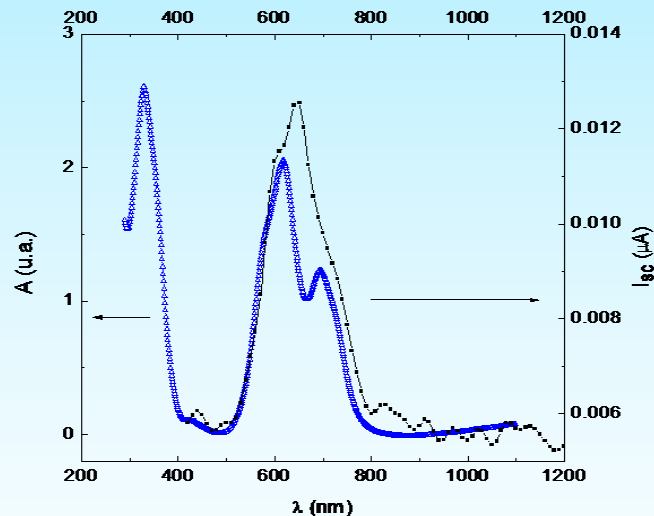
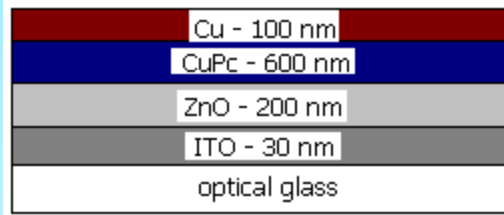
Physical properties of ZnO

- Large optical absorption coefficient;
- Wide and direct band gap of 3.37 eV;
- Very large exciton binding energy (60 meV);
- Good chemical stability;
- Very large piezoelectric coefficients;
- Good candidate for spintronics applications



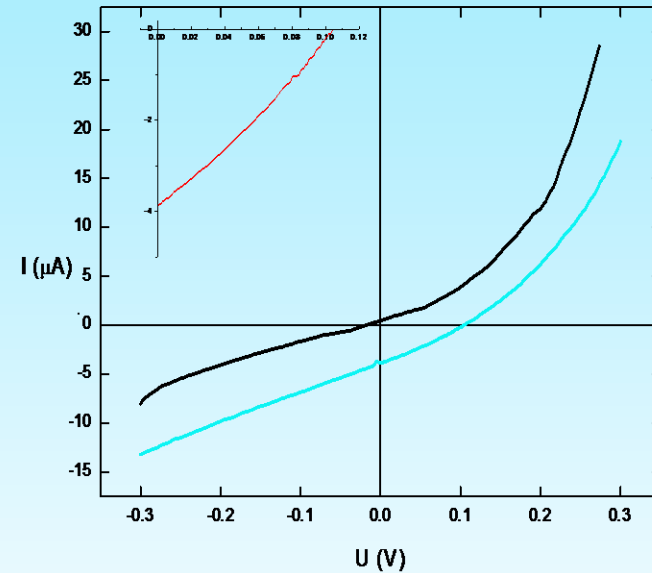
Layered structures based on nanostructured ZnO films and CuPc as organic absorber

ITO/ZnO/CuPc/Cu



Configuration of ITO/ZnO/CuPc/Cu cell (a) and absorption spectrum of CuPc film (up-triangles) and action spectrum of short-circuit photocurrent (filled squares) (b)

(a)



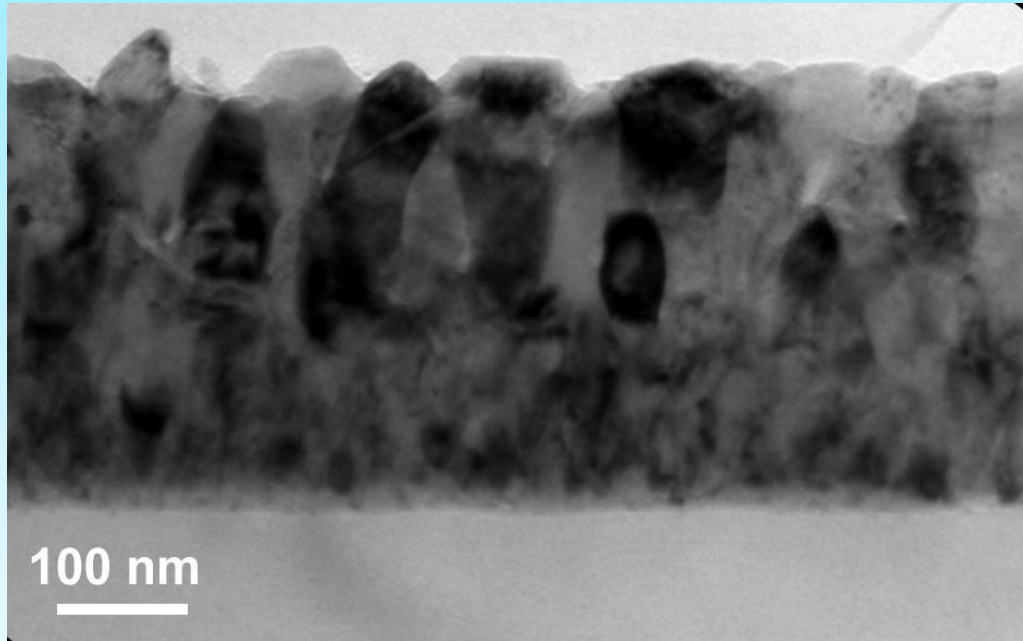
(b)

I-U characteristics of ITO/ZnO/CuPc/Cu cell, recorded in dark (black curve) and under illumination with monochromatic light (660 nm) (red curve)

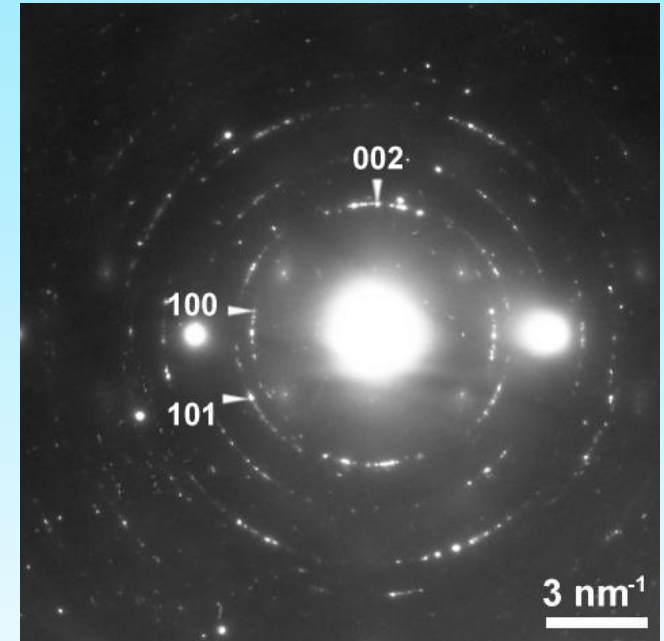
S. Antohe, L. Ion, C. Tazlaoanu, G. Socol, L. Magherusan, I. Enculescu, D. Bazavan, I.N. Mihailescu, and V.A. Antohe, MRS Spring Meeting 2007, SUA, Symp. Z 4.9, pg. 538



Layered structures based on nanostructured ZnO films and CuPc as organic absorber



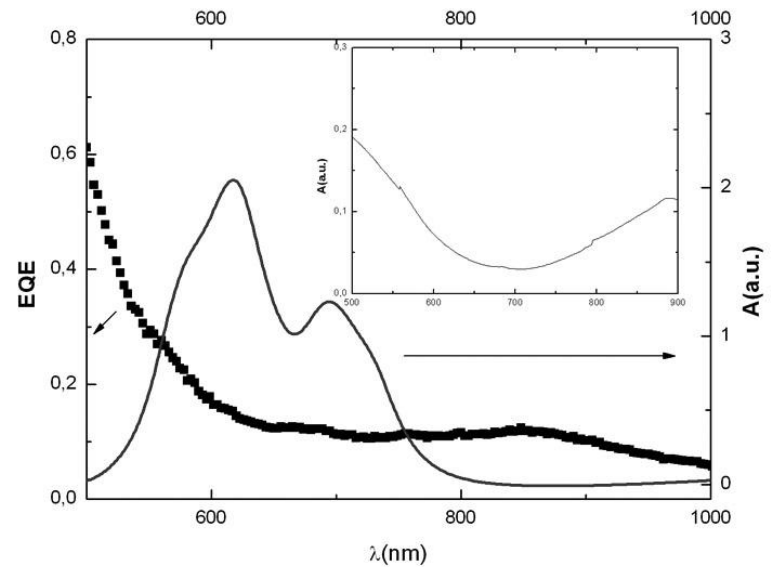
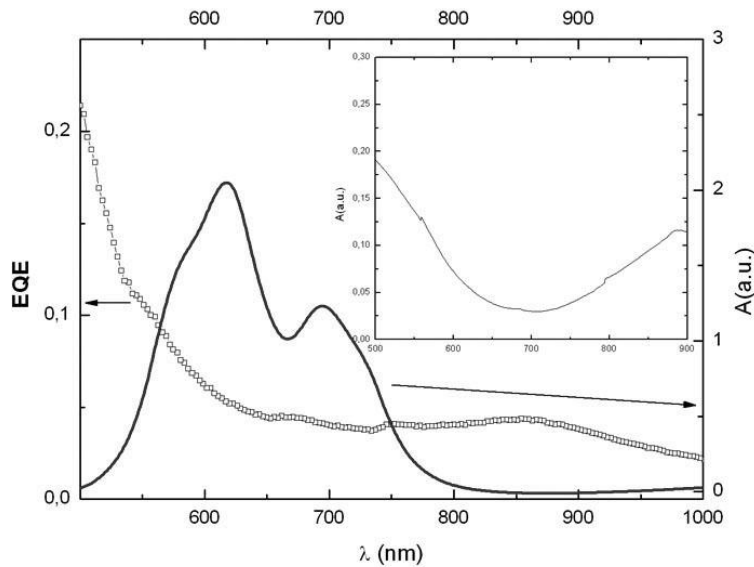
XTEM image of AZO thin film



SAED pattern of an AZO thin film

C.Ghica, L. Ion, G. Epurescu, L. Nistor, S. Antohe, M. Dinescu, **Journal of Nano-science and Nanotech-nology**, volume 10, Number 2, February 2010, pp. 1322-1326 (5)





Spectral dependence of the external quantum efficiency (EQE) of the Al/CuPc/ZnO/glass structure in the case of the ZnO385 layer (a) and the ZnO388 layer (b). The solid line shows the absorption spectrum of CuPc. The absorption spectrum of the ZnO layer is shown in the inset.

The EQE in the Q region of the CuPc absorbent (500-800 nm), measures 6-10% for sample 385. At higher photon energies, the photo generation processes take place both in CuPc and ZnO, increasing EQE up to 30% at wavelengths below 500 nm. In case of sample 388, the EQE value raises up to 14-25% in the spectral range corresponding to the CuPc absorption Q-band.

In the two analyzed cases, the difference consists in the PLD deposition parameters for the AZO films growth. The increased oxygen pressure in the case of sample 388 lead to an AZO film with an increased surface roughness, determining a higher value for the EQE. The explanation comes from two aspects: a rough interface means a higher photoactive area and a better collection efficiency at the AZO electrode; the rough interface determines diffuse scattering of light incident on this interface back into the CuPc absorbing layer, increasing the absorption efficiency.

C.Ghica, L. Ion, G. Epurescu, L. Nistor, S. Antohe, M. Dinescu, **Journal of Nanoscience and Nanotechnology**, volume 10, Number 2, February 2010, pp. 1322-1326 (5)



Layered structures based on nanostructured ZnO films and CuPc as organic absorber

1) Nanostructured ZnO thin films were deposited on optical glass substrates *by pulsed laser deposition* (PLD), their structure and morphology being optimized for photovoltaic applications.

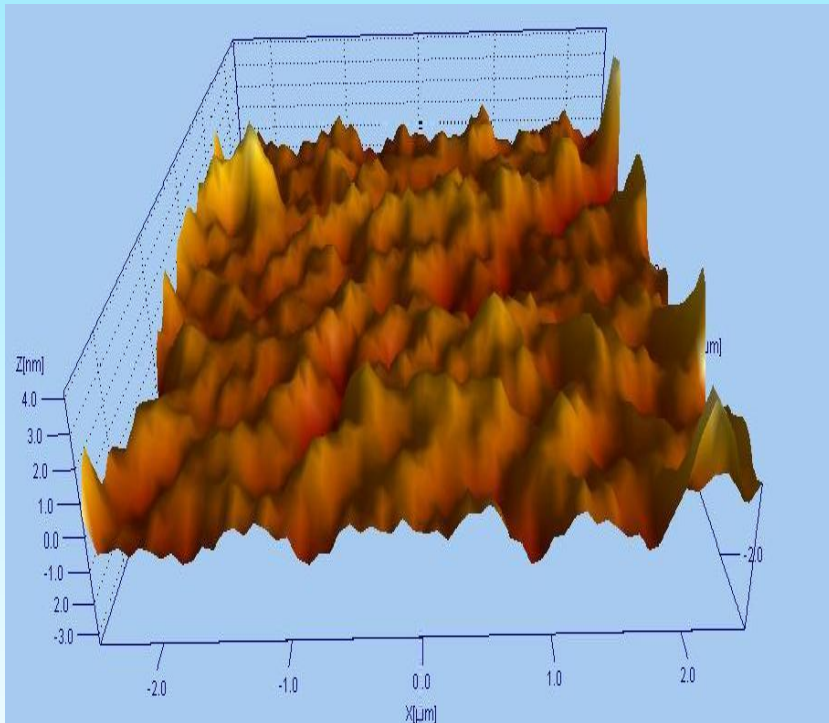


Image of the plasma during PLD deposition

Sample	Target	Temperature (°C)	Pressure (mbar)	Fluence (mJ/cm ²)	Distance (cm)	Thickness (nm)
ZnO_1	In ₂ O ₃ :ZnO (10%)	500	5	1,6	5	513
ZnO_2	In ₂ O ₃ :ZnO (3%)	500	5	1,6	5	430

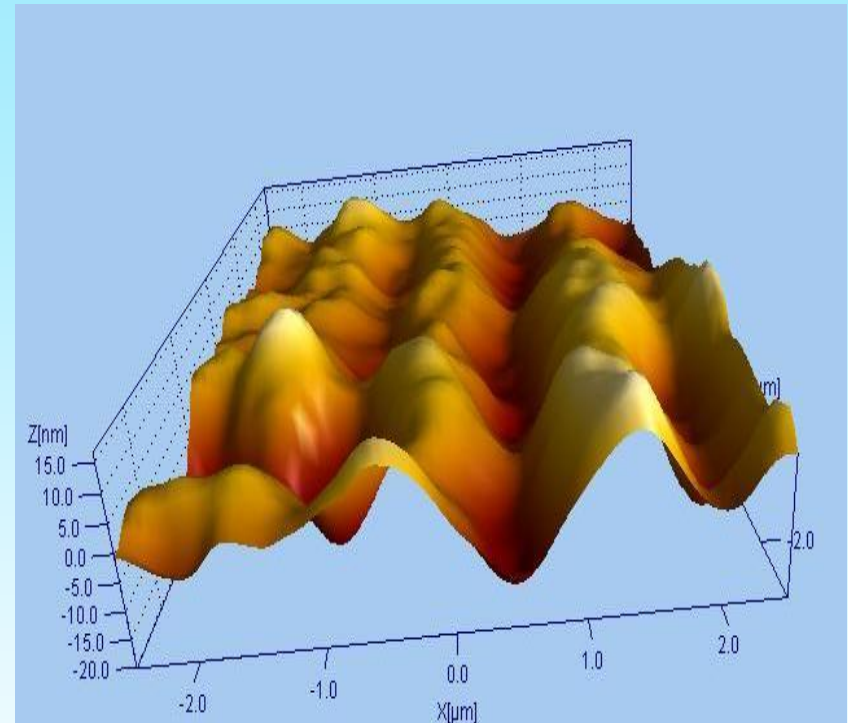


Morphological analysis of the samples by AFM, revealed that the films have low roughness.



AFM image of ZnO_1 sample.

with 7 nm roughness



AFM image of ZnO_2 sample.

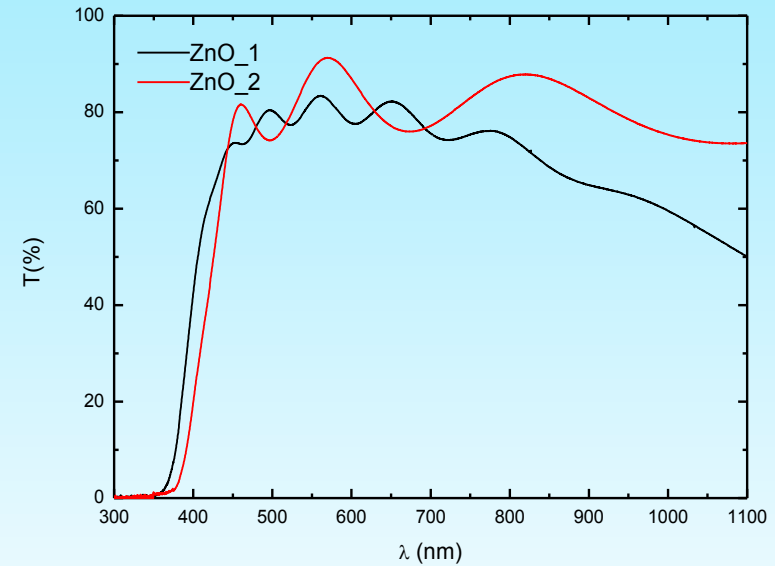
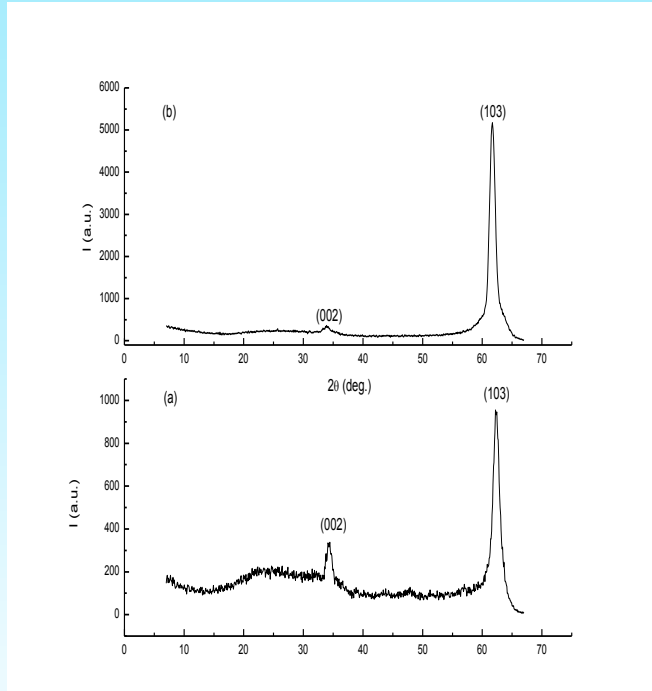
with 10 nm roughness

S. Antohe, I. Enculescu, Cristina Besleaga, Iulia Arghir, V. A. Antohe, V. Covlea, A. Radu, L. Ion, **2010 Ceramics Engineering&Science proceedings (CESP), Volume 31, Issue 7 „Nanostructured Materials and Nanotechnology IV”, pg.71-83, Volume Editors Sanjay Mathur and Tatsuki Ohji, Wiley, ISBN 978-0-470-93495-1**



□ Structural analysis of the samples by X-ray diffraction, revealed that the films consist of a hexagonal-close packed wurtzite type phase ZnO. (002) preferentially oriented in the growth direction,

ZnO films transparency was investigated in the visible region of solar spectrum



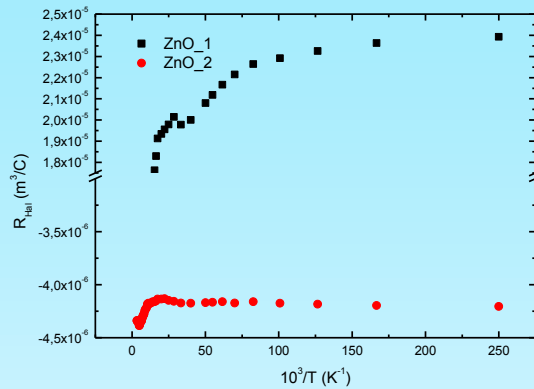
X-ray Diffraction pattern of: (a) ZnO:In₂O₃ (10%), (b) ZnO:In₂O₃ (3%), films

Transmission spectra at room temperature.

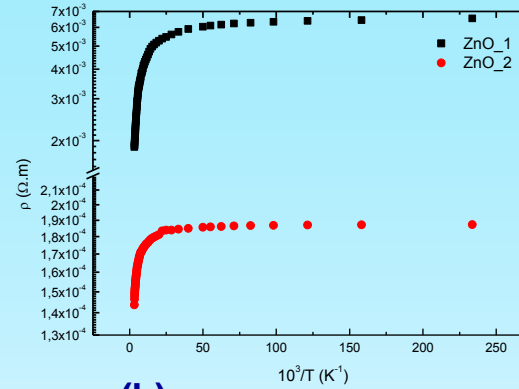
S. Antohe, I. Enculescu, Cristina Besleaga, Iulia Arghir, V. A. Antohe, V. Covlea, A. Radu, L. Ion, **2010 Ceramics Engineering&Science proceedings (CESP), Volume 31, Issue 7 „Nanostructured Materials and Nanotechnology IV”, pg.71-83, Volume Editors Sanjay Mathur and Tatsuki Ohji, Wiley, ISBN 978-0-470-93495-1**



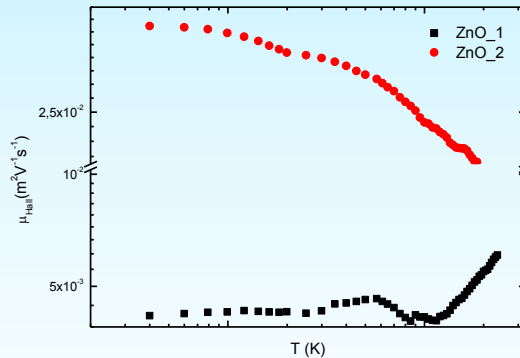
Electrical measurements



(a)



(b)



(c)

Sample	Conduction Type	μ_{Hall} ($\text{m}^2\text{V}^{-1}\text{s}^{-1}$)	E_a (eV)
ZnO_1	electrons (n)	6.2×10^{-3}	0.04
ZnO_2	holes (p)	2.2×10^{-2}	0.07

Temperature dependence of (a) Hall constant (a); resistivity (b); mobility

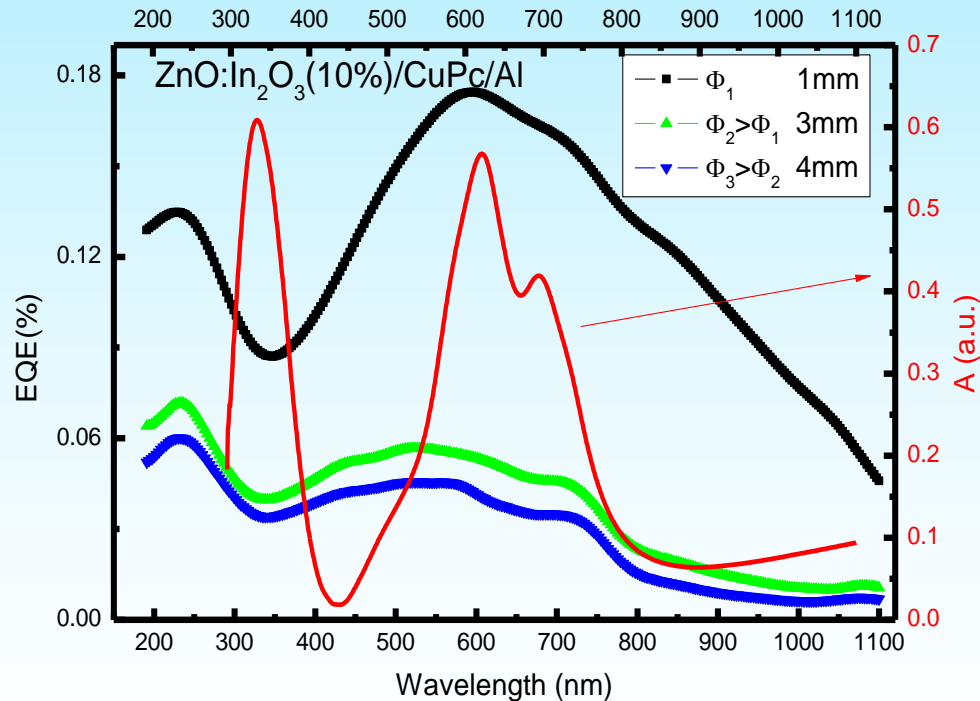


Photovoltaic response of the ZnO:In₂O₃ (10%)/CuPc/Al cell

EQE measured under illumination with monochromatic light, is given by:

$$EQE(\lambda) = \frac{I_{sc}(\lambda)hc}{q\lambda P_{\lambda}}$$

where: P_{λ} is the incident light power, $I_{sc}(\lambda)$ is the short-circuit current, q is the elemental charge, h is Planck's constant, c – speed of light.

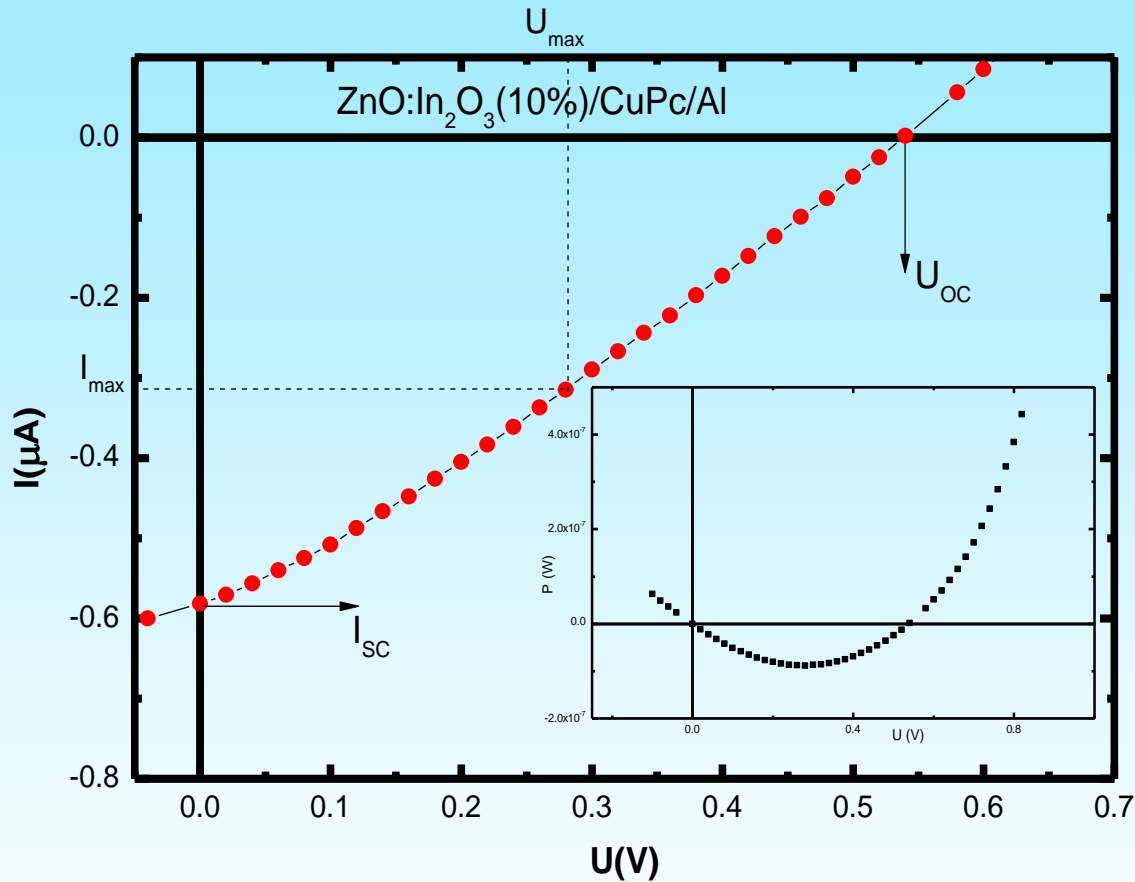


EQE characteristics (dark curve) and absorption spectrum (red curve) for a ZnO/CuPc/Al photovoltaic cell

S. Antohe, I. Enculescu, Cristina Besleaga, Iulia Arghir, V. A. Antohe, V. Covlea, A. Radu, L. Ion, **2010 Ceramics Engineering&Science proceedings (CESP), Volume 31, Issue 7 „Nanostructured Materials and Nanotechnology IV”, pg.71-83, Volume Editors Sanjay Mathur and Tatsuki Ohji, Wiley, ISBN 978-0-470-93495-1**



Photovoltaic response of the ZnO:In₂O₃ (10%)/CuPc/Al cell



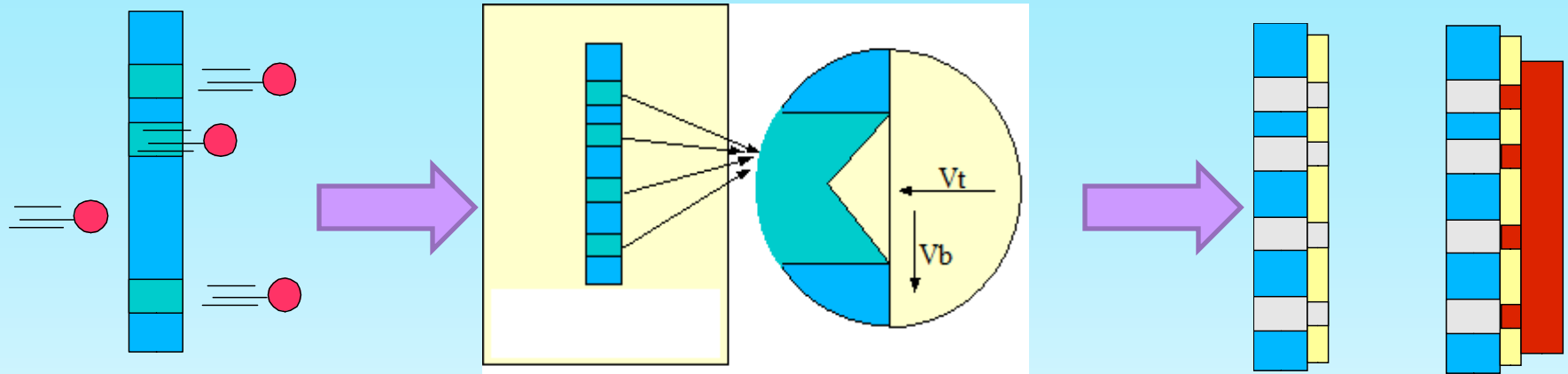
S. Antohe, I. Enculescu, Cristina Besleaga, Iulia Arghir, V. A. Antohe, V. Covlea, A. Radu, L. Ion, **2010** **Ceramics Engineering&Science proceedings (CESP), Volume 31, Issue 7 „Nanostructured Materials and Nanotechnology IV”, pg.71-83, Volume Editors Sanjay Mathur and Tatsuki Ohji, Wiley, ISBN 978-0-470-93495-1**

Current-voltage characteristics for ZnO:In₂O₃(10%)/CuPc/Al photovoltaic cell in the fourth quadrant under AM1.5 illumination (FF=25%), $\eta = 0.03\%$



ZnO Wire Array/CuPc Structures

Growth method of wires arrays using a nuclear track etched polycarbonate membrane as template

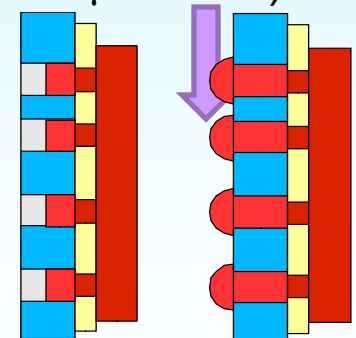


1. Irradiation of the template, (polycarbonate foils -Makrofol N, Bayer, 30 μm thick), with heavy ions (e.g. U, 11.4 MeV/nucleon, at different fluences in the range $10^4 - 10^8$ ions/cm²)

2. Chemical etching of the template (aqueous solutions of 5M NaOH and 10% volume methanol at 50°C. Etching rate of only 200 nm/h allows a good control of the diameter of the created cylindrical pores.

4. ZnO wires deposition

3. Working electrode deposition (Au layer, 50 nm + Cu layer, 10 μm thick)

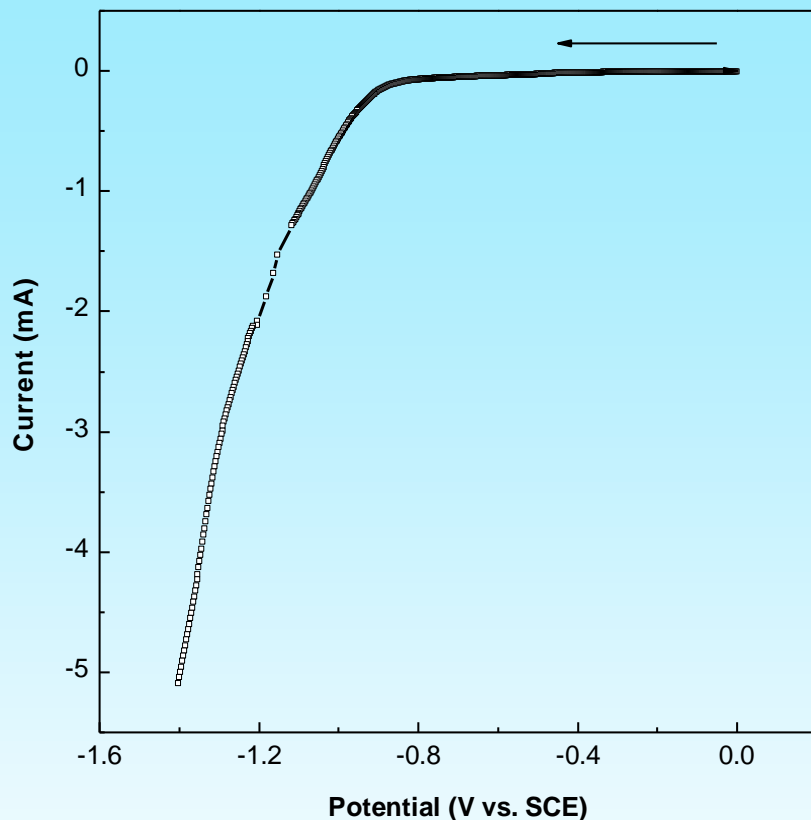


Preparation of multisegment Ni, ZnO, Ni wires

- The electrochemical deposition was performed using a VoltaLab potentiostat controlled by a computer.
- Nickel was deposited at 60°C using a Watts bath.
- ZnO was deposited from a 0.1M Zn(NO₃)₂ aqueous solution at 90°C.
- A three electrode configuration was used with a platinum counterelectrode and a commercial **saturated calomel electrode (SCE)** as reference.
- The following electrode reactions occur during the deposition of the ZnO segments [17]:
 - $2e^- + \text{NO}_3^- + \text{H}_2\text{O} \rightarrow \text{NO}_2^- + 2\text{OH}^-$ (1)
 - $\text{Zn}_2^+ + 2\text{OH}^- \rightarrow \text{Zn}(\text{OH})_2 \rightarrow \text{ZnO} \downarrow + \text{H}_2\text{O}$ (2)
- The deposition potential was chosen at -0.8 V vs. (SCE).

I. Enculescu, M. Sima, M. Enculescu, M. Enache, L. Ion, S. Antohe, R. Neumann, **Phys. stat. solidi (b)**, **244**, 1607 (2007).

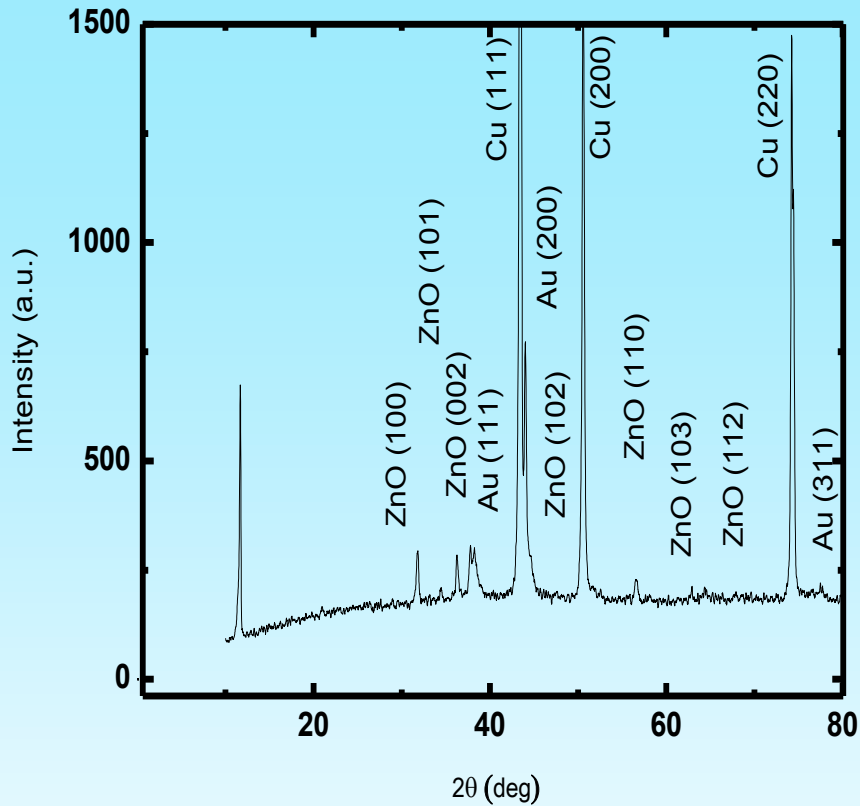




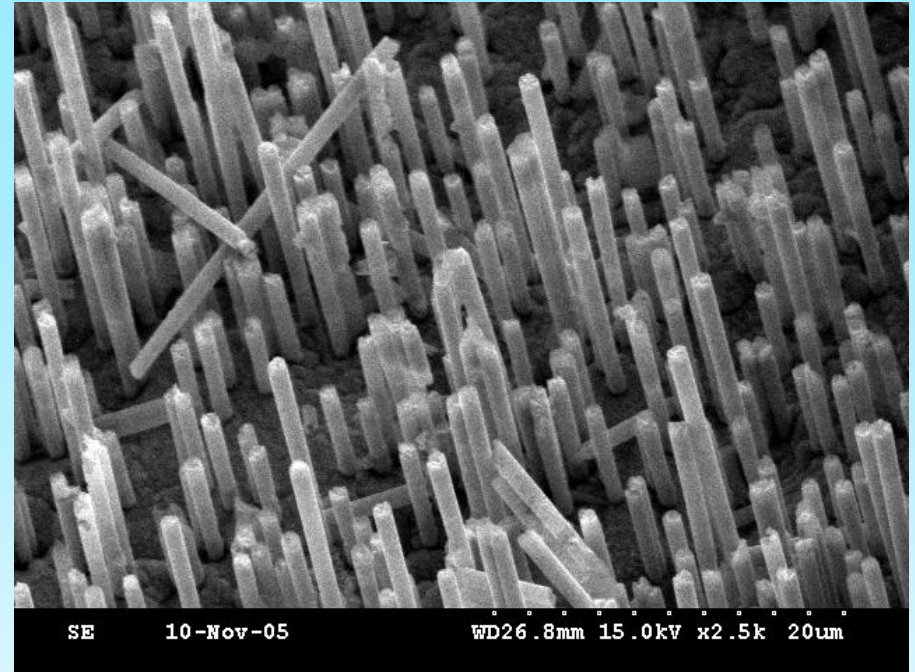
- Voltammetric curve recorded for Au/polycarbonate electrode (0.5 cm² surface) at 89°C in 0.1M Zn(NO₃)₂ solution. The potential scanning rate was 5 mV/s.

C. Tazlaoanu, L. Ion, I. Enculescu, M. Sima, Elena Matei, R. Neumann, Rosemary Bazavan, D. Bazavan, S. Antohe, **Physica E: Low-dimensional Systems and Nanostructures, Vol 40/7 pp 2504-2507, 2007**





XRD spectrum of ZnO nanowire array showing wurtzite type crystalline structure

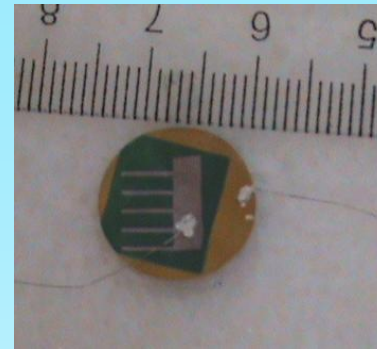
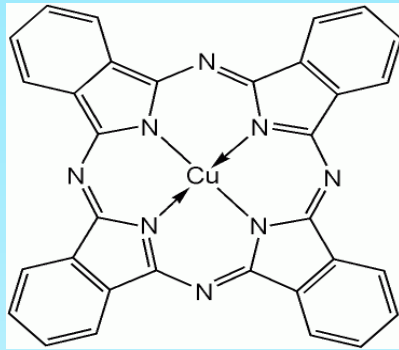


SEM image of ZnO wire arrays

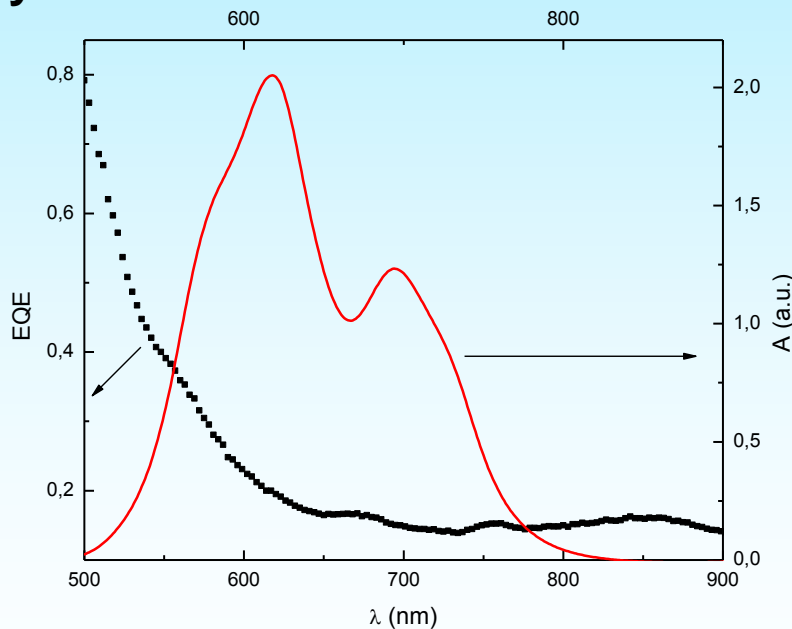
C. Tazlaoanu, L. Ion, I. Enculescu, M. Sima, Elena Matei, R. Neumann, Rosemary Bazavan, D. Bazavan, S. Antohe, [Physica E: Low-dimensional Systems and Nanostructures, Vol 40/7 pp 2504-2507, 2007](#)



Photovoltaic response of the ZnO wire arrays/CuPc/Al cell



Molecular Structures of CuPc and an Image of the ZnO wire array/CuPc/Al cell



EQE characteristics (dark curve) and absorption spectrum (red curve) for a ZnO(nws)/CuPc/Al photovoltaic cell based on ZnO wire array.

S. Antohe, I. Enculescu, Cristina Besleaga, Iulia Arghir, V. A. Antohe, V. Covlea, A. Radu, L. Ion, 2010 Ceramics Engineering&Science proceedings (CESP), Volume 31, Issue 7 „Nanostructured Materials and Nanotechnology IV”, pg.71-83, Volume Editors Sanjay Mathur and Tatsuki Ohji, Wiley, ISBN 978-0-470-93495-1



ITO/ZnO hexagonal column array / CuPc/Al

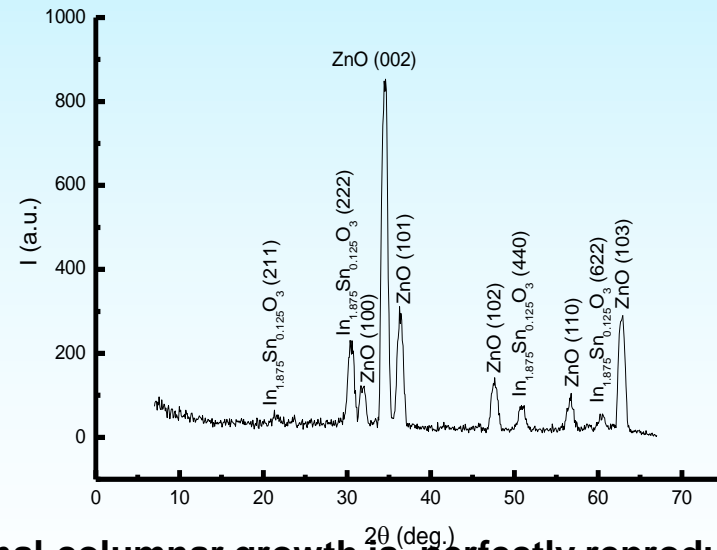
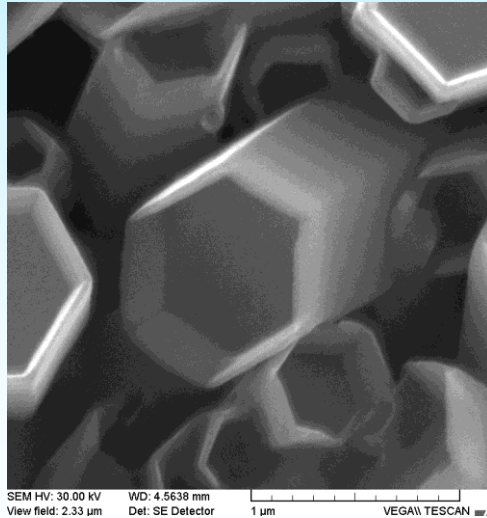
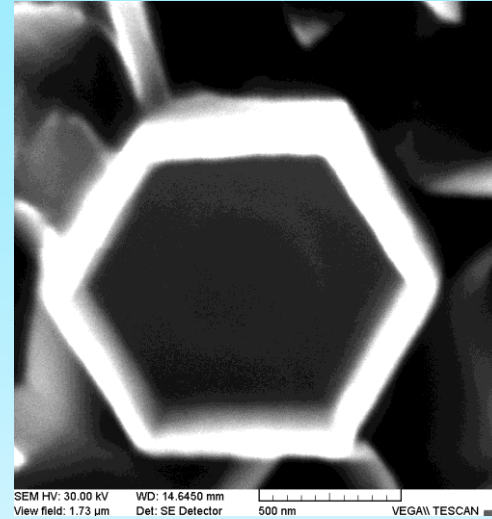
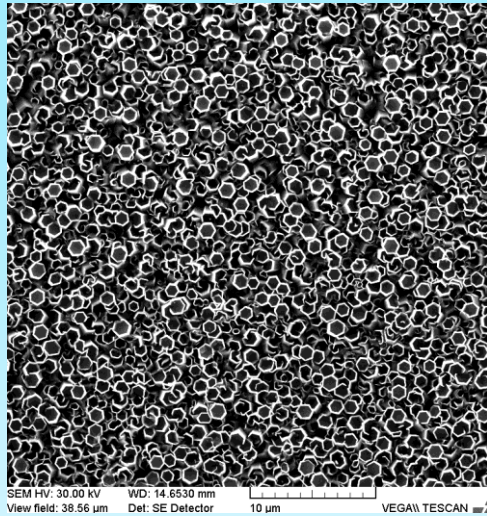
Preparation of ZnO nanotubes

- The electrochemical deposition was performed on a 90 nm ITO covered optical glass, using a VoltaLab potentiostat controlled by a computer.
- A three electrode configuration was used with a platinum counter electrode, a commercial **saturated calomel electrode (SCE)** as reference and ITO as working electrode.
- ZnO was deposited from a 0.1M $\text{Zn}(\text{NO}_3)_2$ aqueous solution at 90°C.
- The deposition potential was chosen at **-850 mV** vs. (SCE).
- The following electrode reactions occur during the deposition of the ZnO segments [17]:
- $2e^- + \text{NO}_3^- + \text{H}_2\text{O} \rightarrow \text{NO}_2^- + 2\text{OH}^-$ (1)
- $\text{Zn}_2^+ + 2\text{OH}^- \rightarrow \text{Zn}(\text{OH})_2 \rightarrow \text{ZnO} \downarrow + \text{H}_2\text{O}$ (2)

Cristina Besleagă, Iulia Arghir, Camelia Florica, T.L. Mitran, Elena Matei, I. Enculescu, N. Dina, L. Ion, (*)S. Antohe, Manuscript Number: MSB-D-09-01352R1, accepted to be published in **Materials Science and Engineering B, 2010**



Nano-engineered ZnO thin films / CuPc/Al structures



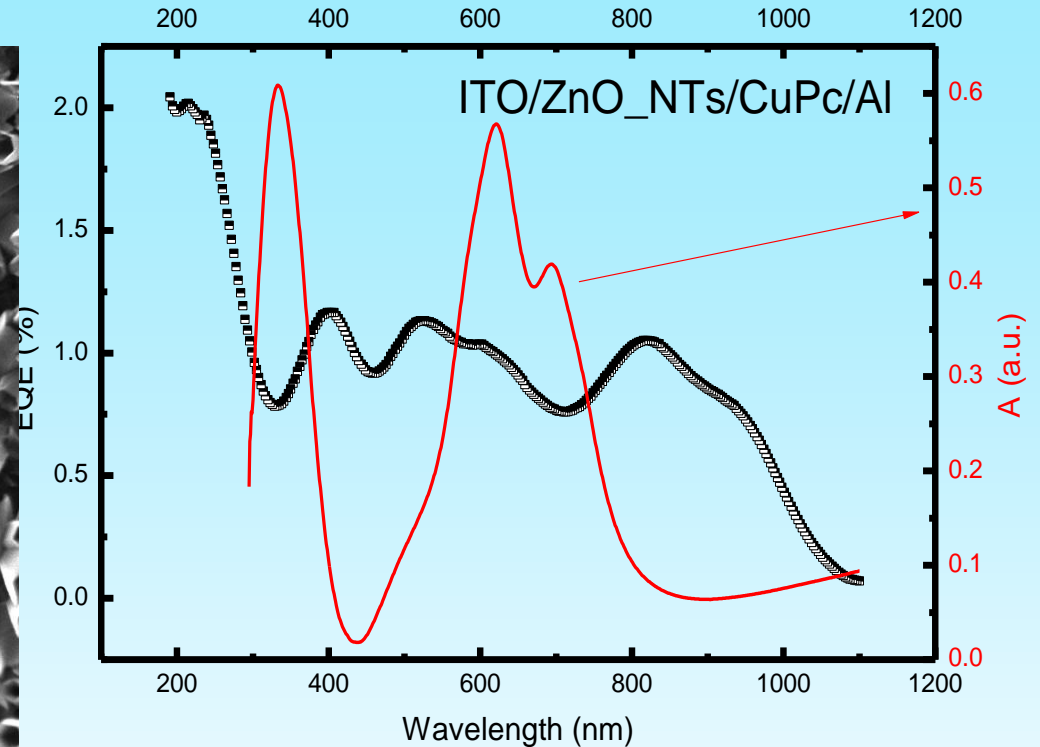
-In the above mentioned conditions, the hexagonal-columnar growth is perfectly reproducible.



ITO/ZnO hexagonal column array/CuPc/Al structures



SEM micrograph of
CuPc/ZnO(NTs)/ITO structure.



Spectral dependence of EQE for an ITO/ZnO(NTs)/CuPc/Al photovoltaic cell (black) and CuPc absorption spectrum (red). EQE one order of degree higher than the previous structures based on ZnO with small roughness

Cristina Besleagă, Iulia Arghir, Camelia Florica, T.L. Mitran, Elena Matei, I. Enculescu, N. Dina, L. Ion, (*)S. Antohe
Manuscript Number: MSB-D-09-01352R1, accepted to be published in **Materials Science and Engineering B**, 2010

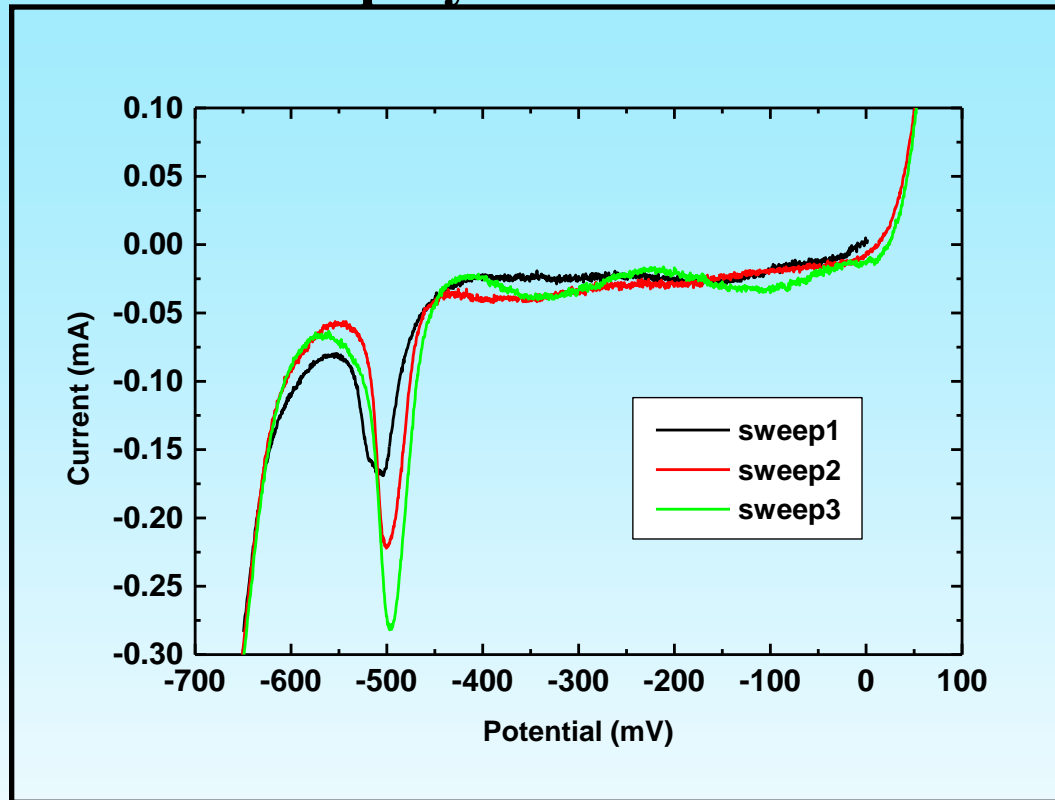


Hybrid structures based on submicron CdTe wire arrays and CuPc as organic absorber

- **Among A_2B_6 semiconductor compounds, CdTe is one of the best candidates for electronic and optoelectronic applications due to:**
 - suitable optical band gap (wide, direct band gap);
 - large optical absorption coefficient;
 - good electronic properties;
- **Specific electronic and optical properties of CdTe (nano)wires, induced by the low dimensionality and high surface to volume ratio, make them suitable for:**
 - electronic applications (FETs)
 - optoelectronic applications (lasers, active waveguides, photovoltaic cells)
 - gas sensors



Preparation of CdTe nanowire arrays using a nuclear track etched polycarbonate membrane as template

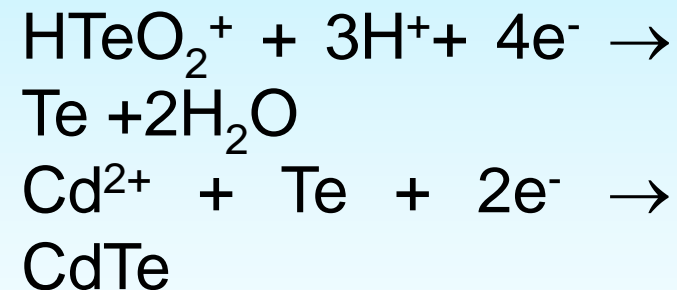


Acidic deposition bath:

➤ 1 M CdSO₄,

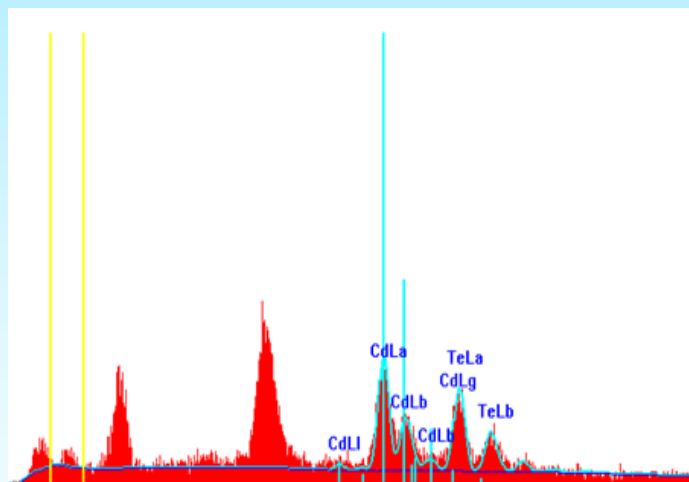
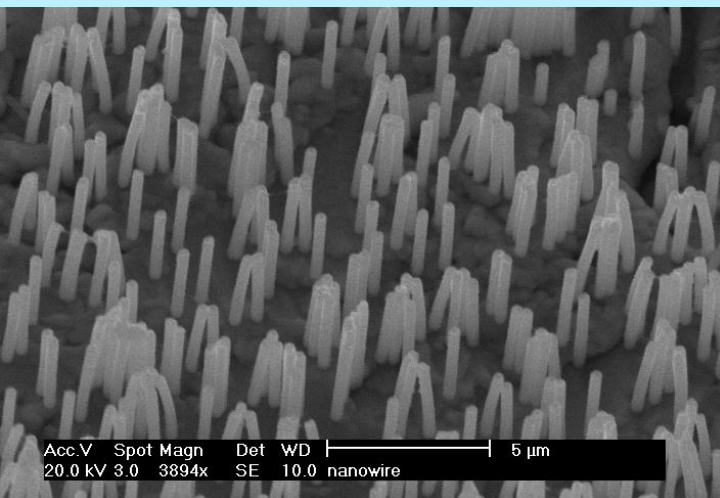
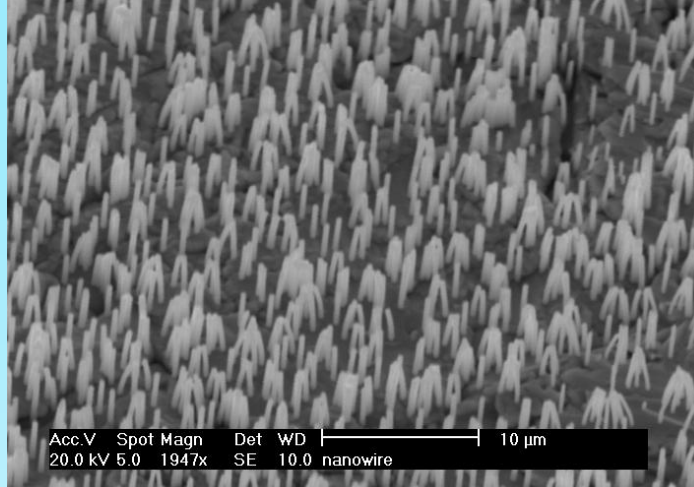
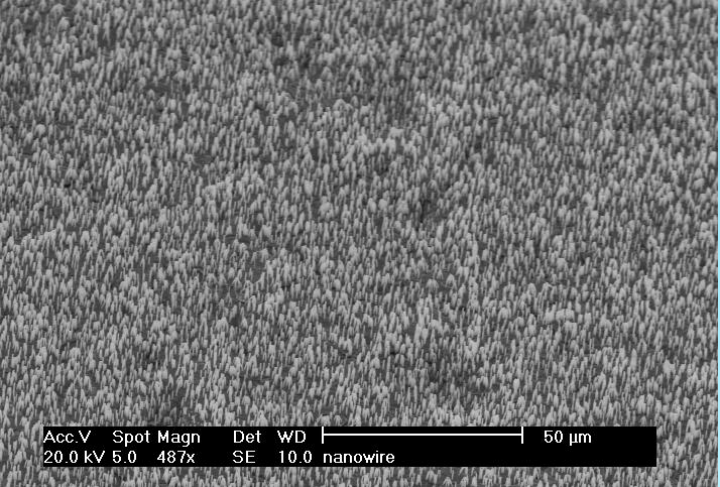
➤ 0.3 mM TeO₂

at a pH of 1.6
adjusted with H₂SO₄)



Polarisation curves for CdTe nanowires deposition. Sweep rate was 5 mV/s. The peak at 500 mV corresponds to the potential where CdTe is deposited. The shift towards more positive potential at the second and third sweep, is due to the fact that the deposition is further favored by the presence in the substrate of Te atoms.



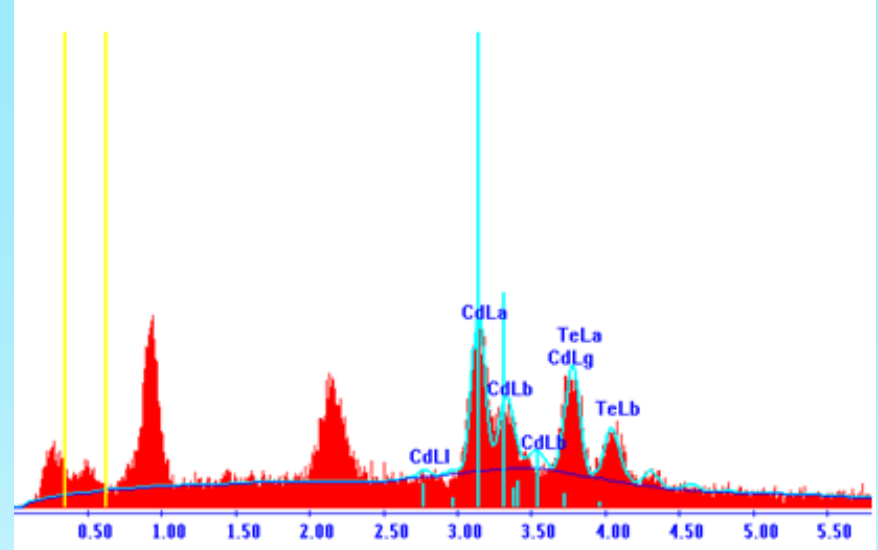
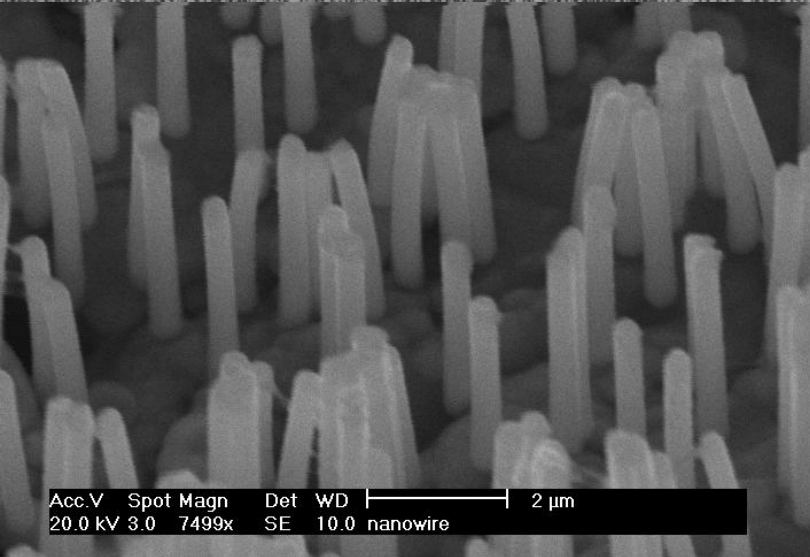
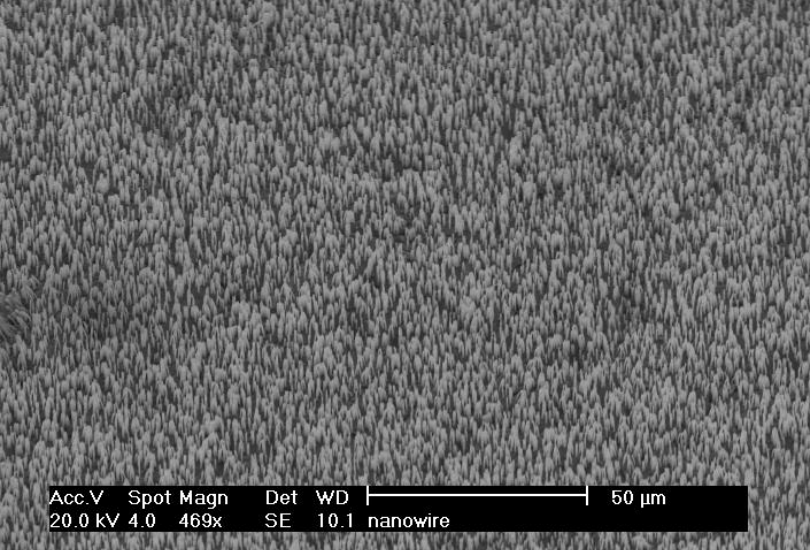


- CdTe nw array
- 10^8 wires/cm²
- 300 nm diameter
- Voltage: -500 mV;
- Composition: 49% Cd; 51%Te

Lucian ION, Ionut ENCULESCU, Stefan ANTOHE, Journal of Optoelectronics and Advanced Materials, Vol. 10 , No. 12, December 2008, 3241-3246

SEM micrographs of an array of CdTe wires (10^8 wires/cm², 300 nm diameter) deposited at -500 mV vs. SCE and the result of Energy Dispersive X-ray (EDX) analysis.





- The stoichiometric composition is obtained at about -530 mV vs. SCE.
- More negative deposition potentials, give rise to wires richer in cadmium
- deposition at -600 mV
- composition:51% Cd 49% Te
- SEM micrographs of an array of CdTe wires (10^8 wires/cm², 300 nm diameter) deposited at -600 mV vs. SCE and the result of EDX analysis.

Lucian ION, Ionut ENCULESCU, Stefan ANTOHE, Journal of Optoelectronics and Advanced Materials, Vol. 10 , No. 12, December 2008, 3241-3246



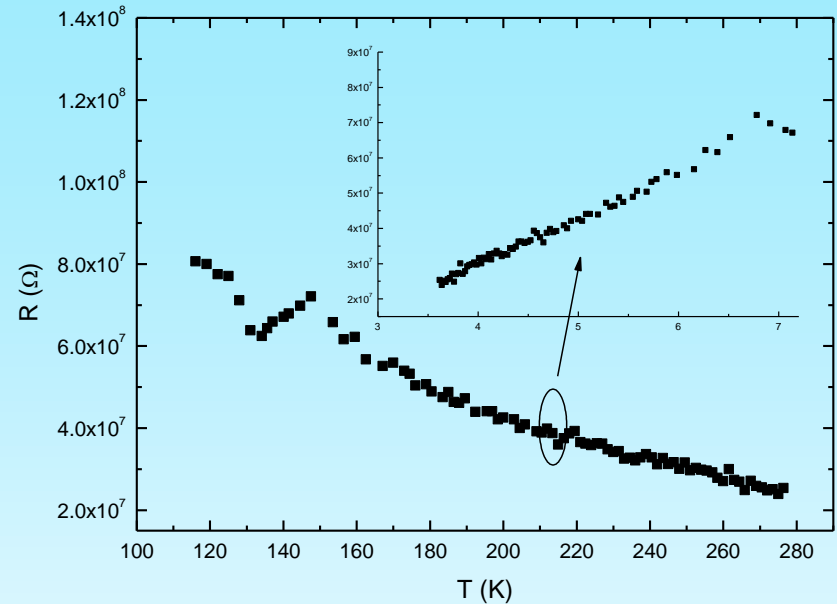
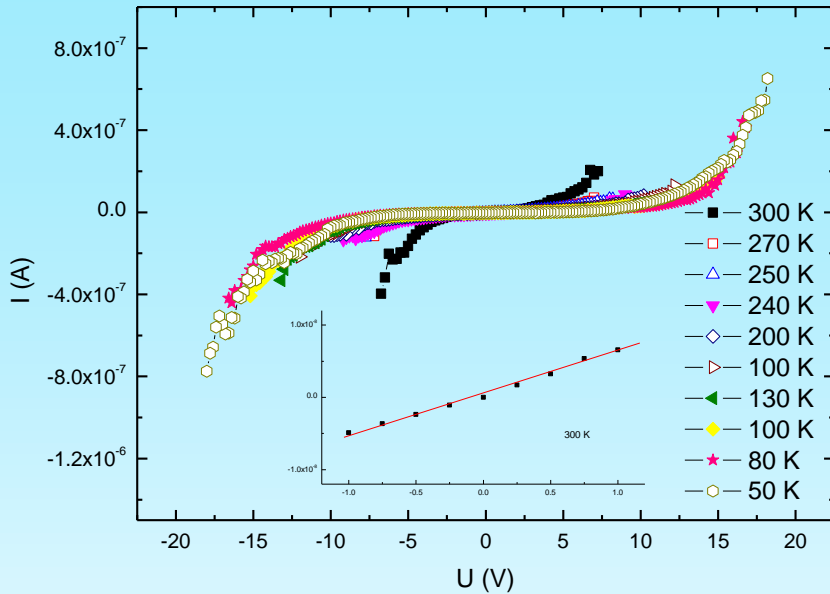


Fig. 15 a) I-V characteristics recorded for a CdTe multisegment wire array (300 nm diameter, 10^6 wires/cm²). The sequence of the segments is specified in Table I (CT8 sample). b) Temperature dependence of the electrical resistance of the sample, measured at applied voltages in the range where I-V curves were linear.

Multisegment wires (300 nm diameter, 10^6 pores/cm²):

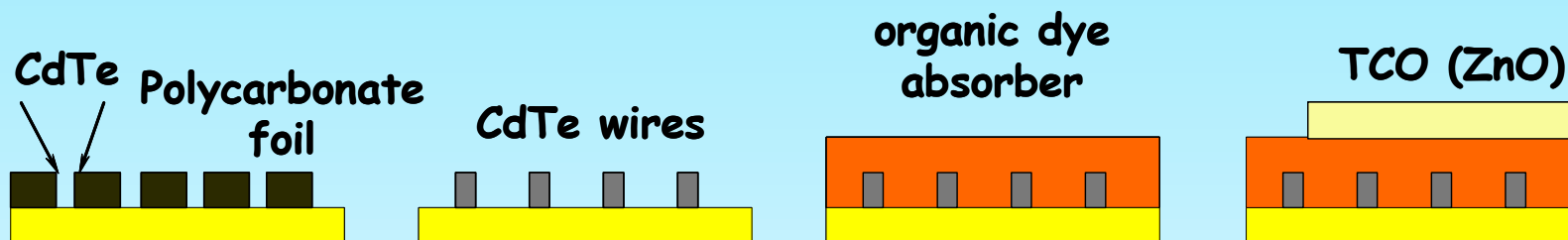
- CdTe, deposited at -680 mV, 700 nm long;
- CdTe stoichiometric, deposited at -510 mV;
- Cd, deposited at -680 mV, 700 nm long.

$$R = R_0 \exp\left(\frac{E_{ac}}{k_B T}\right)$$

The resistance is thermally activated, with an activation energy of 0.03 eV in the high temperature range



The producing of hybrid CdTe wire array/organic dye photovoltaic structures

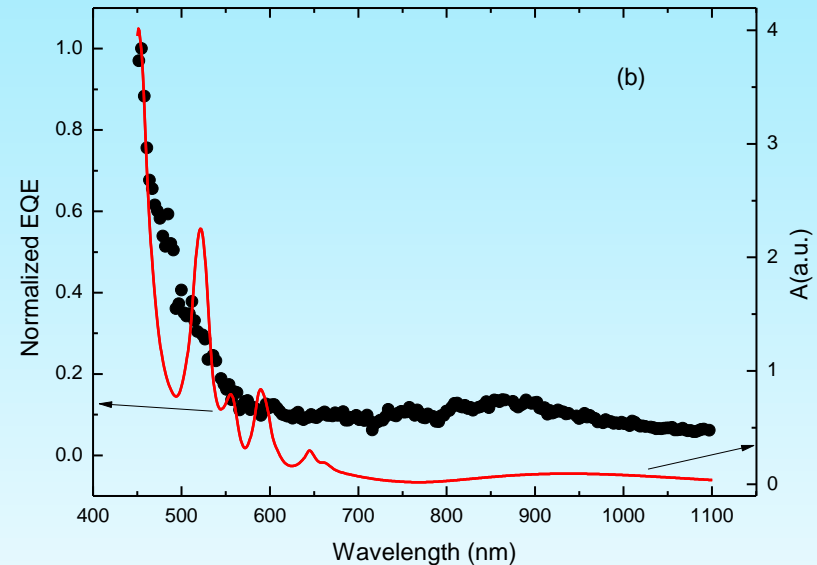
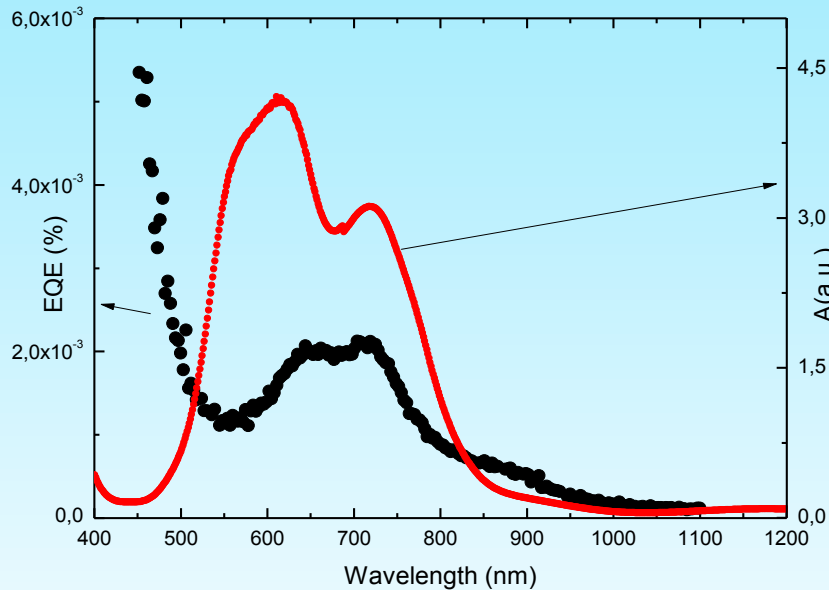


Technological steps in producing hybrid CdTe wire array/organic dye photovoltaic structures.

- After exposing the wire arrays by dissolving the polycarbonate template, an organic dye thin film (400 nm thick) was deposited by thermal vacuum evaporation.
- On top of organic layer, a transparent electrode (ZnO) was grown by Pulsed Electron Deposition. (PED)



The spectral dependence of the external quantum efficiency (EQE) of CdTe(ws)/ZnPc and CdTe (ws)/TPyP structures



EQE of a CdTe wire array/ZnPc structure (a) and, respectively, of CdTe wire array/TPyP (b). For comparison purposes, absorption spectra of ZnPC, TPyP and CdTe films deposited on optical glass in the same conditions are also given (in red and green lines).

Lucian ION, Ionut ENCULESCU, Stefan ANTOHE, Journal of Optoelectronics and Advanced Materials, Vol. 10 , No. 12, December 2008, 3241-3246

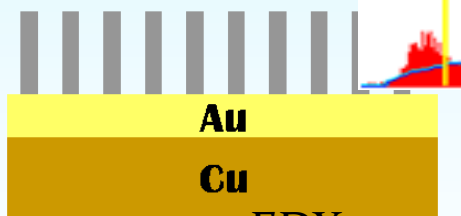


Hybrid CdTe wire array/CdTe/organic dye photovoltaic structures

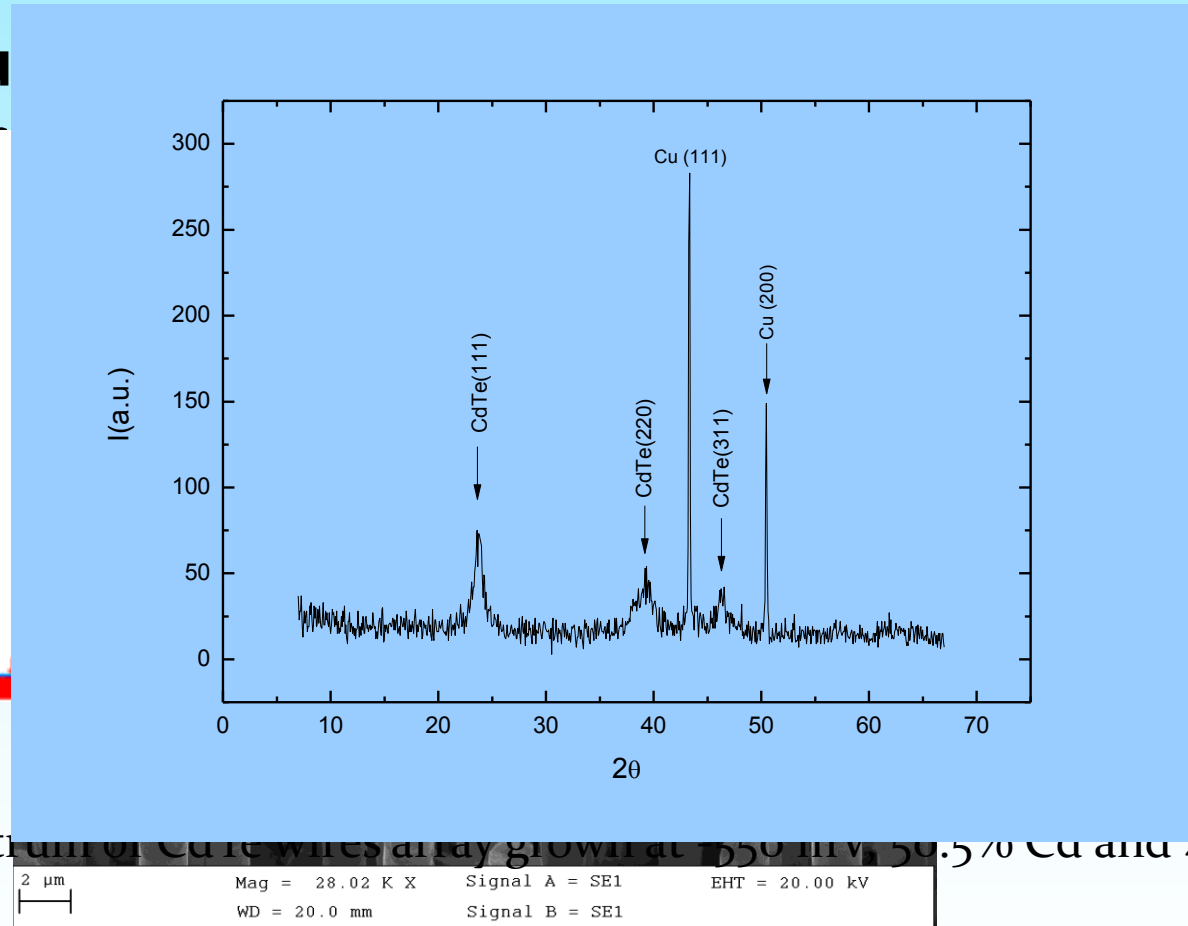
Steps in producing photovoltaic structures

1. After exposing polycarbonate (100 nm thick) was

Exposed CdTe nanowire



EDX spectrum of CdTe wires array grown at 150 mV, 50.5% Cu and 49.5% Te



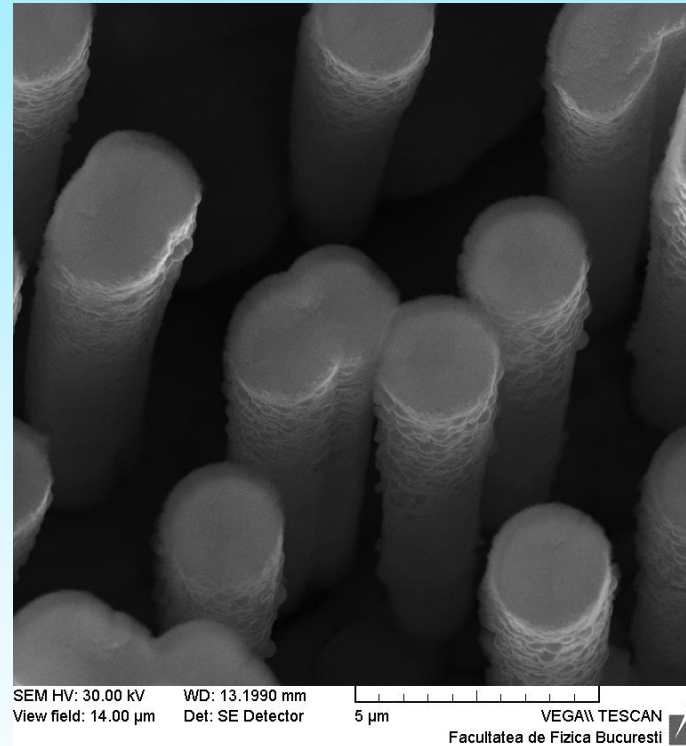
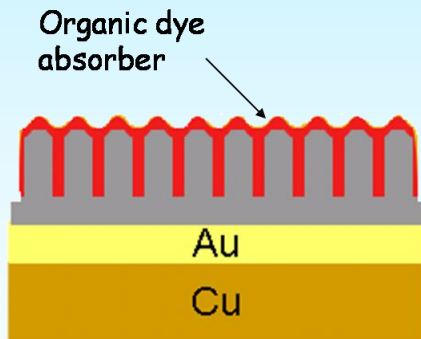
2 μm Mag = 28.02 K X Signal A = SE1 EHT = 20.00 kV
WD = 20.0 mm Signal B = SE1

dye
he
im
n.



Hybrid CdTe wire array/CdTe/organic dye photovoltaic structures

2. An organic dye (TPyP, CuPC or ZnPc) was deposited by vacuum sublimation.

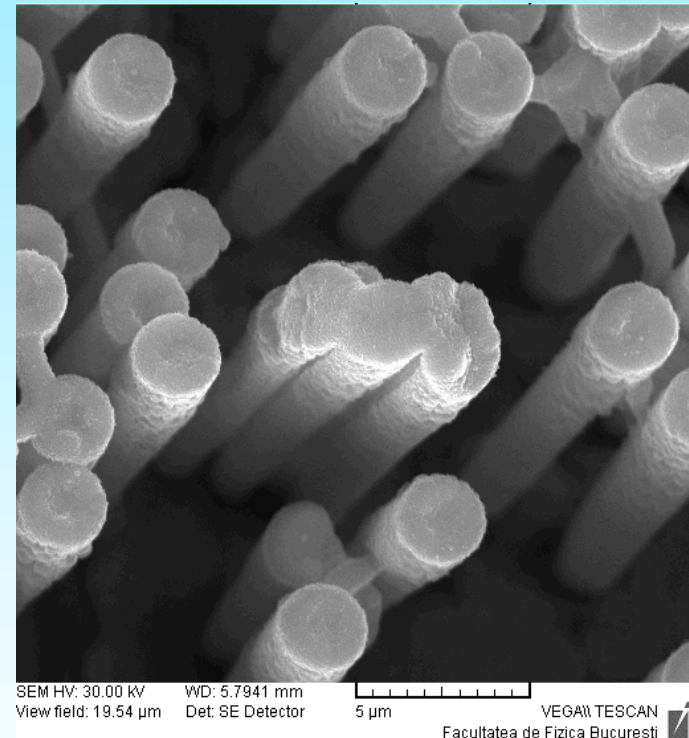
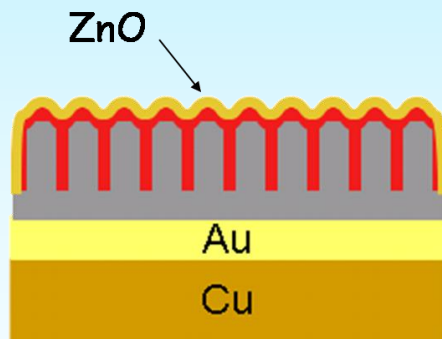


S. Antohe, I. Enculescu, L. Ion, 6th International Conference – NN09& 3rd International Summer School-SS-NN09 on Nanosciences & Nanotechnologies, Aristotle University of Thessaloniki, 13-15 July 2009, Abstract Book, pg.31, oral presentation, in press **Materials Science and Engineering B, 2010**



Hybrid CdTe wire array/CdTe/organic dye photovoltaic structures

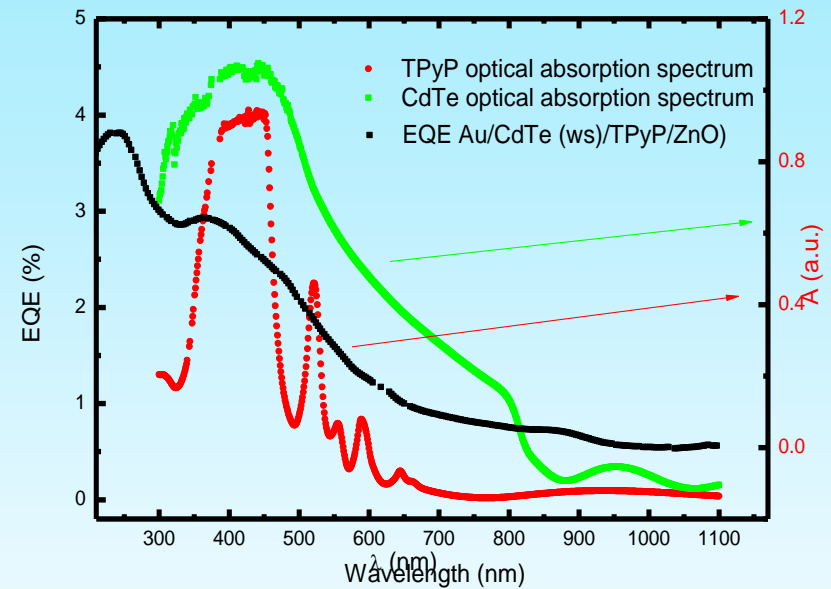
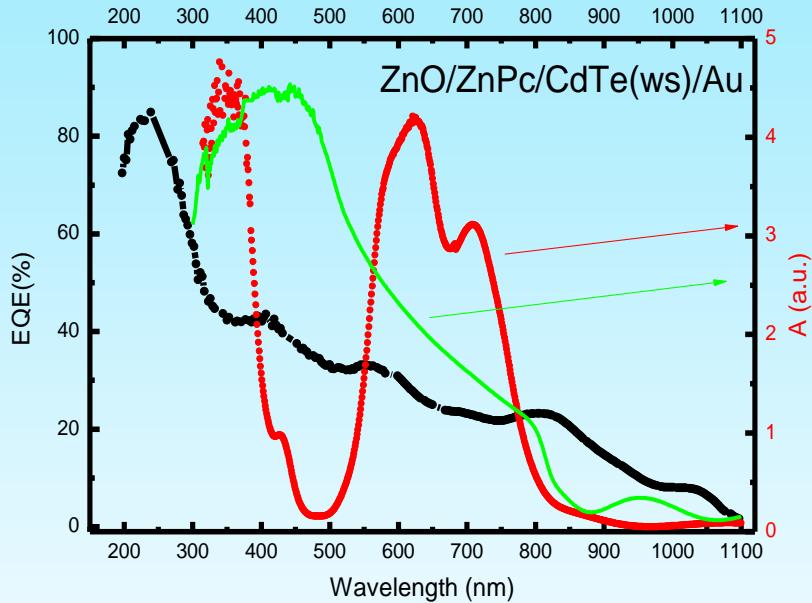
3. The structures were completed by depositing on top a thin ZnO film, by Pulsed Electron Deposition (PED) technique.



L. Ion, I. Enculescu, V. A. Antohe, A. Radu, M. Radu, G. Chisulescu, N. Dina, S. Antohe., 2nd International Symposium on Flexible Organic Electronics, 8-10 July 2009, Porto Carras Grand Resort, halkidiki, Greece, Book of Abstracts, pg.110, in press **Materials Science and Engineering B, 2010**



The spectral dependence of the external quantum efficiency (EQE) of CdTe(ws)/CdTe/ZnPc and CdTe (ws)/CdTe/TPyP structures



EQE of a CdTe wire array/CdTe(200nm)ZnPc structure (a) and, respectively, of CdTe wire array/CdTe(200nm)/TPyP (b). For comparison purposes, absorption spectra of ZnPc, TPyP and CdTe films deposited on optical glass in the same conditions are also given (in red and green lines).



Conclusions

- The single - layer ITO/CuPc/Al and ITO/TPyP/Al cells have a photovoltaic response as a result of the charge carrier photogeneration in CuPc or TPyP layer and their separation in the built electric field present at Al/CuPc and ITO/TPyP interface, respectively.
- The two-layer ITO/CuPc/TPyP/Al cells have a power conversion efficiency of about 100 times greater than that of organic monolayer cells, due to a strong cosensitization effect. The ITO/Chla/TPyP/Al cells show rectification and photovoltaic phenomena due to barrier formed at the Chla/TPyP interface.
- The three-layered organic photovoltaic cells (ITO/CuPc/(CuPc +TPyP)/TPyP/Al), clearly suggest an improvement, although modest, over two-layered cells. The co deposited interlayer acts as an efficient carrier photogeneration layer, as a result of exciton dissociation via the exciplex of (CuPc-TPyP+)* dyes. The power conversion efficiencies of three-layered cells, ranging from 0.07 to 0.35%, are 2-3 times greater as compared to those for double-layered cells.
- The spectral sensitization of an a-Si:H solar cell using an organic layer was obtained. The action spectrum was extended by 30 nm to longer wavelengths range, using a 100 nm thick layer of TPyP.
- The structures based on the P3HT:PCBM (1:1) blend shows a promising photovoltaic response, with a value of 0.58 V for the open-circuit voltage, and a short-circuit current of 1.35×10^{-6} A, and then the fill-factor and power conversion efficiency are increased of about two order of degree, than that measured in the case of structures based on P3HT or PCBM polymers.



Conclusions

- Different kind of nanostructured ZnO electrodes photosensitised with an organic absorber were produce and characterized.
- EQE of ZnO wire arrays /CuPc structures was 4 time larger than that of ZnO nanostructured film/CuPc structures.
- EQE of ZnO nanotubes arrays /CuPc structures was about one order of degree higher than that of ZnO nanostructured film/CuPc structures.
- Large arrays of CdTe submicron wires were successfully produced by electrodeposition, using a template method. Etched nuclear track polycarbonate membranes were used as template.
- Different kind of hybride photovoltaic structures based on CdTe nanowire arrays were prepared using ZnPc and TPyP as organic absorber
- EQE of CdTe nws/CdTe (200nm)/ZnPc structures was two order of magnitude higher than in the case of CdTe nws/ZnPc.
- Currently, work is in progress to improve the efficiency of these structures, by increasing the density of the wire arrays, improving the crystalline quality of both the wires and the organic dyes thin films and improving also the quality of the inner interface of the structures.



REFERENCES

- [1] Tang, C.W. *Appl. Phys. Lett.* 1986, 48, 183.
- [2] Antohe, S., *Phys.Stat.Sol.(a)*1993,136, 401.
- [3] Antohe, S.;Tugulea,L., *Phys.Stat.Sol.(a)*1991, 128, 253.
- [4] Antohe, S.;Ruxandra,V.; Tugulea,L.; Gheorghe,V.;Inascu,D.,*J.Phys.III France* 1996, 6, 1133.
- [5] Schmidt-Mende, L.; Fechtenkötter, A.; Müllen, K., Moons, E.; Friend, R.H., MacKenzie, J.D. *Science* 2001, 293, 1119.
- [6] Padinger, F.; Rittberger, R. S.; Sariciftci, N. S. *Adv. Funct. Mater.* 2003, 13, 85;
- [7] Chirvase, D.; Parisi, J.; Hummelen, J.C.; Dyakonov, V. *Nanotechnology* 2004, 15, 1317;
- [8] Li, G.; Shrotriya, V.; Yao, Y.; Yang, Y. *J. Appl. Phys.* 2005, 98, 043704;
- [9] Schilinsky, P.; Asawapirom, U.; Scherf, U.; Biele, M.; Brabec, C.J. *Chem. Mater.* 2005, 17, 2175;
- [10] Kim, Y.; Choulis, S.A.; Nelson, J.; Bradley, D.D.C.; Cook, S.; Durrant, J.R. *Appl. Phys. Lett.* 2005, 86, 063502.



- [11] S. Antohe, I. Munteanu, I. Dima, *Rev. Roum. Phys.*, 34 (6), 665 (1989)
- [12] S. Antohe, *Rev. Roum. Phys.*, 37, 309 (1992)
- [13] S. Antohe, L. Tugulea, V. Gheorghe, V. Ruxandra, I. Caplanusi and L. Ion, *Phys. Stat. Sol. (a)* 153, 581 (1996)
- [14] L. Tugulea and S. Antohe, *Photosynthesis Research II*, 845 (1993)
- [15] S. Antohe, *Journal of Optoelectronics and Advanced Materials*, 2, 498 (2000)
- [16] S. Antohe, *Romanian Reports in Physics*, 53, 427 (2001)
- [17] S. Antohe, D. Ionascu, V. Ruxandra, L. Tugulea, I. Spânulescu, N. Tomozeiu and I. A. Qazii, *Romanian Reports in Physics*, 48, 581 (1996)
- [18] S. Antohe, L. Ion, N. Tomozeiu, T. Stoica, E. Barna, *Solar Energy Materials&Solar Cells* 62, 207 (2000)
- [19] S. Antohe, Chapter 11 „Electronic and Optoelectronic Devices Based on Organic Thin Films “ in *HANDBOOK OF ORGANIC ELECTRONICS AND PHOTONICS, Electronic Materials and Devices, Edited by Hari Singh Nalwa, Volume 1 : Pages: 433, 440, AMERICAN SCIENTIFIC PUBLISHERS, Los Angeles, California, USA, 2006, ISBN : 1-58883-096-9*
- [20] I. Enculescu, Z. Siwy, D. Dobrev, C. Trautmann, M.E. Toimil-Molares, R. Neumann, K. Hjort, L. Westerberg, R. Spohr, *Appl. Phys. A* 77, 751 (2003).



- [21] I. Enculescu, M. Sima, M. Enculescu, M. Enache, L. Ion, S. Antohe, R. Neumann, *Phys. stat. solidi (b)*, **244**, 1607 (2007).
- [22] C. Tazlaoanu, L. Ion, I. Enculescu, M. Sima, Elena Matei, R. Neumann, Rosemary Bazavan, D. Bazavan, S. Antohe, *Physica E: Low-dimensional Systems and Nanostructures*, Vol 40/7 pp 2504-2507, 2007.
- [23] M. Ghenescu, L. Ion, I. Enculescu, C. Tazlaoanu, V. A. Antohe, M. Sima, M. Enculescu, E. Matei, R. Neumann, O. Ghenescu, V. Covlea, S. Antohe, *Physica E: Low-dimensional systems and Nanostructures*, Vol 40/7 pp 2485-2488, 2007
- [24] S. Antohe, L. Ion, C. Tazlaoanu, G. Socol, L. Magherusan, I. Enculescu, D. Bazavan, I.N. Mihailescu, and V.A. Antohe, *MRS Spring Meeting 2007, SUA, Symp. Z 4.9*, pg. 538
- [25] L. Ion, I. Enculescu, Rosemary Bazavan, R. Neuman and S. Antohe, *IMRC, Chongqing, China, June 9-12 2008, Symposium D, O-D11.14*, Pg.173
- [26] L. Ion, I. Enculescu, Elena Matei, C. Tazlaoanu and S. Antohe, *IMRC, Chongqing, China, June 9-12 2008, Symposium B, P-B3.40*, Pg.55
- [27] L. Ion, I. Enculescu, S. Antohe, *Journal of Optoelectronics and Advanced Materials*, Vol. 10 , No. 12, December 2008, 3241-3246
- [28] C.Ghica, L. Ion, G. Epurescu, L. Nistor, S. Antohe, M. Dinescu, *Journal of Nano-science and Nanotechnology*, volume 10, Number 2, February 2010, pp. 1322-1326 (5)
- [29] S. Antohe, I. Enculescu, Cristina Besleaga, Iulia Arghir, V. A. Antohe, V. Covlea, A. Radu, L. Ion, 2010 *Ceramics Engineering&Science proceedings (CESP), Volume 31, Issue 7 „Nanostructured Materials and Nanotechnology IV”*, pg.71-83, Volume Editors Sanjay Mathur and Tatsuki Ohji, Wiley, ISBN 978-0-470-93495-1
- [30] Larisa Magherusan, Polona Skraba, Cristina Besleaga, Sorina Iftimie, Nicoleta Dina, Mirela Bulgariu, Carmen-Gabriela Bostan, C. Tazlaoanu, A. Radu, L. Ion, M. Radu, A. Tanase, G. Bratina, S. Antohe, *Journal of Optoelectronics and Advanced Materials*, Vol. 12 , No. 2, February 18, 2010, p. 212-218



Thank you for your attention!

